Syntheses of New Polymers Containing Metalloporphyrins and Their Physicochemical Behavior

A Doctoral Thesis

by

Hiroyuki Aota

Submitted to the Faculty

of Science, Osaka University

February, 1993

Approvals

February, 1993

This thesis is approved as to
style and content by

蒲池幹治

Member-in -chief

中村晃

Member

寺本明夫

Member

森島洋太郎

Member

Acknowledgments

This research work was carried out under the direction of Professor Mikiharu Kamachi and Associate Professor Yotaro Morishima at Department of Macromolecular Science, Faculty of Science, Osaka University. The author is greatly indebted to Professor Mikiharu Kamachi and Associate Professor Yotaro Morishima for their continuing guidance and encouragement throughout the course of this work. Grateful acknowledgements are also made to Dr. Masaoki Furue, Dr. Akira Harada, and Dr. Atsushi Kajiwara for their helpful suggestions and to Mr. Hirofumi Fujii, Mr. Shin-ichi Araki, and all of the members of the Kamachi Laboratory for their cooperation and friendship.

The author is greatly indebted to Emeritus Professor Michihiko Kishita, Associate Professor Wasuke Mori, and Dr. Hirokazu Nakayama, College of General Education, Osaka University, for the measurements of magnetic susceptibility and their helpful discussion of the results. The author is very grateful to Kanegafuchi Chemical Industry Co., Ltd. for its scholarship. Finally, the author greatly indebted to Professor Akira Matsumoto, Faculty of Engineering, Kansai University, for his continuing encouragement.

Osaka
February, 1993

青田浩幸
Hiroyuki Aota

Contents

Abbreviations used in this thesis are as follows.

AgTPP	5,10,15,20-Tetraphenylporphyrinatosilver(II) (Silvertetraphenylporphyrin)
AIBN	2,2'-Azobisisobutyronitrile
AMPS	2-Acrylamido-2-methylpropanesulfonate
AOTPP	5-Acryloyloxyphenyl-10,15,20-triphenylporphine
CdMAm	N-cyclododecyl-methacrylamide
$CH_3OCODPE$	2,8,12,18-Tetraethyl-5,10-bis(4-methoxy-carbonylphenyl)-3,7,13,17-tetramethylporphine
CT	Charge-Transfer
CuAAEtio	(5-Acrylamido-2,7,12,17-tetraethyl-3,8,13,18-tetramethylporphyrinato)copper(II)
CuAOMTPP	(2-Acryloyloxymethylene-5,10,15,20-tetraphenylporphyrinato)copper(II)
$CuCH_3OCODPE$	[2,8,12,18-Tetraethyl-5,10-bis(4-methoxy-carbonylphenyl)-3,7,13,17-tetramethyl-porphyrinato]copper(II)
CuCuDPE	poly($CuNH_2DPE$-co-$CuCH_3OCODPE$)
CuMnDPE	poly($CuNH_2DPE$-co-$MnClCH_3OCODPE$)
$CuNH_2DPE$	[5,10-Bis(4-aminophenyl)-2,8,12,18-tetraethyl-3,7,13,17-tetramethyl-porphyrinato]copper(II)
CuTPP	5,10,15,20-Tetraphenylporphyrinatocopper(II) (Coppertetraphenylporphyrin)

DMF	N,N-Dimethylformamide
DPE	2,8,12,18-tetraethyl-3,7,13,17-tetramethyl-5,10-diphenylporphine (Diphenyletioporphyrin)
ET	Electron Transfer
Etio	2,7,12,17-tetraethyl-3,8,13,18-tetramethylporphine (Etioporphyrin)
LaMAm	N-Laurylmethacrylamide
$MnClCH_3OCODPE$	Chloro[2,8,12,18-tetraethyl-5,10-bis(4-methoxycarbonylphenyl)-3,7,13,17-tetramethylporphyrinato]manganese(III)
$MnClNH_2DPE$	Chloro[5,10-bis(4-aminophenyl)-2,8,12,18-tetraethyl-3,7,13,17-tetramethylporphyrinato]manganese(III)
MnMnDPE	poly($MnClNH_2DPE$-co-$MnClCH_3OCODPE$)
MV^{2+}	Methylviologen
NH_2DPE	5,10-Bis(4-aminophenyl)-2,8,12,18-tetraethyl-3,7,13,17-tetramethylporphine
NH_2Etio	5-Amino-2,7,12,17-tetraethyl-3,8,13,18-tetramethylporphine
NH_2Por	5-Aminoporphine
NH_2TPP	5-(4-Aminophenyl)-10,15,20-triphenylporphine
NO_2DPE	2,8,12,18-tetraethyl-3,7,13,17-tetramethyl-5,10-bis(4-nitrophenyl)porphine
NO_2Etio	2,7,12,17-tetraethyl-3,8,13,18-tetramethyl-5-nitroporphine

NO_2Por	5-Nitroporphine
NO_2TPP	5-(4-Nitrophenyl)-10,15,20-triphenylporphine
2-NpMAm	N-(2-Naphthylmethyl)-methacrylamide
PMPS	phenylmethylphenacylsulfonium p-toluenesulfonate
poly(A/Cd/ZnEtio)	poly(AMPS-co-CdMAm-co-ZnAAEtio)
poly(A/Cd/ZnPor)	poly(AMPS-co-CdMAm-co-ZnAAPor)
poly(A/Cd/ZnTPP)	poly(AMPS-co-CdMAm-co-ZnAATPP)
poly(A/La/ZnEtio)	poly(AMPS-co-LaMAm-co-ZnAAEtio)
poly(A/La/ZnPor)	poly(AMPS-co-LaMAm-co-ZnAAPor)
poly(A/La/ZnTPP)	poly(AMPS-co-LaMAm-co-ZnAATPP)
poly(A/Np/ZnEtio)	poly(AMPS-co-2-NpMAm-co-ZnAAEtio)
poly(A/Np/ZnPor)	poly(AMPS-co-2-NpMAm-co-ZnAAPor)
poly(A/Np/ZnTPP)	poly(AMPS-co-2-NpMAm-co-ZnAATPP)
poly(A/ZnEtio)	poly(AMPS-co-ZnAAEtio)
poly(A/ZnPor)	poly(AMPS-co-ZnAAPor)
poly(A/ZnTPP)	poly(AMPS-co-ZnAATPP)
Por	Porphine
S_0	Singlet ground state
S_1	First singlet excited state
T_1	First triplet excited state
T_n	nth triplet excited state
TADF	Thermally activated delayed fluorescence
THF	Tetrahydrofuran
TPP	5,10,15,20-Tetraphenylporphine (Tetraphenylporphyrin)
VOAOMTPP	(2-Acryloyloxymethylene-5,10,15,20-tetraphenylporphyrinato)oxovanadium(IV)

$VOCH_3OCODPE$	[2,8,12,18-Tetraethyl-5,10-bis(4-methoxy-carbonylphenyl)-3,7,13,17-tetramethyl-porphyrinato]oxovanadium(IV)
VOFTPP	(2-Formyl-5,10,15,20-tetraphenyl-porphyrinato)oxovanadium(IV)
VOHOMTPP	(2-Hydroxmethyl-5,10,15,20-tetraphenyl-porphyrinato)-oxovanadium(IV)
VOMnDPE	poly($VONH_2DPE$-co-$MnClCH_3OCODPE$)
$VONH_2DPE$	[5,10-Bis(4-aminophenyl)-2,8,12,18-tetra-ethyl-3,7,13,17-tetramethylporphyrinato]-oxovanadium(IV)
VOTPP	Oxo(5,10,15,20-Tetraphenylporphyrinato)-vanadium(IV) (Vanadyltetraphenylporphyrin)
VOVODPE	poly($VONH_2DPE$-co-$VOCH_3OCODPE$)
ZnAAEtio	5-Acrylamido-2,7,12,17-tetraethyl-3,8,13,18-tetramethylporphyrinato)zinc(II)
ZnAAPor	(5-Acrylamidoporphyrinato)zinc(II)
ZnAATPP	[5-(4-Acrylamidophenyl)-10,15,20-triphenyl porphyrinato]zinc(II)
$ZnNH_2Etio$	(5-Amino-2,7,12,17-tetraethyl-3,8,13,18-tetramethylporphyrinato)zinc(II)
$ZnNH_2TPP$	[5-(4-Aminophenyl)-10,15,20-triphenyl-porphyrinato]zinc(II)
$ZnNH_2Por$	(5-Aminoporphyrinato)zinc(II)
ZnTSPP	5,10,15,20-Tetrakis(4-sulfonatophenyl)-porphyrinatozinc(II)

Chapter 1

Introduction

1.1. Porphyrins and Metalloporphyrins

Porphyrins [1,2] are derived from porphine, which consists of four pyrrole-type rings joined by four methine bridges to give a macrocycle, as shown in Figure 1. The porphyrin macrocycle has 22 π-electrons, of which 18 π-electrons are included in one delocalization system. Accordingly, porphyrins are highly colored. The typical spectra of porphyrins are composed of the Soret band found around 400 nm, whose molar extinction coefficients are around 400,000 $M^{-1}cm^{-1}$, and the four bands, Q-bands, in higher wavelength, whose molar extinction coefficients are much smaller (around 15,000 $M^{-1}cm^{-1}$) than that of the Soret bands. Aromatic character in porphyrin compounds has been confirmed by measurement of their heat of combustion, x-ray investigation, and NMR spectroscopy. According to the IUPAC rules, the porphyrin ring is numbered from 1 to 24, as shown in Figure 1.

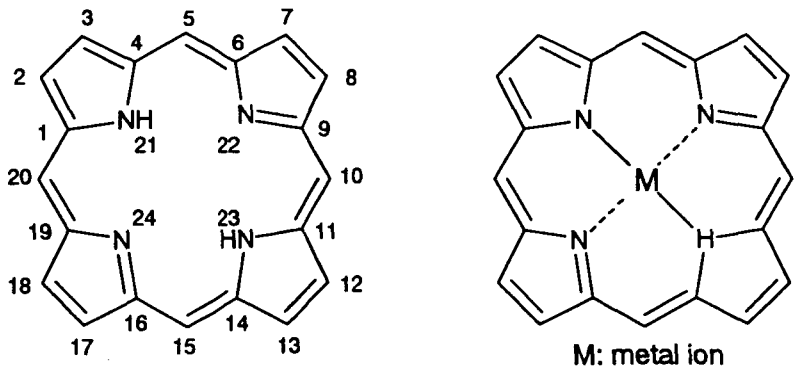

Figure 1. Structures of Porphine and Metalloporphyrin

Porphyrins readily form complexes with a whole variety of metals, as shown in Figure 1. The metal complexes constitute the most abundant colored matters in natural systems. Moreover, metalloporphyrins play an important role as functional groups in wide variety of biological systems: The peripherally modified form of the iron(II) complex is contained in the Cytochromes[3] and enzymes such as peroxidase and catalase,[4] and Chlorophylls, photosynthetic pigments, are composed of a peripherically modified form of the magnesium complex. Special functions of metalloporphyrins such as oxygen-carrying system and photosynthesis system appear in an environment where metalloporphyrin moieties are surrounded by polypeptide or make an aggregation by themselves. Therefore, a lot of papers have been reported on the preparation of polymers containing porphyrin moieties and on the study on their biomimetic functions. Tsuchida and Nishide succeeded in the molecular design of artificial oxygen-carrying system using polyamide containing tetraphenylporphyrin (TPP) moieties.[5] Kamachi et al.[6-11] have firstly succeeded in the preparation of high polymers by radical polymerization of vinyl monomers containing porphyrin moieties or metalloporphyrins in their side chain, and investigated magnetic properties of paramagnetic metalloporphyrin. They found that the homopolymer containing silvertetraphenylporphyrin (AgTPP) had a strong antiferromagnetic interaction[6] and the copolymer containing coppertetraphenylporphyrin (CuTPP) and vanadyltetraphenylporphyrin (VOTPP) had a ferromagnetic interaction.[11]

1.2. Magnetism

It is commonly known that some substances are attracted to a magnetic field while others are repelled from it. The susceptibility of a material in the presence of magnetic field, χ, is defined by the ratio of the magnetization (M) to the magnitude of the magnetic field (H)

$$\chi = M / H \qquad (1)$$

The sign of the magnetic susceptibility usually depends on whether the ground-state electrons in a molecule or an ion are paired or unpaired. Therefore, we can divide all matters into two categories, diamagnetic or paramagnetic. Paramagnetism is characterized by electron spins unpaired in the molecule, and diamagnetism by the repulsion of the electrons from the region of high field. There are four types of magnetic behavior in paramagnetic substances. The first case where the spins oriented randomly due to no magnetic interaction is known as paramagnetism. As a result of some type of interaction, the second case where the randomly oriented spins of the paramagnetic substances orient themselves parallel to one another is known as ferromagnetism, and the third case where the spins having a magnetic moment of the same magnitude orient themselves antiparallel to one another is known as antiferromagnetism, and the last case where the two kinds of spins having magnetic moments of different magnitude orient themselves antiparallel alternatively to one another is known as ferrimagnetism .

A schematic representation of these generalized types of spin orientations for two dimensional lattice is shown in Figure 2.

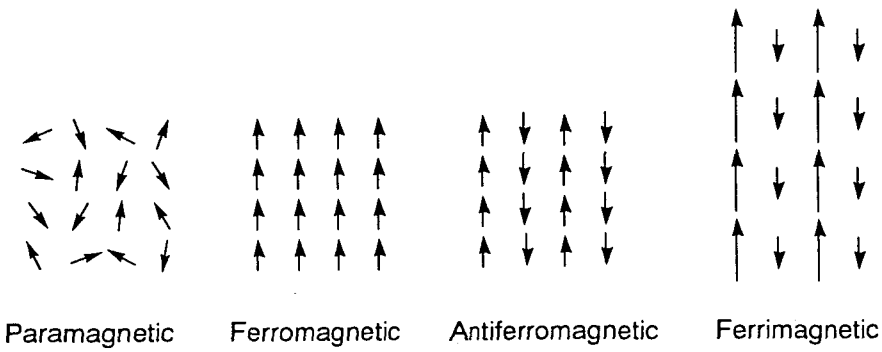

Figure 2. Schematic representation of four types of spin orientation.

Diamagnetism is generated by the tendency of electron moving in a closed orbit, and is independent of temperature. Paramagnetism is generated by the tendency of electron spins to orient themselves in a magnetic field. The magnetic susceptibility of a paramagnetic species depends inversely on the temperature (Curie's law):

$$\chi = C / T \qquad (2)$$

where C is the Curie constant and T is the absolute temperature. The Curie constant is dependent on the number of unpaired electrons and the g value of the compound.[12] The Curie constant for the electron spin only susceptibility is:

$$C = [N_A g^2 \mu_B^2 S(S+1)] / 3k \qquad (3)$$

where N_A is Avogadro's number, μ_B is the Bohr magneton, S is the spin angular momentum, and k is the Boltzmann constant.

A weak magnetic interaction between neighboring spins in a material is approximated as a perturbation in equation. The influence of this interaction may be described by replacing the temperature term of equation with a $(T-\theta)$ term as shown in eq. (4) (Curie-Weiss' law).

$$\chi = C/(T-\theta) \qquad (4)$$

where θ is the Weiss constant, which has the unit of Kelvin.

Figure 3-a shows the magnetic behavior of a sample that obeys Curie's or Curie-Weiss' law. A plot of the inverse of the magnetic susceptibility against temperature for a system that obeys the Curie-Weiss' law yields a straight line as shown in Figure 3-b. The intercept of the line with temperature axis gives both the sign and magnitude of the Weiss constant. A positive value for θ is caused by ferromagnetic interaction, while a negative value shows the presence of an antiferromagnetic spin interaction.

Another convenient way to show the presence of magnetic interaction is temperature dependence of magnetic moment (μ_{eff}) of the substance.

$$\mu_{eff} = 2.83\ (\chi T)^{0.5} \qquad (5)$$

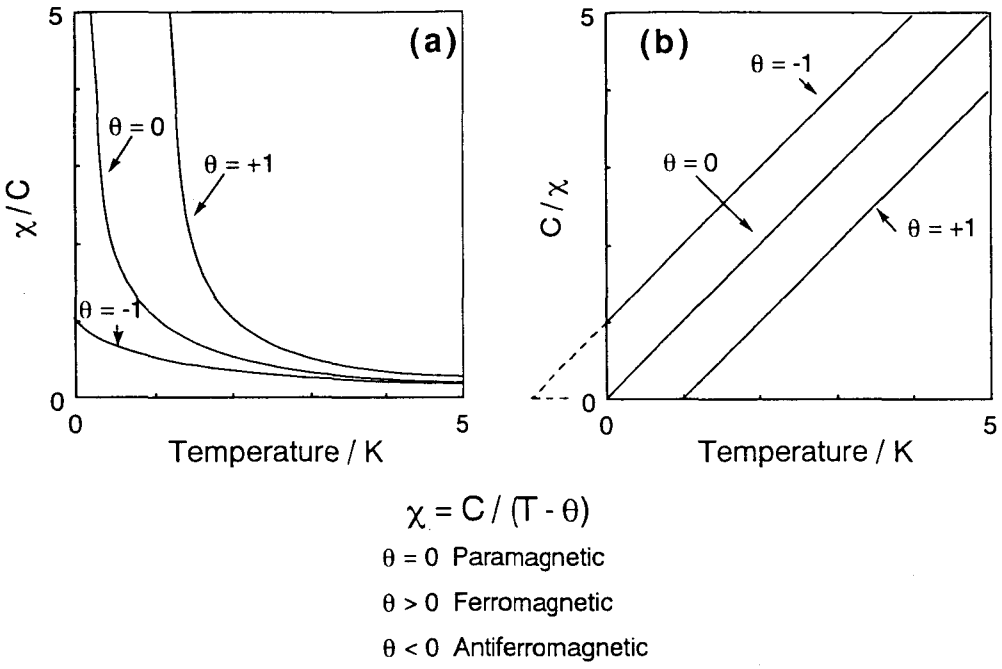

Figure 3. The plots of magnetic susceptibility (**a**) and inverse of magnetic susceptibility (**b**) versus temperature.

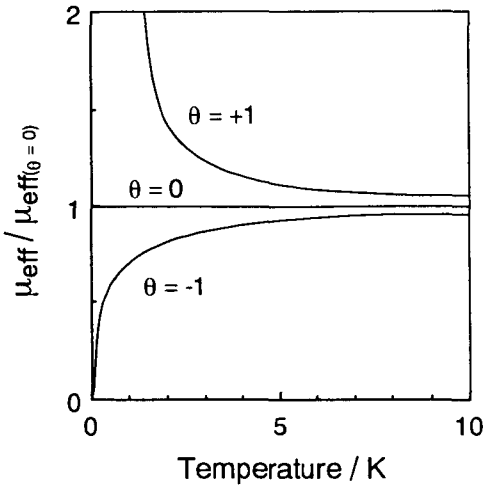

Figure 4. The plot of effective magnetic moment versus temperature.

The magnitude of μ_{eff} is dependent on the number of unpaired electrons and g-value. For a system obeying Curie's law, a plot of μ_{eff} as a function of temperature yields a horizontal straight line in the low temperature region. On the other hand, the presence of spin interaction is denoted by a departure from the horizontal line in the low temperature region. Typical plots of the effective magnetic moment are shown in Figure 4.

1.3. Historical Background of Molecular Based Magnetic Materials.

In 1967, Itoh [13] and independently Wasserman [14] et al. found that the electric ground state of bis(phenyl-methylenyl)-m-phenylene **1** is the quintet state. On the basis of this finding, Mataga [15] proposed an idea that the following polymers **2** and **3** with

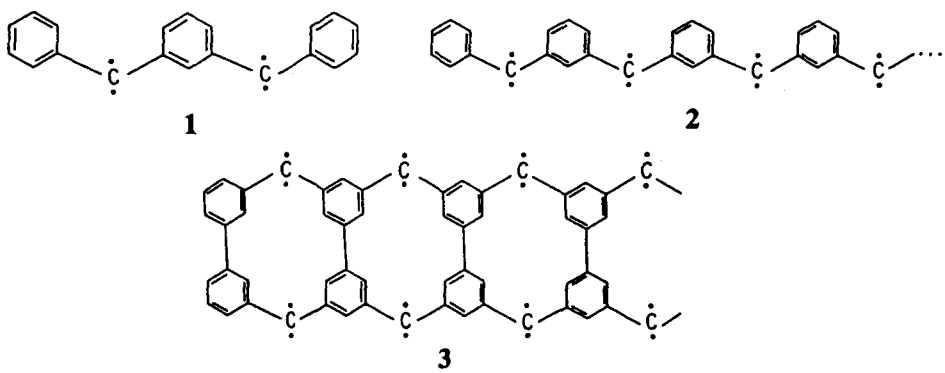

1 **2** **3**

the conjugated π-electron system will show the ferromagnetic spin alignment due to the topological nature of the molecular orbitals, if they can be prepared. In order to confirm this idea, Itoh and

Iwamura et al.[16] prepared bis[(di-phenylmethyl-ene-3-yl)]-m-phenylene with nonet spin multiplicity due to intramolecular spin alignment, and suggested that such high spin state is relevant to the design of organic ferromagnets. However, the temperature dependence of its magnetic susceptibility gave a straight line with a negative Weiss temperature θ = -22K in Curie-Weiss' law. This finding indicates that intermolecular spin alignment is anti-ferromagnetic. In order to get information on a relation between intermolecular spin alignment and relative orientation, the electronic spin-spin interaction between two diphenyl carbene units incorporated in [2,2] paracyclophane skeleton has been investigated by ESR spectroscopy.[17] The pseudo-ortho and pseudo-para bis(phenylmethylenyl) [2,2] paracyclophanes are in the ground quintet state, while the pseudo-meta isomer is singlet. These findings show that intermolecular ferromagnetic interaction is possible in organic free radicals. In 1977, Ovchinnikov[18] theoretically pointed out that organic polymers such as **4** and **5** might be ferromagnetic owing to an exchange interaction. No experimental

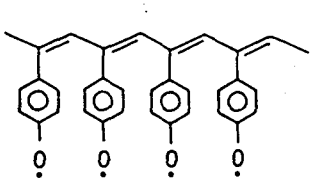

4

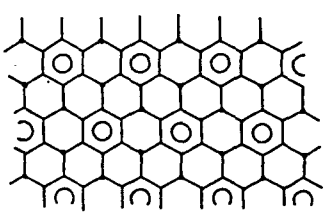

5

data on the polymer for magnetism was reported before 1980, although several papers were published on the preparation of polyradicals. Recently, organic and organometallic compounds with ferromagnetic interaction have been prepared on the basis of theoretical background by Miller et al.[19] In 1986, Ovchinnikov et al.[20] obtained black and insoluble polymers by the polymerization of 1,4-bis(2,2,6,6-tetramethyl-4-hydroxy-4-piperidyl-1-oxyl)butadiyne **6**. The IR spectra of the polymers suggested that the polymer was composed of 1,2-addition unit and 1,4-addition unit as shown in **7** and **8**. The magnetic behavior of the polymers was investigated by

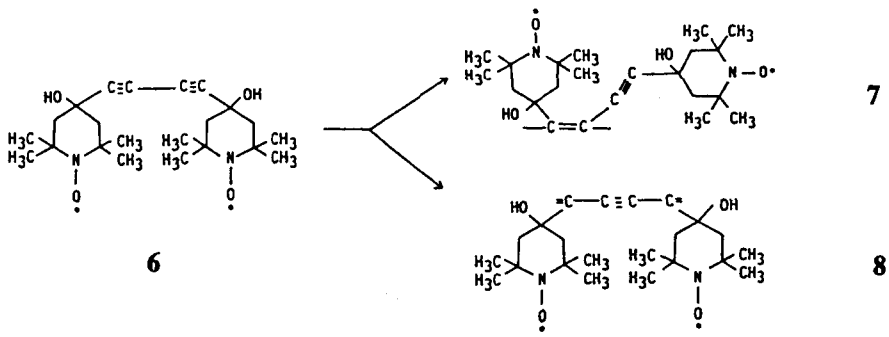

6 **7** **8**

the measurement of temperature dependence of the magnetic susceptibility and field dependence of magnetization, which indicated that some parts of the polymers were ferromagnetic. Because of the poor yield of the ferromagnetic fraction and incomplete characterization of the magnetic properties, the presence of pure organic ferromagnetism was controversial. A structural analogue of this polymer which exhibited similar ferromagnetic behavior

supported the existence of organic ferromagnetism.[21] Independently, Torrance et al.[22] reported that some parts of black, insoluble polymers **9** obtained by the reaction of triaminobenzene with iodine showed ferromagnetic behavior in the relation between magnetic moments and magnetic field.

In 1989, Ohtani et al.[23] found that ferromagnetic polymers **10** were formed by dehydrogenation from triarylmethane resins by irradiation of UV light or laser light in the presence of a photooxidizing agent. This finding led to the idea that conjugated polymer chains were necessary for the occurrence of ferromagnetism. Recently, Tanaka et al.[24] prepared a polymer with an indigo unit in the main chain **11**, and reported that the resulting insoluble polymer contained the fraction which was attracted by a permanent magnet and showed a definitive hysteresis loop at room temperature.

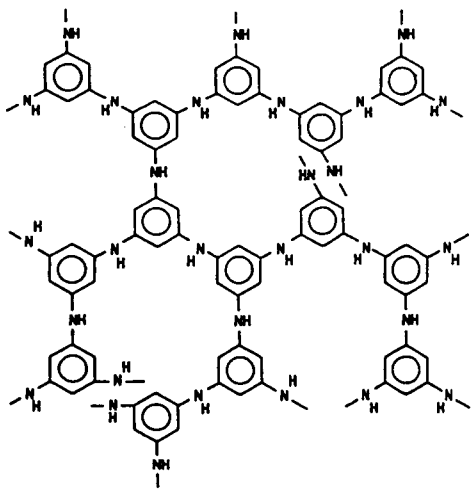

9

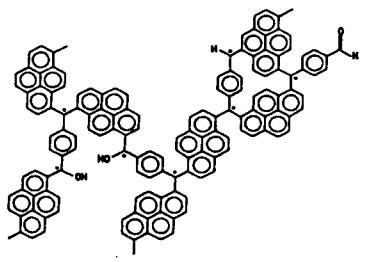

10

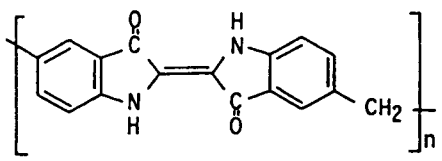

11

Based on the idea of Ovchinnikov, molecular designs for high-spin polymers have been attempted. Examples are shown in **1 2** and **1 3** [25,26].

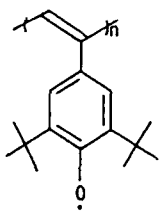

12

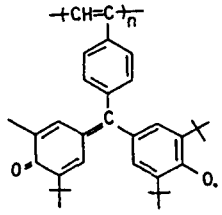

13

Tabata et al.[27] prepared high spin polymers by thermal annealing of polyphenylacetylene and its derivatives at 120°C. The concentration of radicals increased several orders of magnitude after thermal annealing, and the magnetic behavior suggests the presence of spin-glass. Recently, Murata et al.[28] found that carbon powder prepared by pyrolysis of a mixture of COPNA (condensed polynuclear aromatic) resin and activated carbon showed an apparent saturation magnetization and a hysteresis loop.

1.4. Historical Background of Magnetically Interacting Metalloporphyrin Polymers.

In the course of ESR study on polymers containing 2,2,6,6-tetramethylpiperidin-1-oxyl in their side chains, Kamachi et al.[29] came across the fact that an electron exchange interaction took place between the side chains. This phenomenon suggests the possibility that organic polymers containing paramagnetic species might be a new type of magnetic material owing to the magnetically long-range

ordering of unpaired electrons through a spin-spin interaction. On the basis of this idea, they investigated the temperature dependence of this magnetic susceptibility of polymethacrylate containing 2,2,6,6-tetramethylpiperidin-1-oxyl or verdazyl in their side chains, **14** or **15**. A weak antiferromagnetic interaction took place between the

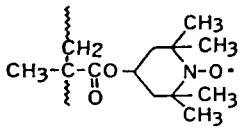

14

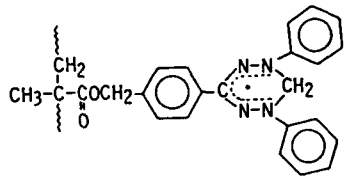

15

unpaired electrons of the polymers[29]. Since no magnetic interaction between unpaired electrons was found in the case of the corresponding monomer radical, it was concluded that a polymer effect was observed on the magnetic behavior of free radicals. However, the interaction is too weak to be paid attention as a magnetic material.

Usually, magnetism is caused by the spin-alignment due to an intermolecular exchange of electrons in d- or f-orbitals of metal ions. Accordingly, magnetic behavior of organic polymers containing paramagnetic metal ions has been paid attention as a new strategy for a polymer ferromagnet.

Kamachi et al.[6,7] prepared polymers containing TPP moieties, which had been considered to be an inhibitor for radical polymerization of the corresponding acrylic or methacrylic

compounds (AOTPP or MAOTPP), and found that the TPP moieties in the obtained polymers are forced to make some interaction due to their close approach. Accordingly, Kamachi et al. introduced paramagnetic metal ions (Cu(II), Ag(II), VO(II), and Co(III)) into TPP moieties (polyAOTPPM(X) **1 6** or polyMAOTPPM(X) **1 7**; M(X): Ag(II), VO(II), and Co(III)), and investigated their magnetic behavior.

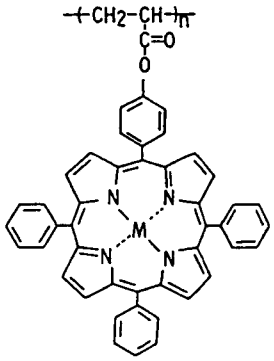

16

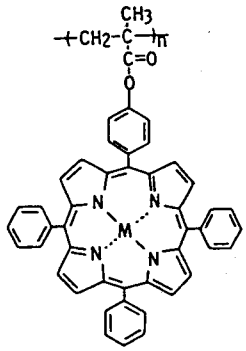

17

The measurement of magnetic susceptibility (X_M) of these polymers showed that paramagnetic species bound to polymer chains interact antiferromagnetically, and that the interaction is much larger than that of the corresponding monomer units.[9] Especially, an antiferromagnetic polymer was obtained in the case of AgTPP and the origin of the antiferromagnetic behavior has been ascribed to the superexchange interaction through the C=O group between Ag(II) ions.[6] They attempted to expand this study to polymers containing other paramagnetic ions. Rare earth metal ions Er(III) and Yb(III) were chosen instead of Ag(II) ions, because these ions have electrons

in the f-orbital and accordingly are considered to be effective for the occurrence of magnetic interaction.[10] The temperature dependence of X_M of AOTPPEr(III)OH showed a straight line through the origin, indicating that there is no magnetic interaction between AOTPPEr(II)OH molecules. Similar straight line was also observed in the case of polyAOTPPEr(III)OH, but a detailed study showed some deviation from AOTPPEr(III)OH below 5K: a weak ferromagnetic interaction was found below 5K. However, the magnetic interaction was much weaker than they expected. A copolymer containing both CuTPP and VOTPP moieties in their side chains was prepared by the radical copolymerization of CuAOTPP and VOAOTPP, whose metal ions have d^9 and d^1 configurations, respectively.[11] The temperature dependence of the magnetic susceptibility follows Curie-Weiss' law with θ=50K, indicating the existence of the ferromagnetic interaction between CuTPP and VOTPP moieties. Since polyCuAOTPP and polyVOAOTPP are respectively antiferromagnetic, the ferromagnetic interaction in the copolymer might be ascribed to the results of an interaction between CuTPP and VOTPP moieties located casually in the position suitable for the occurrence of long-range ferromagnetic interaction.

1.5. Photophysics and Photochemistry of Zincporphyrin

It is well-known that the primary process in photosynthesis involves a fast photoinduced electron transfer followed by an efficient charge separation. Magnesium-porphyrin moieties are

known to play an important role in such critical functions in photosynthetic system. Since magnesium complexes of porphyrins are not so stable, molecular understanding of the photochemical process has been indirectly investigated by photochemical system of zinc-porphyrin, which is more stable and more convenient in quantitative research. Therefore, a lot of fundamental data on photochemical behavior and photochemical reaction have been reported so far.[30] Forward and backward electron transfer reactions between zinc-porphyrin and quinones were studied from the point of molecular design of an artificial photosynthetic system.[31] The cation radicals prepared by electron transfer reactions from zincporphyrin moieties to electron acceptors has been detected by the photochemical reaction of a reaction system which is composed of zinctetra(pyridylmethyl)porphyrin ($ZnTMPyP^{4+}$) and methylviologen (MV^{2+}). This detection is ascribable to a charge repulsion between $ZnTMPyP^{5+}$. and MV^{+}..[32] On the contrary, no cation radical was detected by photochemical reaction of a reaction system of zinctetra(sufonylphenyl)porphyrin ($ZnTSPP^{4-}$)-MV^{2+}, because a backward electron transfer occurred rapidly between $ZnTSPP^{3-}$. and MV^{+}..[33] Electron repulsion seems to be important for the charge separation.

In recent years, much attention has been paid to the photophysical and photochemical processes of a hydrophobic chromophore bound to an amphiphilic polyelectrolyte, because a dramatic effect on the photophysical and photochemical behaviors of the chromophore has been brought about by the interfacial

electrostatic potential and/or the existence of microphase separation.

Morishima et al.[34] showed that photophysical and photochemical behavior of polycyclic aromatic chromophores such as phenanthrene and pyrene compartmentalized in amphiphilic polyelectrolyte were very different from those of homogeneous system: fast electron transfer occurred from compartmentalized photoexcited aromatics to methylviologen, while back electron transfer was considerably slowed, and thus charge separation was achieved. Porphyrins, which play a role in the photosystem, seems to be a good chromophore for the compartmentalized system. In this thesis, photophysical and photochemical behaviors of zinc-porphyrin compartmentalized in hydrophobic domain of amphiphilic polyelectrolytes were investigated.

1.6. Scope and Outline of This Thesis

In our laboratory, magnetic behavior of the polymers containing metallotetraphenylporphyrins has been studied.[6-11] But the phenyl groups of metallotetraphenylporphyrin are considered to hinder the stacking of the porphyrins because of their bulkiness. In order to obtain a stronger magnetic interaction, a distance between paramagnetic sites should be shortened and the order of the paramagnetic sites should be controlled. Chapter 2 describes the syntheses of monomers containing metalloporphyrins and their polymerizations. PolyCuAOMTPP and polyVOAOMTPP, in which the distances between main chain and metal center are shorter than

those in polyCuAOTPP and polyVOAOTPP which have been studied in our laboratory previously,[6] were prepared from TPP. Vinyl monomers containing etioporphyrin (Etio) and porphine (Por), which we expected to induce better stacking of the porphyrin moieties without the phenyl groups, were prepared. But homopolymers could not be obtained from these monomers. Polyamides containing diphenyletioporphyrin (DPE) in their main chains were prepared to study a magnetic interaction through amide bond, and to obtain a ferrimagnet in which two kinds of spins having magnetic moments of different magnitude are ordered antiparallel, as shown in Figure 2.

Previously, Morishima et al.[34] found that an amphiphilic polyelectrolyte having a sufficiently high mole fraction of bulky hydrophobic pendant groups forms a unimolecular micelle in dilute aqueous solution due to intramolecular self-organization of hydrophobic pendant groups. When a small mole fraction of hydrophobic chromophore is covalently incorporated into the amphiphilic polyelectrolyte, it is found to be encapsulated in the hydrophobic domain of the micelle, leading to the "compartmentalization" of the chromophore. In order to apply this compartmentalization to design photoinduced electron transfer system, amphiphilic polyelectrolytes with zinctetraphenylporphyrin (ZnTPP) as a chromophore were prepared.

In Chapter 3, magnetic behavior of the polymers studied by using an ESR spectrometer and a magnetic balance is described. The polyamides prepared from DPEs, which we expected the ferrimagnetism, had only very weak antiferromagnetic interaction.

PolyVOAOMTPP consists of two different magnetic parts, which are magnetoactive and magnetoinactive. ESR spectra of the magnetoactive part suggest that a ferromagnet exists in part. The temperature dependence of the effective magnetic moment of magnetoinactive part shows that the ferromagnetic interaction occurs between the vanadyl sites.

In Chapter 4, photophysical behavior of amphiphilic polyelectrolytes containing ZnTPP was studied by absorption, fluorescence, phosphorescence, and transient absorption spectra. ZnTPP moieties of the amphiphilic polyelectrolytes were compartmentalized in their hydrophobic microdomains in water. Lifetimes of the triplet state of compartmentalized ZnTPP were much longer than that of ZnTPP that was not compartmentalized. Phosphorescence and thermally activated delayed fluorescence of ZnTPP moieties were found, for the first time, in solution at room temperature.

In Chapter 5, photoinduced electron transfer from the compartmentalized ZnTPP to MV^{2+} is described. The formation of grand state charge transfer (CT) complexes was hindered by compartmentalization, rate constants of electron transfers (ET) from excited compartmentalized ZnTPP to MV^{2+} were estimated. Accumulations of photoproducts, $ZnTPP^{+\cdot}$ and $MV^{+\cdot}$, were found in the microsecond time region in the compartmentalized systems.

In Chapter 6, photoinduced electron transfer from the compartmentalized ZnTPP to phenylmethylphenacylsulfonium p-toluenesulfonate (PMPS), which is an irreversible electron acceptor, is

described. $ZnTPP^{+\cdot}$ moieties in the compartmentalized systems were detected by laser photolysis, visible spectra, and ESR measurements. The naphthyl and cyclododecyl groups were effective to accumulate $ZnTPP^{+\cdot}$ which persisted over 20 min.

Chapter 7 is the summary of this thesis.

References

1) *The Porphyrins* ; Dolphin, D., Ed.; Academic Press: New York, 1978.

2) *Porphyrins and Metalloporphyrins* ; Smith, K. M., Ed.; Elsevier Scientific Publishing: Amsterdam, 1975.

3) Ferguson-Miller, S.; Brautigan, D. L.; Margoliash, E. The electron transfer function of cytochrome c. In *The Porphyrins* ; Dolphin, D., Ed.; Academic Press: New York, 1979; Vol. VII, pp 149.

4) Hewson, E.; Hager, L. P. Peroxidases, catalases, and chloroperoxidase. In *The Porphyrins* ; Dolphin, D., Ed.; Academic Press: New York, 1979; Vol. VII, pp 295.

5) Tsuchida, E.; Nishide, H.; Ohyanagi, M.; Okada, O. *J. Phys. Chem.* **1988**, *92*, 6461.

6) Kamachi, M.; Akimoto, H.; Mori, W.; Kishita, M. *Polym. J.* **1984**, *16*, 23.

7) Kamachi, M.; Cheng, X. S.; Kida, T.; Kajiwara, A.; Shibasaka, M.; Nagata, S. *Macromolecules* **1987**, *20*, 2665.

8) Kajiwara, A.; Kamachi, M. *Polym. J.* **1989**, *21*, 593.

9) Nozakura, S.; Kamachi, M. *Makromol. Chem. Suppl.* **1985**, *12*, 255

10) Kamachi, M.; Cheng, X. S.; Nozakura, S. *Fifth Rare Earth Symposium.* (Tokyo, 1987), Preprints 2B05.

11) Kamachi, M.; Cheng, X. S.; Aota, H.; Mori, W.; Kishita, M. *Chem. Lett.* **1987**, 2331.

12) Yoshida, K. *Jisei*; Asakura: Tokyo, 1972

13) Itoh, K. *Chem. Phys. Lett.* **1967**, 235.

14) Wasserman, E.; Murray, R. W.; Yager, W. A.; Trozzolo, A. M.; Smolynsky, G. *J. Am. Chem. Soc.* **1967**, *89*, 5076.

15) Mataga, N. *Theor. Ghem. Acta.* **1968**, *10*, 372.

16) Teki, Y.; Takui, T.; Itoh, K.; Iwamura, H.; Kobayashi, K. *J. Am. Chem. Soc.* **1986**, *108*, 2147.

17) Iwamura, H. *Pure & Appl. Chem.* **1986**, *58*, 187.

18) Ovchinnikov, A. A. *Dokl. Nauk. Acad. USSR.* **1977**, *236*, 957.

19) Miller, J. S.; Epstein, A. J.; Reiff, W. M. *Chem. Rev.* **1988**, *88*, 201.

20) Korshak, Y. U.; Medvedeva, T. V.; Ovchinnikov, A. A.; Spektor, V. N. *Nature* **1987**, *325*, 370.

21) Cao, Y. et al. *Solid State Comm.* **1988**, *68*, 817.

22) Torrance, J. B.; Costra, S.; Nazzal, A. *Synth. Metal* **1987**, *19*, 709.

23) Ohta, M.; Otani, S. *Chem. Lett.* **1989**, 1179.

24) Tanaka, H.; Tokuyama, K.; Sato, T.; Ota, T. *Chem. Lett.* **1990**, 1813.

25) Yoshioka, T.; Nishide, H.; Tsuchida, E. *Macromolecules* **1988**, *21*, 3119.

26) Yoshioka, T.; Nishide, H.; Tsuchida, E. *Polym Preprint Jpn* **1989**, *38*, 2108.

27) Tabata, M. *Kobunshi* **1990**, *39*, 359.

28) Murata, K.; Masuda, T.; Ueda, H. *Chemistry Express* **1990**, *8*, 597.

29) Kamachi, M.; Tamaki, Y.; Morishima, Y.; Nozakura, S.; Mori, W.; Kishita, M. *Polym. J.* **1982**, *14*, 363.

30) (a) Mosseri, S.; Mialocq, J. C.; Perly, B.; Hambright, P. *J. Phys. Chem.* **1991**, *95*, 2196. (b) Davila, J.; Harriman, A. *J. Am. Chem. Soc.* **1990**, *112*, 2686. (c) Neta, P.; Harriman, A. *J. Chem. Soc., Faraday Trans. 2* **1985**, *81*, 123. (d) Richoux, M.-C.; Harriman, A. *J. Chem. Soc., Faraday Trans. 1* **1982**, *78*, 1873. (e) Kalyanasundaram, K. *J. Chem. Soc., Faraday Trans. 2* **1983**, *79*, 1365.

31) (a) Harriman, A.; Porter, G.; Searle, N. *J. Chem. Soc., Faraday Trans. 2* **1979**, *75* 1515. (b) Kong, J. L. Y.; Spears, K. G.; Loach, P. A. Photochem. Photobiol. 1982, 35, 545. (c) Osuka, A.; Maruyama, K.; Mataga, N.; Asahi, T.; Yamazaki, I.; Tamai, N.; Nishimura, Y. *Chem. Phys. Lett.* **1991**, *181*, 413.

32) (a) Harriman, A.; Porter, G.; Richoux, M.-C. *J. Chem. Soc., Faraday Trans. 2* **1981**, *77*, 833. (b) Harriman, A.; Porter, G.; Richoux, M.-C. *J. Chem. Soc., Faraday Trans. 2* **1982**, *78*, 1955.

33) (a) Harriman, A.; Richoux, M.-C. *J. photochem.* **1980**, *14*, 253. (b) Harriman, A.; Richoux, M.-C. *J. Chem. Soc., Faraday Trans. 2* **1980**, *76* 1618.

34) (a) Morishima, Y.; Itoh, Y.; Nozakura, S. *Makromol. Chem.* **1981**, *182*, 3135. (b) Morishima, Y.; Kobayashi, T.; Nozakura, S. *J. Phys. chem.* **1985**, *89*, 4081. (c) Morishima, Y.; Kobayashi, T.; Furui, T.; Nozakura, S. *Macromolecules* **1987**, *20*, 1707. (d) Morishima,

Y.; Kobayashi, T.; Nozakura, S. *Polym. J.* **1989**, *21*, 267. (e) Morishima, Y.; Furui,T.; Nozakura, S.; Okada, T.; Mataga, N. *J. Phys. chem.* **1989**, *93*, 1643. (f) Morishima, Y. *Prog. Polym. Sci.* **1990**, *15*, 949. (g) Morishima, Y.; Tominaga, Y.; Kamachi, M.; Okada, T.; Hirata, Y.; Mataga, N. *J. Phys. chem.* **1991**, *95*, 6027. (h) Morishima, Y.; Tominaga, Y.; Nomura, S.; Kamachi, M. *Macromolecules* **1992**, *25*, 861. (i) Morishima, Y.; Tsuji, M.; Kamachi, M.; Hatada, K. *Macromolecules* **1992**, *25*, 4406.

Chapter 2

Syntheses of Monomers Containing Metalloporphyrins and Their Polymerizations

2.1. Introduction

Before 1983, several studies had been reported on the preparation of polymers containing porphyrin moieties.[1-6] These polymers were prepared by polymer reaction with porphyrin derivatives,[1,2] the copolymerization of protoporhyrin derivatives or heme derivatives[3-6] with vinyl monomers, and condensation polymerization of esters and amines containing porphyrin moieties.[5] Kamachi et al.[7-11] have firstly succeeded in the preparation of high homopolymers by radical polymerization of vinyl monomers containing porphyrin moieties, which had been considered to be an inhibitor for radical polymerization, in their side chain, and investigated magnetic properties of paramagnetic metalloporphyrin. They found that the polymer containing AgTPP had a strong antiferromagnetic interaction[7] and the copolymer containing CuTPP and VOTPP had a ferromagnetic interaction.[11] In order to obtain a stronger magnetic interaction, the distance between paramagnetic sites should be shorten and the order of the paramagnetic sites should be controlled. This Chapter describes the syntheses of monomers containing metalloporphyrins which are based on tetraphenylporphyrin (TPP), etioporphyrin (Etio), porphine (Por), and diphenyletioporphyrin (DPE), and polymerizations of the monomers. Moreover, amphiphilic polyelectrolytes, which have a sufficiently high mole fraction of bulky hydrophobic pendant groups and a small amount of zincporphyrin derivatives, are prepared to study the photophysical and photochemical behaviors.

2,2. Nomenclature

Several types of nomenclature are used for porphyrin derivatives.[12] In this Chapter, the nomenclature of porphyrin compounds is used according to the IUPAC rules, e.g., tetraphenylporphyrin (TPP) and zinctetraphenylporphyrin (ZnTPP) are named 5,10,15,20-tetraphenylporphine and (5,10,15,20-tetraphenylporphyrinato)zinc(II), respectively.

2,3. Syntheses of Monomers Containing Metallo-porphyrins

2,3,1. Vinyl Monomers

2,3,1,a. (2-Acryloyloxymethylene-5,10,15,20-tetraphenyl-porphyrinato)oxovanadium(IV) **(VOAOMTPP)**

Synthetic pathway of VOAOMTPP is shown in Scheme I.

5,10,15,20-Tetraphenylporphine **(TPP)** was prepared from benzaldehyde and pyrrole according to the method of Adler et al.[13]

Oxo(5,10,15,20-Tetraphenylporphyrinato)vanadium(IV) **(VOTPP)** was prepared in a 86% yield by refluxing a solution of 32 g of TPP and 50 g of vanadium (IV) oxide sulfate in a mixed solvent of 2.5 L of N,N-dimethylformamide (DMF) and 300 mL of acetic acid for 27 h. A crude product was obtained by removal of solvents, dissolved again in chloroform, and chromatographed on a silica gel column using chloroform as an eluent.

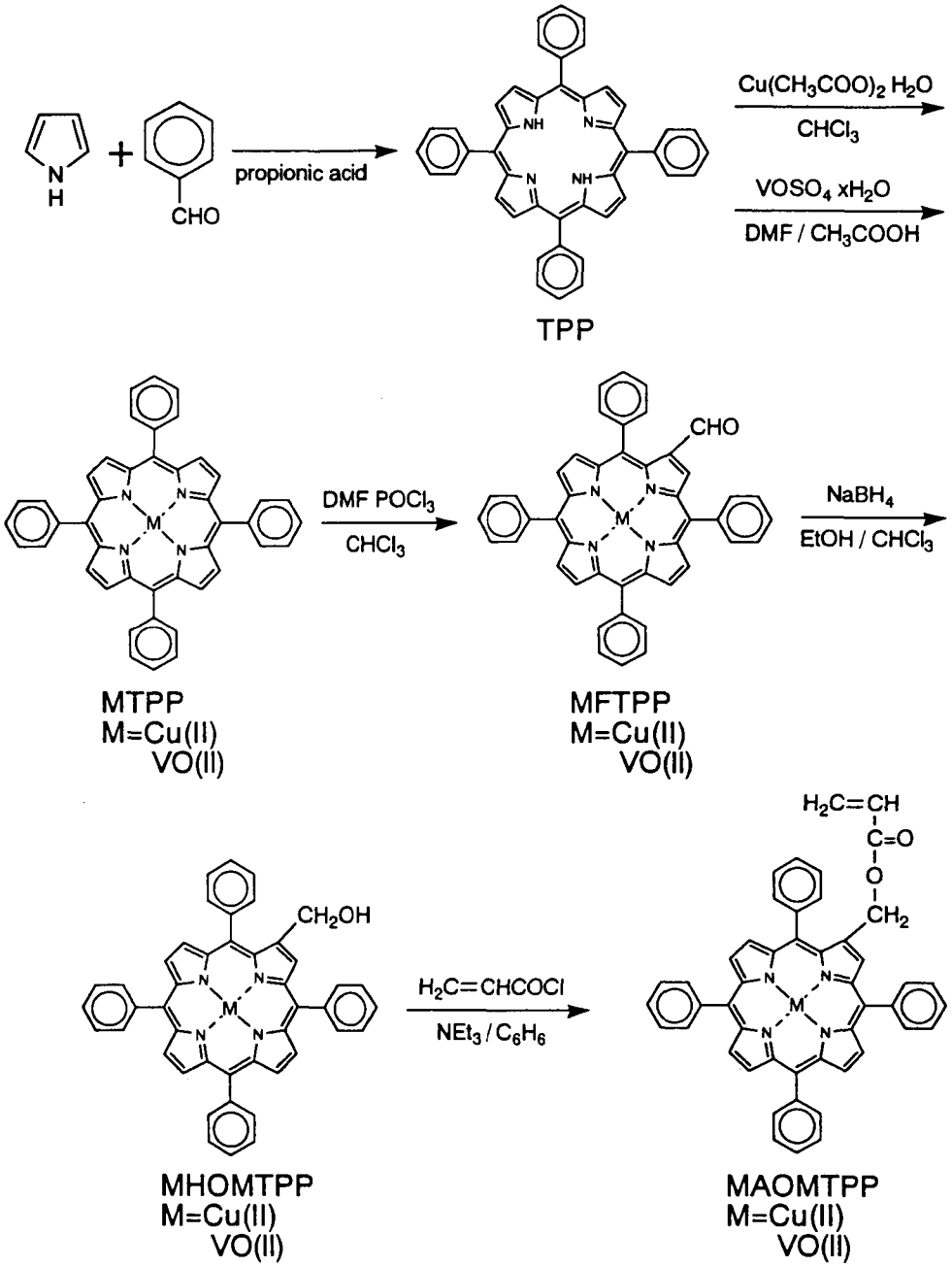
propionic acid
TPP
$Cu(CH_3COO)_2\ H_2O$
$CHCl_3$
$VOSO_4\ xH_2O$
DMF / CH_3COOH
DMF $POCl_3$
$CHCl_3$
$NaBH_4$
$EtOH / CHCl_3$
MTPP
M=Cu(II)
VO(II)
MFTPP
M=Cu(II)
VO(II)
$H_2C{=}CHCOCl$
NEt_3 / C_6H_6
MHOMTPP
M=Cu(II)
VO(II)
MAOMTPP
M=Cu(II)
VO(II)

Scheme I

(2-Formyl-5,10,15,20-tetraphenylporphyrinato)-oxovanadium(IV) (**VOFTPP**) was prepared using Vilsmeier reaction. Vilsmeier reagent was prepared by mixing phosphoryl chloride with DMF according to the literature.[14] A solution of 8.0 g of VOTPP in 1.2 L of chloroform was added to the Vilsmeier reagent, and then the mixture was refluxed for 3 h. After cooling, a solution of 500 g of sodium acetate in 1 L of water was added to the reaction mixture, and then refluxed for 2 h. The chloroform layer was concentrated, and chromatographed on a silica gel column using chloroform as an eluent. VOFTPP was isolated in 60% yield by removal of the solvent from the second fraction and recrystallized from benzene. Anal. Calcd for $C_{45}H_{28}N_4O_2V$: C, 76.38; H, 3.99; N, 7.92%. Found: C,76.05; H,4.05; N,7.88%.

(2-Hydroxmethyl-5,10,15,20-tetraphenylporphyrinato)-oxovanadium(IV) (**VOHOMTPP**) was prepared as follows: a suspension of 2.0 g of sodium borohydride in 150 mL of ethanol was added to a solution of 6.0 g of VOFTPP in 1 L of chloroform with stirring at room temperature. After 10 min, the reaction mixture was filtered to remove excess sodium borohydride. The filtrate was washed with water and dried over magnesium sulfate. VOHOMTPP was quantitatively isolated by removal of the solvent.

VOAOMTPP was prepared as follows: 10 mL of acryloyl chloride was added dropwise to a solution of 6.0 g of VOHOMTPP and 20 mL of triethylamine in 300 mL of benzene with stirring at room temperature. After 1 h, the reaction mixture was filtered to remove triethylammonium chloride. The filtrate was evaporated, and the

residue was dissolved in benzene and chromatographed on a silica gel column using benzene as an eluent. VOAOMTPP was isolated by removal of solvent from the second fraction, and recrystallized from benzene-hexane: yield 60%. Anal. Calcd for $C_{48}H_{32}N_4O_3V$: C, 75.49; H, 4.22; N, 7.34; V, 6.67%. Found: C,75.23; H,4.31; N,7.30; V, 6.54%. IR spectrum is shown in Figure 1-a.

2 , 3 , 1 , b . (2-Acryloyloxymethylene-5,10,15,20-tetraphenylporphyrinato)copper(II) **(CuAOMTPP)**

CuAOMTPP was prepared by a method similar to the preparation of VOAOMTPP. Anal. Calcd for $C_{48}H_{32}N_4O_2Cu$: C, 75.82; H, 4.24; N, 7.37; Cu, 8.36%. Found: C,76.11; H,4.41; N,7.23; Cu, 8.16%.

2 , 3 , 1 , c . [5-(4-Acrylamidophenyl)-10,15,20-triphenylporphyrinato]zinc(II) **(ZnAATPP)**

Synthetic pathway of ZnAATPP is shown in Scheme II.

5-(4-Nitrophenyl)-10,15,20-triphenylporphine **(NO_2TPP)** and 5-(4-Aminophenyl)-10,15,20-triphenylporphine **(NH_2TPP)** were synthesized according to the literature.[15)]

[5-(4-Aminophenyl)-10,15,20-triphenylporphyrinato]zinc(II) **(ZnNH_2TPP)** was synthesized by the following method. To a 250 mL of tetrahydrofuran (THF) solution containing 2.50 g (3.97 mmol) of NH_2TPP was added 5.0 g (19 mmol) of zinc acetylacetonate. The solution was refluxed for 1 h, and concentrated to a-tenth of its original volume followed by an addition of 600 mL of methanol. The mixture was allowed to stand overnight at 0°C. Resulting crystals were collected and washed with methanol and dried to give 2.2 g (78%) of ZnNH_2TPP.

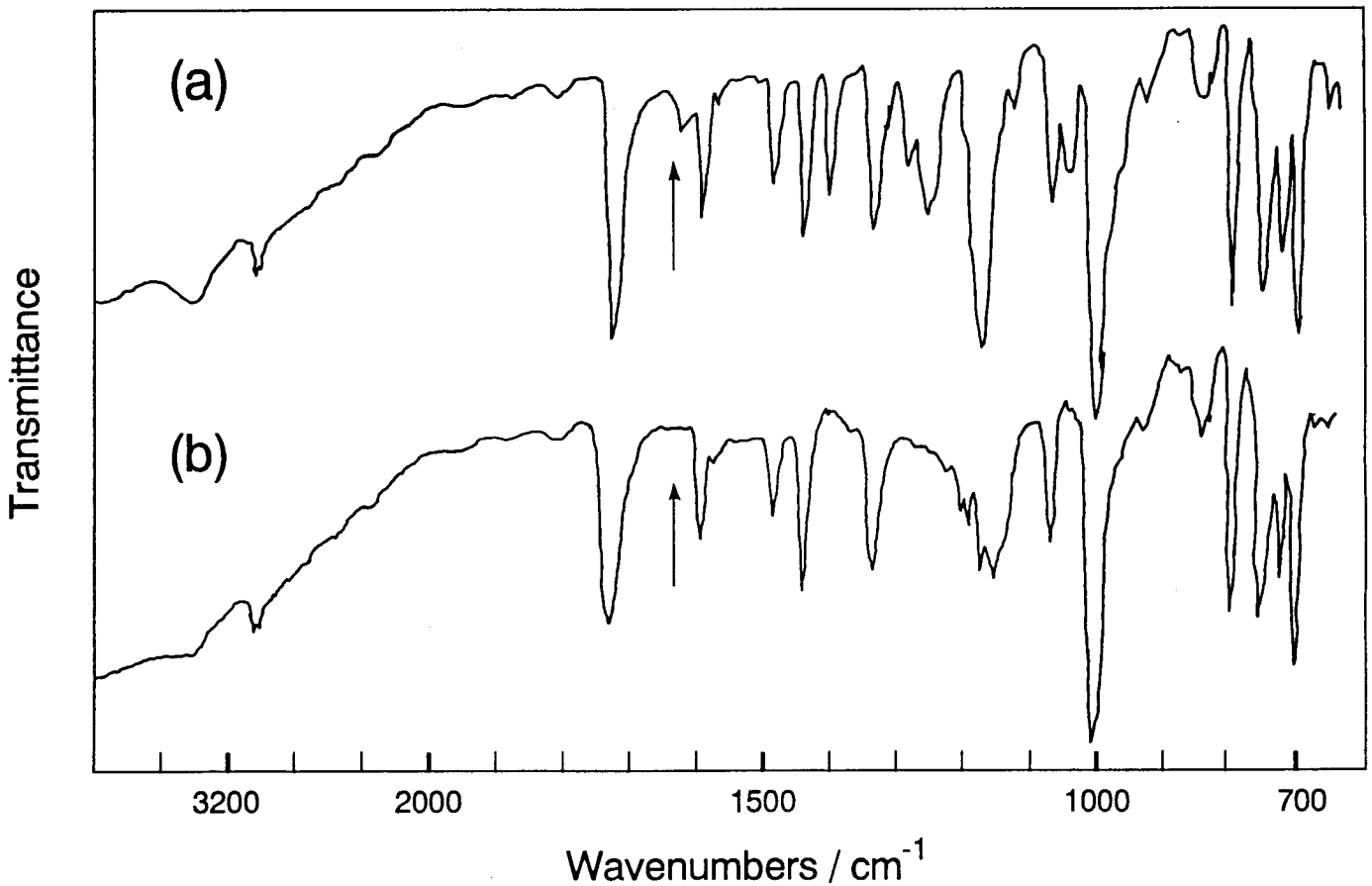

Figure 1. IR spectra of VOAOMTPP (**a**) and polyVOAOMTPP (**b**)

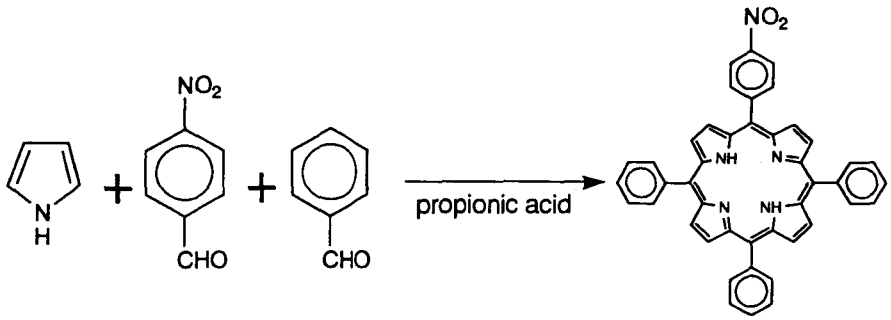
NO2
CHO
CHO
propionic acid
NO2TPP

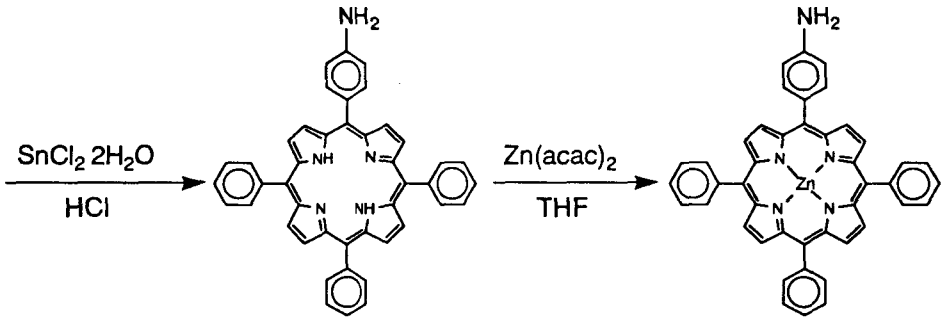
NH2
SnCl2 2H2O
HCl
Zn(acac)2
THF
NH2TPP
ZnNH2TPP

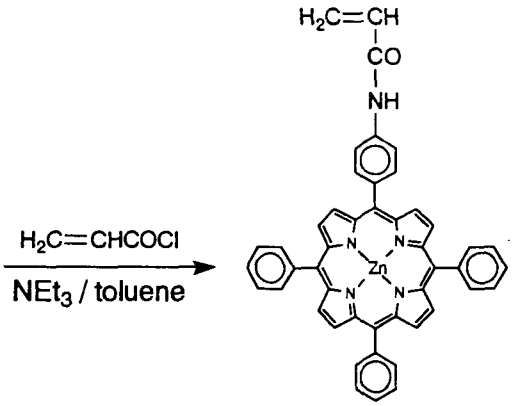
H2C=CH
CO
NH
H2C=CHCOCl
NEt3 / toluene
ZnAATPP

Scheme II

ZnAATPP was synthesized as follows: a solution of 2.5 mL (3.1 mmol) of acryloyl chloride in 50 mL of toluene was added to a solution of 2.2 g (3.1 mmol) of $ZnNH_2TPP$ and 5 mL (36 mmol) of triethylamine in 1 L of toluene with stirring at 15°C. The reaction mixture was heated at 25°C for 10 min, and then 50 mL of methanol was added. The reaction mixture was filtered to remove triethylammonium chloride, and the filtrate was washed with 5% of aqueous sodium hydrogen carbonate and dried over anhydrous sodium sulfate. A crude product was obtained by removal of the solvent, chromatographed on a silica gel column using toluene-methanol (9/1:v/v) as an eluent. ZnAATPP was isolated by removal of the solvent, and recrystallized from benzene-acetone (4/1:v/v): yield 0.95 g (1.3 mmol, 32%). NMR (DMSO-d_6) δ 5.84 (d, 1H, vinyl), 6.45-6.63 (m, 2H, vinyl), 7.77-7.89 (m, 11H, phenyl), 8.13-8.21 (m, 8H, phenyl), 8.77-8.82 (m, 8H, pyr), 10.57 (s, 1H, NHCO); IR (KBr) 1632cm^{-1} (C=C), 1658cm^{-1} (C=O); MS m/e 745.3. Anal. Calcd for $C_{47}H_{31}N_5OZn$: C, 75.55; H, 4.18; N, 9.37%. Found: C,75.09; H,4.35; N,9.25%. Visible spectrum in DMF is shown in Figure 1-a in Chapter 4.

2 , 3 , 1 , d . (5-Acrylamido-2,7,12,17-tetraethyl-3,8,13,18-tetramethylporphyrinato)zinc(II) **(ZnAAEtio)**

Synthetic pathway of ZnAAEtio is shown in Scheme III.

2,7,12,17-tetraethyl-3,8,13,18-tetramethylporphine **(Etio)** was prepared from ethylacetoacetate, sodium nitrite and acetylacetone according to synthetic methods of octaethylporphine reported by Inhoffen et al.[16]. Anal. Calcd for $C_{32}H_{38}N_4$: C, 80.29; H, 8.00; N,

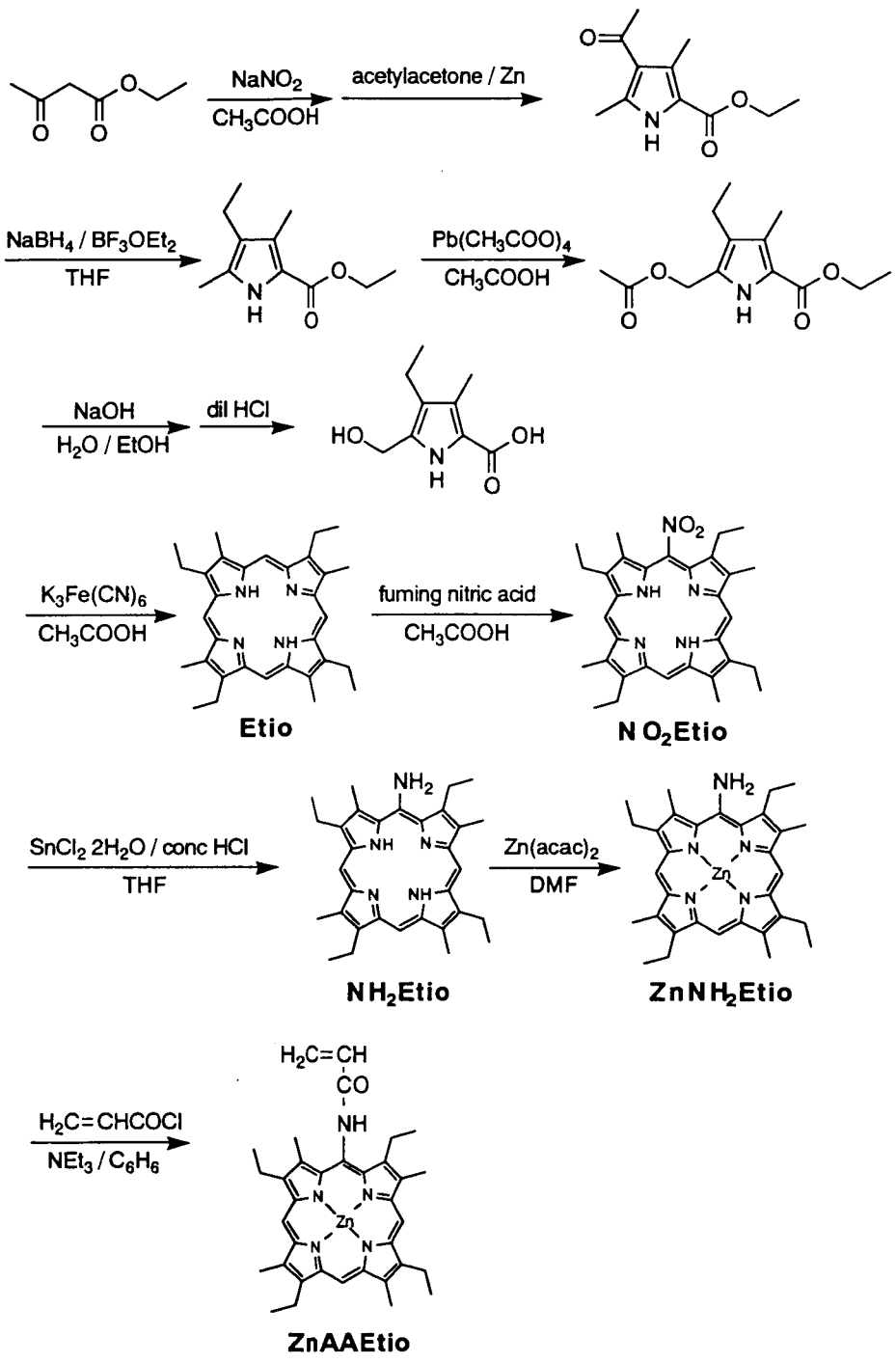
NaNO2
CH3COOH
acetylacetone / Zn
NaBH4 / BF3OEt2
THF
Pb(CH3COO)4
CH3COOH
NaOH
H2O / EtOH
dil HCl
K3Fe(CN)6
CH3COOH
fuming nitric acid
CH3COOH
Etio
NO2Etio
SnCl2 2H2O / conc HCl
THF
Zn(acac)2
DMF
NH2Etio
ZnNH2Etio
H2C=CHCOCl
NEt3 / C6H6
ZnAAEtio

Scheme III

11.70%. Found: C,80.30; H,7.89; N,11.66%.

2,7,12,17-tetraethyl-3,8,13,18-tetramethyl-5-nitroporphine (**NO_2Etio**) was prepared from Etio according to the manner similar to a preparation of 5-nitrooctaethylporphine [17] from octaethylporphine with some modification: a suspension of 19.46 g (40.7 mmol) of Etio in 500 mL of acetic acid was added rapidly to an ice-cold mixture of 1 L of fuming nitric acid and 500 mL of acetic acid with stirring. The reaction mixture was stirred for 3 min, and then poured into 7 L of ice water. A precipitate was filtered off , and washed with an aqueous sodium acetate, water, and dried *in vacuo*. NO_2Etio was recrystallized from toluene: yield 15.76 g (30.1 mmol, 74%).

5-Amino-2,7,12,17-tetraethyl-3,8,13,18-tetramethylporphine (**NH_2Etio**) was prepared as follows: a solution of 19.3 g (36.9 mmol) of NO_2Etio in 2 L of THF was added to a solution of 83.25 g (369 mmol) of tin(II) chloride dihydrate in 500 mL of conc. HCl at 10-20°C. The reaction mixture was stirred for 2 h at room temperature, and then neutralized with aqueous sodium hydroxide. An organic layer was separated, the solvent was evaporated, and the residue was dried *in vacuo*. NH_2Etio was recrystallized from toluene: yield 9.55 g (19.3 mmol, 52%). Anal. Calcd for $C_{32}H_{39}N_5$: C, 77.85; H, 7.96; N, 14.19%. Found: C,77.46; H,7.91; N,13.84%.

(5-Amino-2,7,12,17-tetraethyl-3,8,13,18-tetramethyl-porphyrinato)zinc(II) (**ZnNH_2Etio**) was prepared as follows: 2.00 g (4.05 mmol) of NH_2Etio was added to a solution of zinc acetylacetonate in 100 mL of DMF. The mixture was heated at 60°C for 3 h, and then poured into 200 mL of water. A crude product was

separated by filtration, washed with methanol, and recrystallized from 80 mL of toluene: yield 1.10 g (1.97 mmol, 49%). Anal. Calcd for $C_{32}H_{39}N_5Zn$: C, 69.00; H, 6.69; N, 12.57%. Found: C,69.10; H,6.72; N,12.50%

ZnAAEtio was synthesized as follows: a solution of 5 mL (62.7 mmol) of acryloyl chloride in 50 mL of toluene was added to a solution of 3.50 g (6.28 mmol) of $ZnNH_2Etio$ in 1 L of toluene containing 10 mL (72 mmol) of triethylamine with stirring at 15°C. The reaction mixture was stirred for 10 min, and then 50 mL of methanol was added to the mixture. The solution was filtered and the filtrate was washed with 3% of an aqueous sodium hydrogencarbonate, dried over sodium sulfate. A crude product was obtained by removal of the solvent, chromatographed on a silica gel column using toluene-acetone (10/1:v/v) as an eluent. ZnAAEtio was isolated by removal of the solvent, and recrystallized from toluene: yield 0.754 g (1.23 mmol, 20%). NMR (DMSO-d_6) δ 1.78-1.84 (m, 12H, CH_2CH_3), 3.43 (s, 3H, pyr-CH_3), 3.61 (s, 9H, pyr-CH_3), 4.12 (q, 8H, pyr-CH_2-Me), 6.16 (d, 1H, vinyl), 6.65 (d, 1H, vinyl), 7.16 (q, 1H, vinyl), 10.08 (s, 3H, *meso*), 11.70 (s, 1H, NHCO); IR (KBr) 1610cm^{-1} (C=C), 1654cm^{-1} (C=O); MS m/e 610 (M+1). Anal. Calcd for $C_{35}H_{39}N_5OZn$: C, 68.79; H, 6.43; N, 11.46%. Found: C,68.91; H,6.42; N,11.37%

2,3,1,e. (5-Acrylamido-2,7,12,17-tetraethyl-3,8,13,18-tetramethylporphyrinato)copper(II) **(CuAAEtio)**

CuAAEtio was prepared by the method similar to ZnAAEtio. IR (KBr) 1610cm^{-1} (C=C), 1654cm^{-1} (C=O); Anal. Calcd for $C_{35}H_{39}N_5OCu$: C, 69.00; H, 6.45; N, 11.49%. Found: C,69.09; H,6.38; N,11.47%

2,3,1,f. (5-Acrylamidoporphyrinato)zinc(II) **(ZnAAPor)**

Synthetic pathway of ZnAAPor is shown in Scheme IV.

2-Formylpyrrole[18] and 2-hydroxymethylpyrrole[19] were prepared according to the literatures.

Porphine was prepared from 2-hydroxymethylpyrrole by modifying the procedure of Longo et al.[20] as follows: 2.5 L of xylene was maintained at 125°C and oxygen gas was added slowly. A solution of 4.00 g (41.2 mmol) of 2-hydroxymethylpyrrole in 500 mL of xylene was added about 30 h to the heated xylene under oxygen atmosphere. After 15 h from complete addition, the reaction mixture was filtered. A crude porphine was obtained by removal of solvent from the filtrate, chromatographed on a silica gel column using benzene as an eluent, and recrystallized from benzene: yield 190 mg (0.60 mmol,5.8%).

5-Nitroporphine **(NO_2Por)** was prepared according to the literature.[21]

5-Aminoporphine **(NH_2Por)** was synthesized as follows: a solution of 4.0 g (18 mmol) of tin(II) chloride in 6 mL of conc. HCl was added rapidly to a suspended solution of 0.40 g (1.1 mmol) of NO_2Por in 40 mL of conc. HCl at 0-5°C. The reaction mixture was stirred for 1 h, poured into 200 mL of ice water, and then neutralized with aqueous sodium hydroxide. The crude product was separated by filtration, washed with methanol, and dried *in vacuo*: yield 0.23 g.

(5-Aminoporphyrinato)zinc(II) **(ZnNH_2Por)** was prepared as follows: a solution of 0.21 g (0.65 mmol) of NH_2Por and 0.30 g (1.1 mmol) of zinc(II) acetylacetonate in 50 mL of THF was refluxed for 2

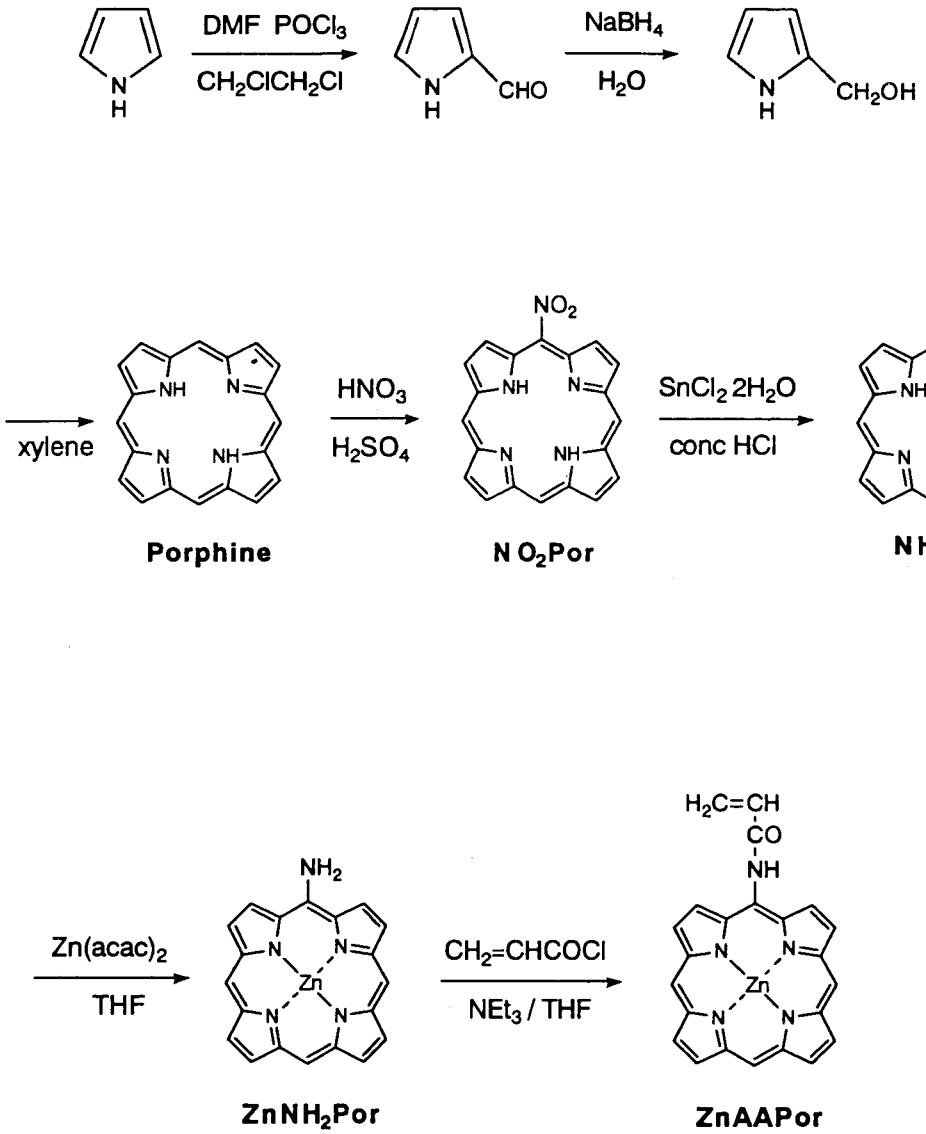
DMF POCl3
CH2ClCH2Cl
NaBH4
H2O
CHO
CH2OH
xylene
HNO3
H2SO4
SnCl2 2H2O
conc HCl
NO2
NH2
Porphine
NO2Por
NH2Por
Zn(acac)2
THF
CH2=CHCOCl
NEt3 / THF
H2C=CH
CO
NH
ZnNH2Por
ZnAAPor

Scheme IV

h. The solvent was removed *in vacuo*, the residue was dissolved in a mixed solvent of 50 mL of THF and 100 mL of chloroform, and then insoluble part was filtered off. A crude product was obtained by removal of the solvent from the filtrate, and dried *in vacuo*.

ZnAAPor was prepared as follows: the crude $ZnNH_2Por$ and 10 mL (7.2 mmol) of triethylamine was dissolved in 50 mL of THF, and cooled in an ice water bath. 0.50 mL (6.2 mmol) of acryloyl chloride was added dropwise to the THF solution. After 5 min, 20 mL of methanol was added, the reaction mixture was filtered. A crude product was obtained by removal of the solvent from the filtrate, chromatographed on a silica gel column using toluene-acetone (4/1:v/v) as an eluent. ZnAAPor was isolated by removal of the solvent, and recrystallized from THF-toluene: yield 64 mg (0.14 mmol, 22% from NH_2Por). NMR (DMSO-d_6) δ 6.19 (d, 1H, vinyl), 6.70 (d, 1H, vinyl), 7.28 (q, 1H, vinyl), 9.50-9.58 (m, 8H, pyr), 10.34 (s, 3H, *meso*), 12.14 (s, 1H, NHCO); IR (KBr) 1614cm^{-1} (C=C), 1650cm^{-1} (C=O); MS m / e 444.0 (M, Zn=68). Anal. Calcd for $C_{23}H_{15}N_5OZn$: C, 62.39; H, 3.41; N, 15.82%. Found: C,62.14; H,3.56; N,15.49% .

2,3,2. Metallodiphenyletioporphyrin Monomers for Condensation Polymerization

Synthetic pathway of metallodiphenyletioporphyrins is shown in Scheme V-1 and V-2.

2,8,12,18-Tetraethyl-5,10-bis(4-methoxycarbonylphenyl)-3,7,13,17-tetramethylporphine (**CH_3OCODPE**) and 2,8,12,18-tetraethyl-3,7,13,17-tetramethyl-5,10-bis(4-nitrophenyl)porphine

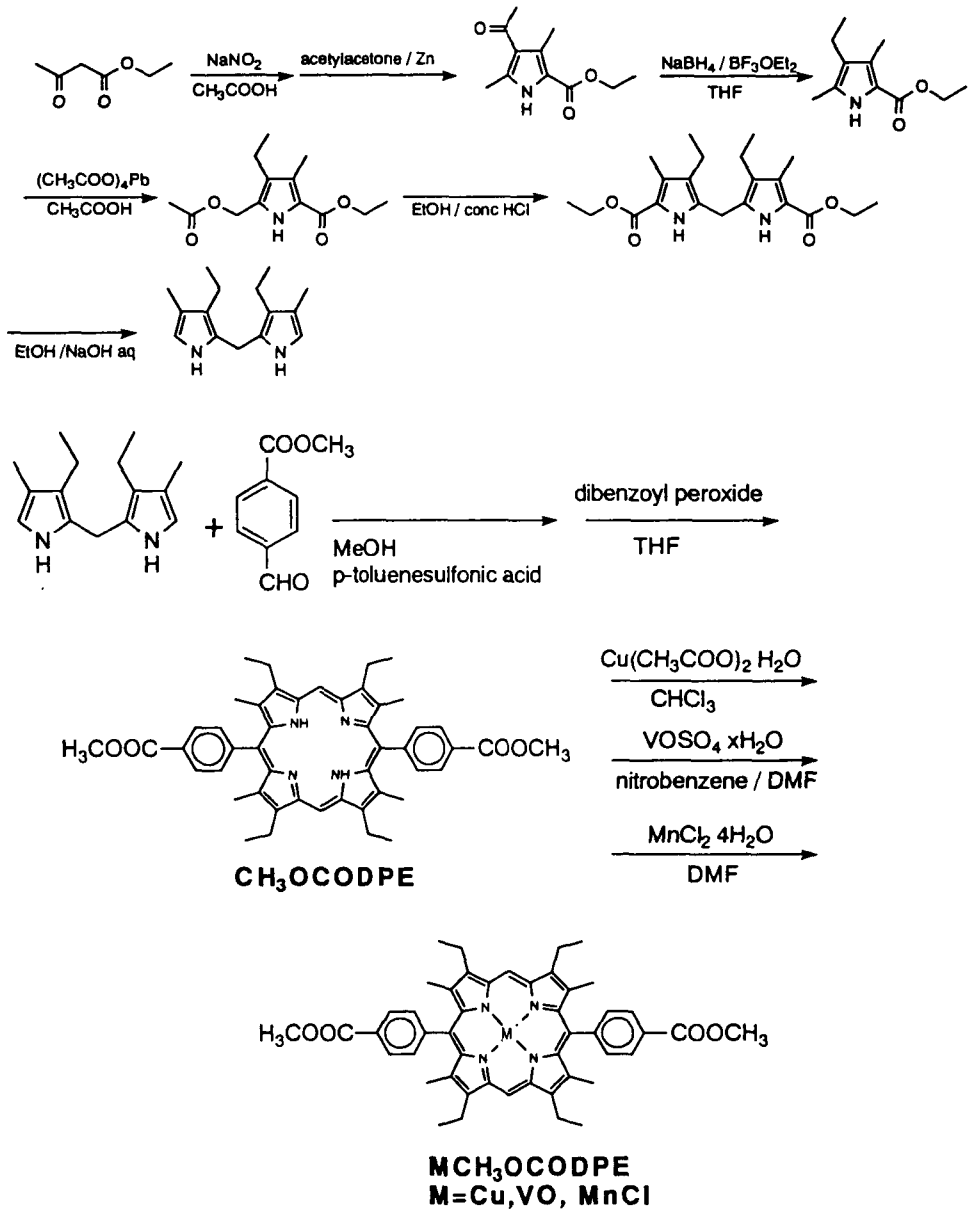
NaNO2
CH3COOH
acetylacetone / Zn
NaBH4 / BF3OEt2
THF
(CH3COO)4Pb
CH3COOH
EtOH / conc HCl
EtOH /NaOH aq
COOCH3
CHO
MeOH
p-toluenesulfonic acid
dibenzoyl peroxide
THF
Cu(CH3COO)2 H2O
CHCl3
VOSO4 xH2O
nitrobenzene / DMF
MnCl2 4H2O
DMF
H3COOC
COOCH3
CH3OCODPE
MCH3OCODPE
M=Cu,VO, MnCl

Scheme V-1

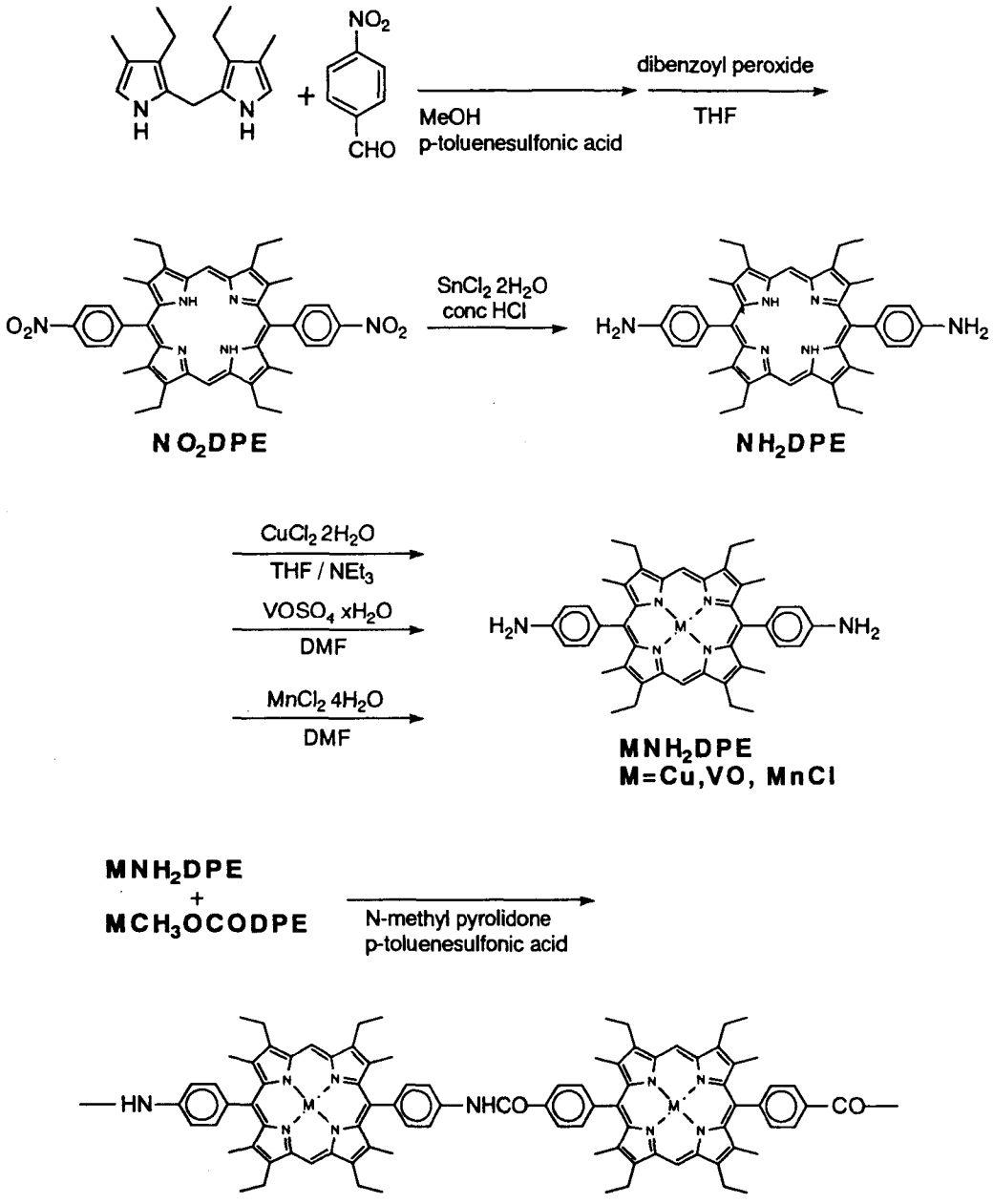
NO2
CHO
MeOH
p-toluenesulfonic acid
dibenzoyl peroxide
THF
O2N
NO2
SnCl2 2H2O
conc HCl
H2N
NH2
NO2DPE
NH2DPE
CuCl2 2H2O
THF / NEt3
VOSO4 xH2O
DMF
MnCl2 4H2O
DMF
MNH2DPE
M=Cu,VO, MnCl
MNH2DPE
+
MCH3OCODPE
N-methyl pyrolidone
p-toluenesulfonic acid
HN
NHCO
CO

Scheme V-2

(**NO_2DPE**) were prepared from 3,3'-diethyl-4,4'-dimethyl-2,2'-dipyrrylmethane and p-methoxycarbonylbenzaldehyde and p-nitrobenzaldehyde, respectively, according to the literature,[22] except for using dibenzoyl peroxide instead of o-chloranil as an oxidizing agent. 5,10-Bis(4-aminophenyl)-2,8,12,18-tetraethyl-3,7,13,17-tetramethylporphine (**NH_2DPE**) was synthesized from NO_2DPE according to the literature.[22] CH_3OCODPE and NH_2DPE were recrystallized from nitrobenzene and THF, respectively. Anal. of CH_3OCODPE: Calcd for $C_{48}H_{50}N_4O_4$: C, 77.18; H, 6.75; N, 7.50%. Found: C,76.98; H,6.70; N,7.47%. Anal. of NH_2DPE: Calcd for $C_{44}H_{48}N_6$: C, 79.96; H, 7.32; N, 12.72%. Found: C,79.41; H,7.28; N,12.32%.

2,3,2,a. [2,8,12,18-Tetraethyl-5,10-bis(4-methoxycarbonylphenyl)-3,7,13,17-tetramethylporphyrinato]copper(II) (**CuCH_3OCODPE**) was prepared as follows: 3.00 g (4.02 mmol) of CH_3OCODPE and 1.60 g (8.04 mmol) of copper (II) acetate in 2 L of chloroform was refluxed for 5 min. The reaction mixture was evaporated to dryness. The residue was washed with methanol, water, methanol, and recrystallized from benzonitrile: yield 3.40 g (3.71 mmol, 92%). MS m/e 808.6 (M+1). Anal.: Calcd for $C_{48}H_{48}N_4O_4Cu$: C, 71.31; H, 5.98; N, 6.93%. Found: C,71.43; H,5.92; N,7.11%.

2,3,2,b. [2,8,12,18-Tetraethyl-5,10-bis(4-methoxycarbonylphenyl)-3,7,13,17-tetramethylporphyrinato]oxovanadium(IV) (**VOCH_3OCODPE**) was prepared as follows: 4.00 g (5.36 mmol) of CH_3OCODPE and 20 g of vanadium (IV) oxide sulfate in 400 mL of DMF was heated at 150°C for 17 h. After cooling, the precipitate in the

reaction mixture was filtered off, washed with water, methanol, dried *in vacuo*, and recrystallized from nitrobenzene: yield 1.76 g (2.17 mmol, 40%). MS m/e 812.6 (M+1). Anal. : Calcd for $C_{48}H_{48}N_4O_5V$: C, 71.01; H, 5.96; N, 6.90%. Found: C,70.96; H,6.00; N,6.99%.

2 , 3 , 2 , c . Chloro[2,8,12,18-tetraethyl-5,10-bis(4-methoxy-carbonylphenyl)-3,7,13,17-tetramethylporphyrinato]manganese(III) (**MnClCH$_3$OCODPE**) was prepared as follows: a solution of 20.0 g (101 mmol) of manganese (II) chloride tetrahydrate in 400 mL of DMF was added to 4.00 g (5.36 mmol) of CH_3OCODPE in 400 mL of nitrobenzene at 150°C. The reaction mixture was maintained at 150°C for 2 h, and then cooled at room temperature, and poured into 2 L of ether. A precipitate in the ether solution was filtered off, washed with water, dissolved in 1 L of methanol, and filtered. The filtrate was poured into 1 L of water, the precipitate in the water was filtered off, dried *in vacuo*, and recrystallized from methanol: yield 2.05 g (2.45 mmol, 45.7%). MS m/e 799.5 (M-Cl). Anal. : Calcd for $C_{48}H_{48}N_4O_4ClMn$: C, 69.02; H, 5.79; N, 6.71; Cl, 4.24%. Found: C,68.81; H,5.83; N,6.68; Cl, 4.40%.

2 , 3 , 2 , d . [5,10-Bis(4-aminophenyl)-2,8,12,18-tetraethyl-3,7,13,17-tetramethylporphyrinato]copper(II) (**CuNH$_2$DPE**) was prepared as follows: 2.50 g (3.78 mmol) of NH_2DPE and 2.50 g (14.7 mmol) of copper (II) chloride dihydrate was heated in mixed solvent of 500 mL of THF and 25 mL of triethylamine at 60°C for 30 min. The reaction mixture was filtered, and the filtrate was poured into 1.5 L of water. A crude product was filtered off, washed with methanol, dried *in vacuo*, and recrystallized from THF-hexane: yield 0.99 g (1.4

mmol, 36%). MS m/e 721.5. Anal. Calcd for $C_{44}H_{46}N_6Cu$: C, 73.15; H, 6.42; N, 11.63%. Found: C,72.81; H,6.42; N,11.06%.

2,3,2,e. [5,10-Bis(4-aminophenyl)-2,8,12,18-tetraethyl-3,7,13,17-tetramethylporphyrinato]oxovanadium(IV) **($VONH_2DPE$)** was prepared as follows: 4.00 g (6.05 mmol) of NH_2DPE and 20 g of vanadium (IV) oxide sulfate in 400 mL of DMF was heated at 140°C for 2.5 h. The reaction mixture was poured into 400 mL of water, the precipitate was filtered off, washed with water, methanol, dried *in vacuo*, and recrystallized from THF-hexane: yield 0.65 g(0.90 mmol, 15%). MS m/e 726.5 (M+1). Anal. Calcd for $C_{44}H_{46}N_6OV$: C, 72.81; H, 6.39; N, 11.58%. Found: C,71.54; H,6.28; N,10.80%.

2,3,2,f. Chloro[5,10-bis(4-aminophenyl)-2,8,12,18-tetraethyl-3,7,13,17-tetramethylporphyrinato]manganese(III) **($MnClNH_2DPE$)** was prepared as follows: 4.00 g (6.05 mmol) of NH_2DPE and 20.0 g of manganese (II) chloride tetrahydrate (101 mmol) in 400 mL of DMF was heated at 150°C for 4 h. The reaction mixture was poured into 500 mL of water, the precipitate was filtered off, washed with water, dried *in vacuo*, and recrystallized from methanol: yield 2.18 g(2.91 mmol, 48%). MS m/e 713.5 (M-Cl). Anal. Calcd for $C_{44}H_{46}N_6ClMn$: C, 70.53; H, 6.19; N, 11.22; Cl, 4.73%. Found: C,70.09; H,6.33; N,10.96; Cl, 3.86%.

2,4. Polymerization

2,4,1. Radical Homopolymerization

Homopolymerization of VOAOMTPP was carried out as follows:

0.50 g of VOAOMTPP and 1.1 mg of 2,2'-azobisisobutyronitrile (AIBN) were put into an ampoule, and then dissolved in benzonitrile. The solution was degassed on a vacuum line by six freeze-pump-thaw cycles and then sealed under vacuum. Polymerization was carried out at 60°C for 50 h. The reaction mixture was poured into acetone to precipitate the resulting polymer. The polymer was purified by reprecipitating from benzene into a large excess of acetone three times. Anal. Calcd for $C_{48}H_{32}N_4O_3V$: C, 75.49; H, 4.22; N, 7.34; V, 6.67%. Found: C,75.36; H,4.43; N,7.07; V, 6.65%. The IR spectrum is shown in Figure 1-b. Molecular weight of the polymer was determined by GPC measurement using THF as an eluent. The molecular weight was calibrated by a standard polystyrene.

Radical homopolymerizations of other vinyl monomers were performed in a similar manner. Results of the homopolymerizations were listed in Table I.

2,4,2. Copolymerization

N-Laurylmethacrylamide (LaMAm)[23] and N-cyclododecyl-methacrylamide (CdMAm)[24] were prepared according to the method reported in our laboratory. N-(2-Naphthylmethyl)-methacrylamide (2-NpMAm) was prepared in a manner similar to N-(1-naphthyl-methyl)methacrylamide reported in our laboratory.[25] 2-Acrylamido-2-methylpropanesulfonate (AMPS) was a gift from Nitto Chemical Industry Co. and was used without further purification.

Copolymerization was carried out as follows: 1.04 g (5.00 mmol) of AMPS, 1.01 g (10.0 mmol) of triethylamine, 1.13 g (5.00 mmol) of

Table I. Radical Homopolymerization of Vinyl Monomers Containing Metalloporphyrins at 60°C

entry	monomer	solvent	[Monomer] [a]	[AIBN] [a]	time/h	conversion(%)	$\overline{M}_w$ [c]	$\overline{M}_w/\overline{M}_n$ [c]
1	VOAOMTPP	benzonitrile	330	3.4	50	25	7800	1.49
2	VOAOMTPP	benzonitrile	660	6.8	50	34	11000	1.49
3	VOAOMTPP	benzonitrile	1320	13.6	50	40	15000	1.56
4	VOAOMTPP	benzonitrile	330	3.4	100	28	7900	1.28
5	CuAOMTPP	benzonitrile	330	3.4	50	35	12000	1.89
6	CuAOMTPP	benzonitrile	660	6.8	50	27	18000	1.98
7	CuAOMTPP	benzonitrile	1320	13.6	50	26	21000	2.48
8	CuAOMTPP	benzonitrile	330	3.4	100	35	14000	1.54
9	ZnAATPP	DMF	110	3.3	50	98[b]	16500	1.46
10	CuAAEtio	benzonitrile	820	8.2	38	0.8[b]	900	—
11	ZnAAPor	DMF	110	3.3	50	1.6[b]	1200	—

[a] compound (mmol) / solvent (dm^3).

[b] estimated by GPC.

c measured on GPC (THF): calibrated by standard polystyrene.

2-NpMAm, 7.48 mg (10 μmol) of ZnAATPP and 4.12 mg (25 μmol) of AIBN were added in this order to a glass ampule containing 10 mL of DMF. The solution was degassed on a vacuum line by six freeze-pump-thaw cycles and then sealed under vacuum. Polymerization was carried out at 60°C for 24 h. The reaction mixture was poured into 150 mL of ether to precipitate the resulting polymer. The polymer was purified by reprecipitating from methanol into a large excess of ether twice and then dissolved in dilute aqueous NaOH whose pH was adjusted to 13. Triethylamine was evaporated by heating the aqueous solution at 90°C for 30 min with vigorous agitation followed by extraction with n-hexane three times. After evaporating remaining n-hexane by heating, the aqueous solution was dialyzed against dilute aqueous NaOH at pH 10 for a week. The polymer was recovered by freeze-drying technique. The conversion was 18.3% (0.410 g) on the basis of the total monomers. The contents of 2-NpMAm in the terpolymer was determined by elemental analysis and the ZnTPP units was determined by UV-vis absorption spectroscopy on the assumption that molar extinction coefficient (ε) at Soret band of the ZnTPP moiety in the terpolymer is the same as that of ZnAATPP ($\varepsilon=6.42\times10^5$ M^{-1}) in DMF shown in Figure 1-a in Chapter 4. This terpolymer containing AMPS, 2-NpMAm and ZnAATPP is represented as poly(A/Np/ZnTPP) shown in Scheme VI.

The copolymer of AMPS and ZnAATPP (poly(A/ZnTPP)) (Scheme VI) was also prepared from 4.14 g (20.0 mmol) of AMPS and 29.8 mg (39.9 μmol) of ZnAATPP by the method as described above. The

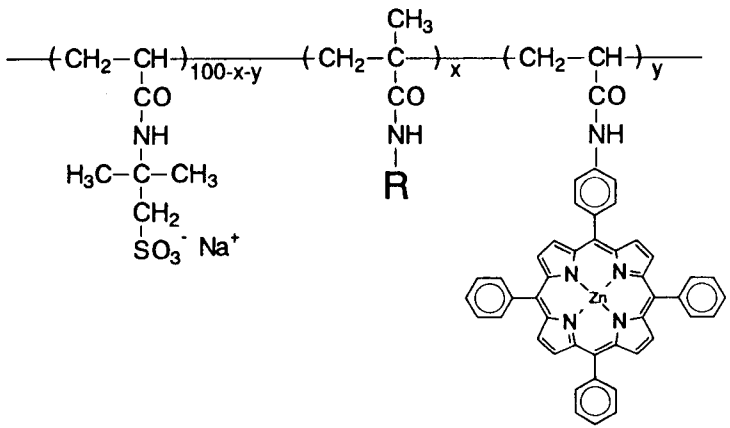

R= La —$(CH_2)_{11}CH_3$ **poly(A/La/ZnTPP)**
x=61
y=0.19

Cd **poly(A/Cd/ZnTPP)**
x=64
y=0.13

Np **poly(A/Np/ZnTPP)**
x=63
y=0.15

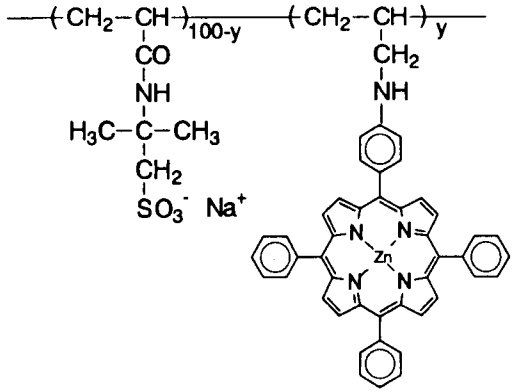

poly(A/ZnTPP)
y=0.34

Scheme VI

conversion was 10.8% (0.452 g) on the basis of the total monomers.

Other terpolymers and copolymers containing other methacrylamides and/or porphyrin monomers were prepared in a similar manner. The compositions of the polymers were summarized in Table II.

2,4,3. Condensation Polymerization

Condensation polymerization of $CuNH_2DPE$ and $MnClCH_3OCODPE$ was carried out as follows: 144.50 mg (200 μmol) of $CuNH_2DPE$ and 167.10 mg (200 μmol) of $MnClCH_3OCODPE$ was put into an glass ampule, and then 2.0 mL of N-methypyrrolidone containing 10 μmol of p-toluenesulfonic acid was added to the ampule. The reaction mixture was heated at 200°C for 70 h under Ar atmosphere, and then poured into chloroform. The resulting precipitate was filtered off. The monomers in the precipitate was removed by extraction with chloroform and with methanol. The insoluble part was filtered off and dried *in vacuo*: yield 247 mg. Anal Calcd for ($C_{44}H_{44}N_6Cu$)($C_{46}H_{42}N_4O_2ClMn$): C, 72.37; H, 5.80; N, 9.38; Cl,2.37; Cu,4.25; Mn,3.68%. Found: C, 65.28; H, 5.16; N, 9.29; Cl,0.27; Cu,2.78; Mn,1.96%. Cu/Mn=1.23(mol/mol). This product was represented as CuMnDPE.

CuCuDPE, VOVODPE, MnMnDPE, and VOMnDPE were also prepared in an analogous manner. VO/Mn in VOMnDPE was 0.84(mol/mol).

2.5. Discussion

Table II. Compositions of the Co- and Terpolymers Containing Zincporphyrins.

polymer code	RMAm (mol%) [a]	zincporphyrin (mol%) [b]
poly(A/ZnTPP)	0	0.34
poly(A/La/ZnTPP)	61	0.19
poly(A/Np/ZnTPP)	63	0.15
poly(A/Cd/ZnTPP)	64	0.13
poly(A/ZnEtio)	0	0.047
poly(A/La/ZnEtio)	62	0.036
poly(A/Np/ZnEtio)	60	0.016
poly(A/Cd/ZnEtio	66	0.021
poly(A/ZnPor)	0	0.34
poly(A/La/ZnPor)	67	0.088
poly(A/Np/ZnPor)	64	0.10
poly(A/Cd/ZnPor)	54	0.15

[a] mole fraction of hydrophobic monomer unit calculated from elementary analysis.

[b] determined by UV-vis absorption spectroscopy by assuming molar extinction coefficients (ε) at Soret bands of the zincporphyrin moieties in the polymers are the same as those of the monomers in DMF: ZnAATPP ($\varepsilon=6.42\times10^5$ M^{-1}), ZnAAEtio ($\varepsilon=3.63\times10^5$ M^{-1}), and ZnAAPor ($\varepsilon=4.15\times10^5$ M^{-1}).

2,5,1. Synthesis of Porphine

It is written in "The Porphyrins" [26] that synthesis of porphine, which is the simplest in porphyrin compounds, is the most difficult. Some groups have synthesized porphine [27], but the procedures were not useful to prepare a large amount of porphine which was necessary to synthesize a monomer containing metalloporphine. Longo et al. [20] have studied the synthesis of porphine in detail. They synthesized porphine in 8-10% yields by the following method: 0.1 g of 2-hydroxymethylpyrrole was added, twice in a day, to 3 L of ethylbenzene at 100°C, this procedure was repeated for 10 days, and then the reaction system was maintained for 4 days. Thus, more than two weeks were needed to obtain about 130 mg of porphine. They pointed out some important conditions to synthesize porphine in the literature [20]: (1) The synthesis of porphine should be carried out at 100°C. Over 100°C, the yield decreased with increasing temperature although the reaction time became shorter, and below 100°C, the yield decreased with decreasing temperature. (2) Oxygen was needed to prepare porphine from porphyrinogen, which consists of four pyrrole rings joined by four methylene bridges to give a macrocycle, but the preparation of the porphyrinogen from 2-hydroxymethylpyrrole was hindered by oxygen. (3) The reaction time became shorter in the presence of a catalyst, but the yield decreased. (4) Low concentration of 2-hydroxymethylpyrrole was needed to prepare porphine in good yield.

In order to obtain a larger amount of porphine in a shorter time, it is considered to be important to control the temperature, the

amount of oxygen, and the adding rate of 2-hydroxymethylpyrrole into the reaction system. Therefore, we modified the conditions as follows. The preparation of porphine was carried out at 125°C although the reaction over 100°C had given lower yield as described in the literature.[20] To control the reaction system at 125°C has two important meanings in this porphine synthesis. First, it is possible to shorten the reaction time. Second, the solubility of oxygen in a solvent decreases and may be moderate to prepare not only porphine but also porphyrinogen. Solvent was refluxed before use to remove oxygen because the preparation of the porphyrinogen is hindered by oxygen. Oxygen was kept flowing slowly into the reaction system because oxygen is needed to prepare porphine, and then 2-hydroxymethylpyrrole in dilute solution was added continuously for about 30 h. The reaction was continued for 15 h after complete addition, and then yield was 8.2 % estimated by UV-visible absorption spectrum. After purification by chromatography and recrystallization, porphine was obtained in 5.8 % yield.

2,5,2. Polymerization of Monomers Containing Metalloporphyrin

IR spectra of VOAOMTPP and polyVOAOMTPP are shown in Figure 1. The IR bands of the monomer at 1630 and 1730 cm^{-1} are assignable to absorptions due to olefinic and carbonyl bonds of unsaturated ester, respectively. In polyVOAOMTPP, the former disappeared and the latter shifted to 1733cm^{-1}, which indicates that carbonyl bond of unsaturated ester changed to that of saturated ester.

No change was found in absorption bands due to the porphyrin ring in the range 700-800 cm^{-1}, after polymerization. Clear change was observed in comparison with IR spectra of CuAOMTPP and polyVOAOMTPP similar to the VOAOMTPP system. These findings show that the polymerization takes place through the C=C bond of the monomers. Elemental analysis of the polymers obtained was consistent with the results of the corresponding monomers, indicating that addition polymerizations took place.

Visible spectra of VOAOMTPP and polyVOAOMTPP are shown in Figure 2. VOAOMTPP has Soret band at 425 nm and Q band at 548 nm, while polyVOAOMTPP has Soret band at 422 nm, Q band at 549 nm, and a new absorption band at 638 nm. The Soret band of polyVOAOMTPP at 422 nm is much weaker and broader than that of monomer. The decrease in the intensity at 422 nm and appearance of new absorption band at 638 nm is probably due to some electronic interactions between the porphyrin moieties caused by their connection with a polyacrylate chain. Similar changes in all absorption bands were also observed in comparison with visible spectra of CuAOMTPP and polyVOAOMTPP.

Degree of the homopolymerization of the acrylamide monomers are different for different porphyrin moieties, the results are summarized in Table I . Polymerization of ZnAATPP could occur and the polymer with a weight-average molecular weight of 16500 was obtained. On the contrary, no polymers were obtained in CuAAEtio and ZnAAPor systems. These differences may be caused by steric hindrance around vinyl groups. Although porphine and etioporphine

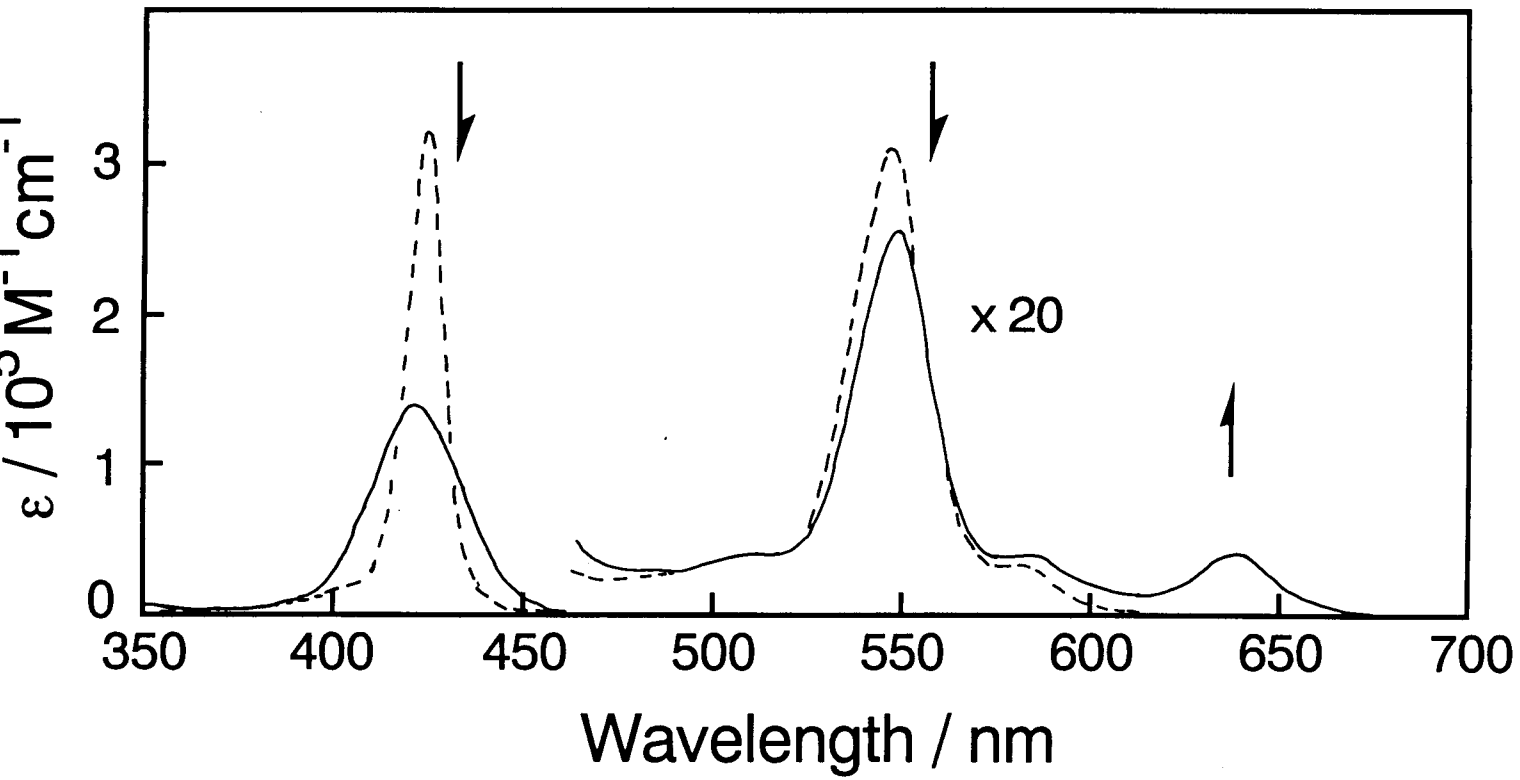

Figure 2. Visible spectra of VOAOMTPP(----) and polyVOAOMTPP(——) in benzene.

moieties are smaller than TPP moiety, the acrylamide moieties in ZnAAPor and CuAAEtio are joined directly at the *meso* position of porphyrin rings, while acrylamide moiety in ZnAATPP is joined at para position of the phenyl group. The steric hindrance around the vinyl group in ZnAATPP may be the smallest and that in CuAAEtio may be the largest in these porphyrin monomers. Other factors for reactivities in the radical polymerizations, for example, Q-e values of monomers, cannot be discussed at present.

Absorption spectra of the copolymer, the terpolymers containing ZnTPP moieties, and the monomer are shown in Figure 1 in Chapter 4, other spectra for ZnEtio and ZnPor systems are shown in Figure 3 and Figure 4 in this Chapter, respectively. The spectra show that the porphyrin moieties are bound to the polymer chains and surroundings of the porphyrin moieties are different for different hydrophobic groups in aqueous solution. The details will be described in Chapter 4.

In the copolymerizations with AMPS which is much smaller than porphyrin monomers, ZnAATPP and ZnAAPor compositions in copolymers are slightly larger than those in monomer feed (0.2 mol%) shown in Table II. On the other hand, ZnAAEtio composition in copolymer is an order of magnitude smaller than that in monomer feed. The results from homopolymerization and copolymerization show that the order of reactivities of monomers in radical polymerization is

$$\text{ZnAAEtio} < \text{ZnAAPor} < \text{ZnAATPP}$$

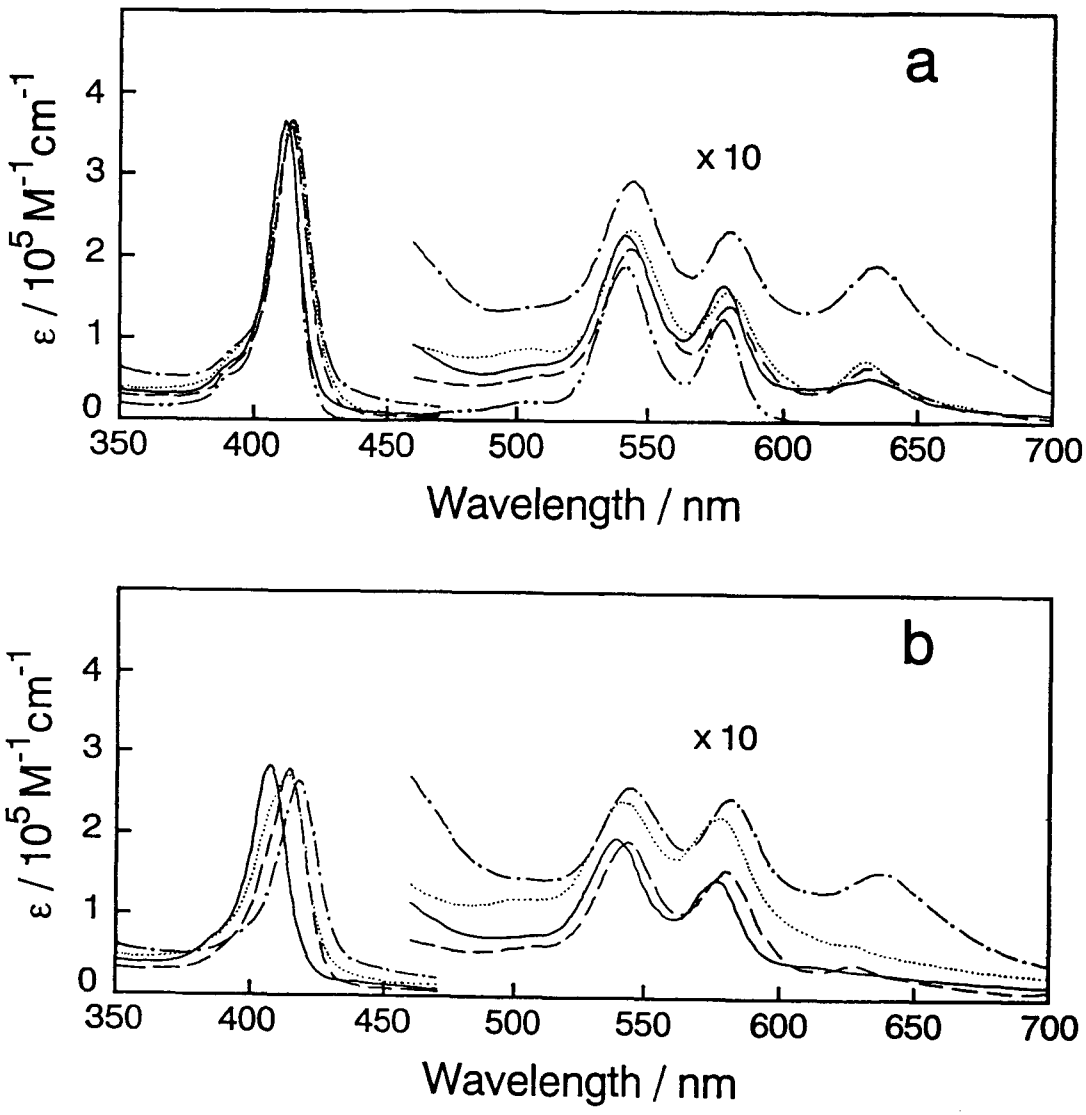

Figure 3. Absorption spectra of the terpolymers, the copolymer, and ZnAAEtio: **a**, in DMF for the terpolymers and ZnAAEtio and DMF/water (9/1 : v/v) for the copolymer; **b**, in water; — — —, poly(A/La/ZnEtio); —— • ——, poly(A/Np/ZnEtio); ·····, poly(A/Cd/ZnEtio); ————, poly(A/ZnEtio); —— • • ——, ZnAAEtio.

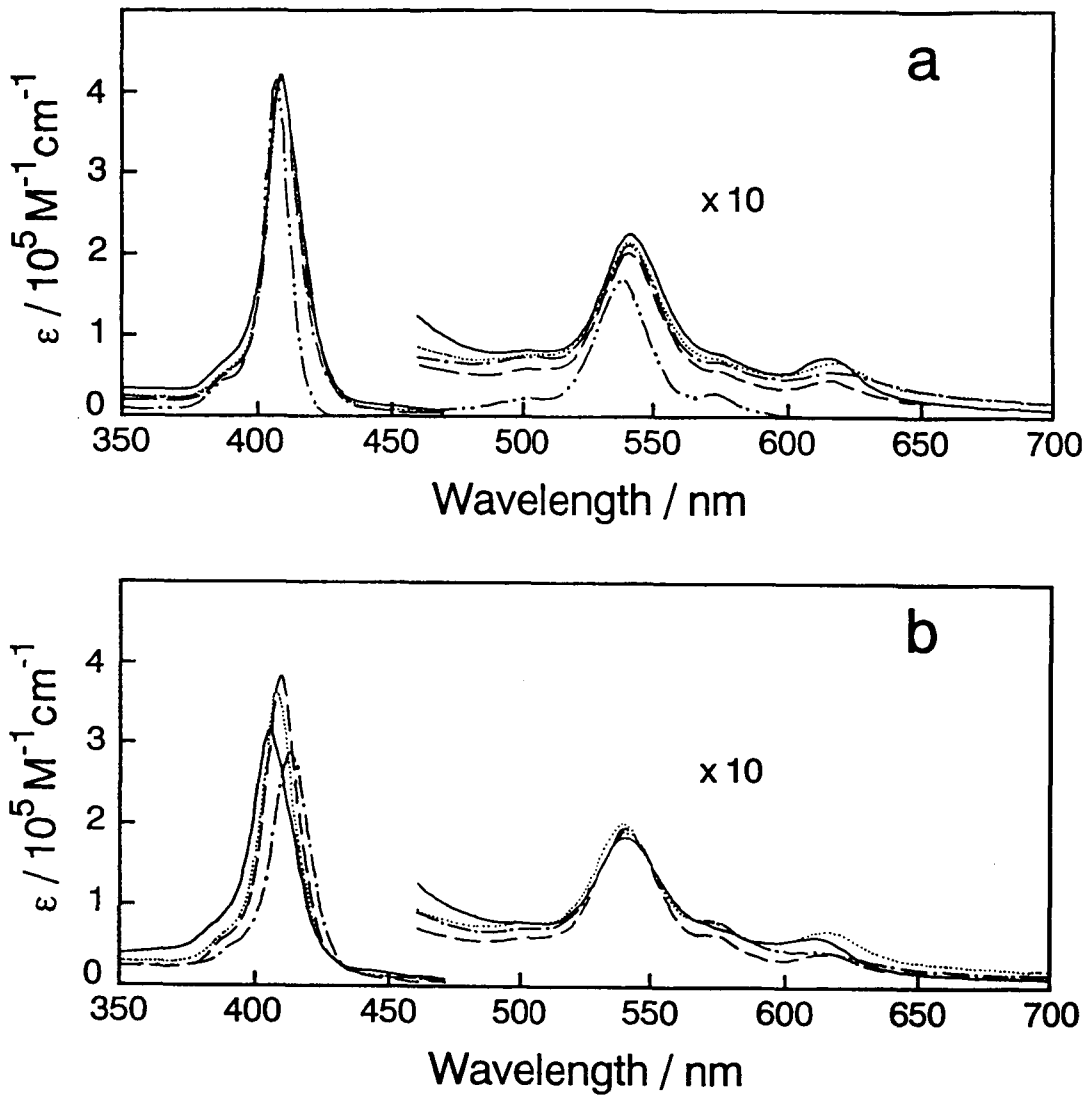

Figure 4. Absorption spectra of the terpolymers, the copolymer, and ZnAAPor: **a**, in DMF for the terpolymers and ZnAAPor and DMF/water (9/1 : v/v) for the copolymer; **b**, in water; — — —, poly(A/La/ZnPor); —— • ——, poly(A/Np/ZnPor); ·····, poly(A/Cd/ZnPor); ————, poly(A/ZnPor); —— • • ——, ZnAAPor.

IR spectra of $CuNH_2DPE$, $MnClCH_3OCODPE$, and CuMnDPE are shown in Figure 5. Broad absorption appeared in CuMnDPE. The IR band of a carbonyl group of $MnClCH_3OCODPE$ (1720 cm^{-1}) was shifted to a lower wavenumber in CuMnDPE (1700 cm^{-1}). This result suggests presence of an amide bond in CuMnDPE. The values found by elemental analysis of CuMnDPE was not in agreement with the calculated values. Since the total of the found values was 84.74%, 15.26% of the weight of CuMnDPE may be oxygen. It has been shown in our laboratory that some oxygen had been absorbed by one porphyrin unit in homopolymers containing porphyrin moieties.[8] These condensation polymers cannot be identified sufficiently because of their insoluble character.

2.6. Conclusion

Several new monomers containing metalloporphyrins were synthesized.

The homopolymers of the acrylate monomers, CuAOMTPP and VOAOMTPP, with the weight average molecular weight of about 15000 were obtained by radical polymerization.

The order of reactivities of the acrylamide monomers in radical polymerization was ZnAAEtio < ZnAAPor < ZnAATPP. This order may be explained by the bulkiness around vinyl group.

Insoluble polymers were obtained by condensation polymerization of DPE compounds. But these insoluble polymers could not be identified sufficiently as polyamides containing

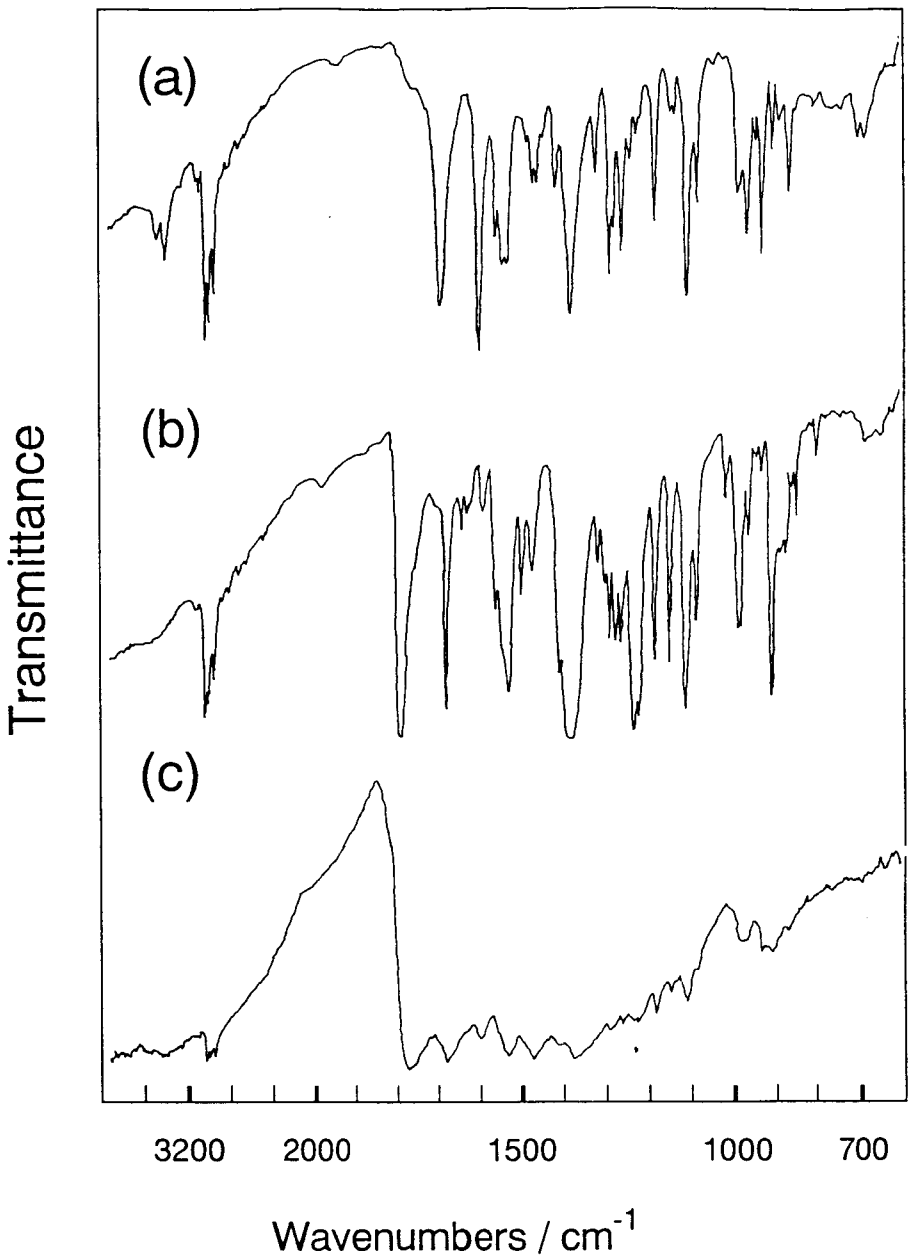

Figure 5. IR spectra of $CuNH_2DPE$ (a), $MnClCH_3OCODPE$ (b), and CuMnDPE (c).

metalloporphyrins in their main chain.

References

1) Lautch, W.; Brocer, W.; Rothkegel, W.; Biederman, W.; Doering, U.; Zoschke, H. *J. Polym. Sci.* **1952**, *8*, 191.

2) Lautch, W.; Brocer, W.; Biederman, W.; Gnichel, H. *J. Polym. Sci.* **1955**, *17*, 479.

3) Tsuchida, E. *J. Makromol. Sci., Chem.* **1979**, *A13*, 545.

4) Finkenauer, L. A.; Dickinson, C. L.; Chein, W. C. *Macromolecules* **1983**, *16*, 728.

5) Kamogawa, M. *J. Polym. Sci.,Polym. Chem. Ed.* **1974**, *12*, 2317.

6) Nishide, H.; Shinohara, K.; Tsuchida, E. *J. Polym. Sci.,Polym. Chem. Ed.* **1981**, *19*, 1109.

7) Kamachi, M.; Akimoto, H.; Mori, W.; Kishita, M. *Polym. J.* **1984**, *16*, 23.

8) Kamachi, M.; Cheng, X. S.; Kida, T.; Kajiwara, A.; Shibasaka, M.; Nagata, S. *Macromolecules* **1987**, *20*, 2665.

9) Nozakura, S.; Kamachi, M. *Makromol. Chem. Suppl.* **1985**, *12*, 255

10) Kamachi, M.; Cheng, X. S.; Nozakura, S. *Fifth Rare Earth Symposium.* (Tokyo, 1987), Preprints 2B05.

11) Kamachi, M.; Cheng, X. S.; Aota, H.; Mori, W.; Kishita, M. Chem. Lett. **1987**, 2331.

12) Bonnett, R. Nomenclature. In *The Porphyrins* ; Dolphin, D., Ed.; Academic Press: New York, 1978; Vol. I, pp 1.

13) Adler, A. D.; Longo, F. R.; Finarelli, J. D.; Goldmacher, J.; Assour, J.; Korsakoff, L. *J. Org. Chem.* **1967**, *32*, 476.

14) Callot, H. J. *Tetrahedron* **1973**, *29*, 899.

15) Hasegawa, E.; Nemoto, J.; Kanayama, T.; Tsuchida, E. *Eur. Polym. J.* **1978**, *14*, 123.

16) Inhoffen, H. H.; Fuhrhop, J.-H.; Voigt, H.; Brockmann jr, H. *Justus Liebings Ann. Chem.* **1966**, *695*, 133.

17) Bonnett, R.; Stephenson, G. F. *J. Org. Chem.* **1965**, *30*, 2791.

18) Silverstein, R. M.; Ryskiewicz, E. E.; Willard, C. *Org. Synth.* **1956**, *36*, 74.

19) Silverstein, R. M.; Ryskiewicz, E. E.; Chaikin, S. W. *J. Am. Chem. Soc.* **1954**, *76*, 4485.

20) Longo, F. R.; Thorne, E. J.; Adler, A. D.; Dym, S. J. *Heterocyclic Chem.* **1975**, *12*, 1305.

21) Drach, J. E.; Longo, F. R. *J. Org. Chem.* **1974**, *39*, 3282.

22) Young, R.; Chang, C. K. *J. Am. Chem. Soc.* **1985**, *107*, 898.

23) Morishima, Y.; Kobayashi, T.; Nozakura, S. *Polym. J.* **1989**, *21*, 267.

24) Morishima, Y.; Tominaga, Y.; Kamachi, M.; Okada, T.; Hirata, Y.; Mataga, N. *J. Phys. chem.* **1991**, *95*, 6027.

25) Morishima, Y.; Tominaga, Y.; Nomura, S.; Kamachi, M. *Macromolecules* **1992**, *25*, 861.

26) Kim, J. B.; Adler, A. D.; Longo, F. R. Synthesis of Porphyrins from Monopyrroles. In *The Porphyrins* ; Dolphin, D., Ed.; Academic Press: New York, 1978; Vol. I, pp 85.

27) (a) Fischer, H.; Gleim, W. *Justus Liebings Ann. Chem.* **1935**, *521*,

157. (b) Rothemund, P. *J. Am. Chem. Soc.* **1935**, *57*, 2010. (c) Rothemund, P. *J. Am. Chem. Soc.* **1936**, *58*, 625. (d) Krol, S. *J. Org. Chem.* **1959**, *24*, 2065. (e) Eisner, U.; Linsted, R. P. *J. Chem. Soc.* **1955**, 3742. (d) Badger, G. M.; Ward, A. D. *Aust. J. Chem.* **1964**, *17*, 649.

Chapter 3

Magnetic Behavior of Polymers Containing Metalloporphyrins

3.1. Introduction

Kamachi et al.[1-5] prepared polymers containing paramagnetic tetraphenylporphyrinato metal complexes, and investigated their magnetic behavior. The measurement of magnetic susceptibility (X_M) of these polymers containing Ag(II), Cu(II), VO(II), and Co(III) showed that paramagnetic species bound to polymer chains interact antiferromagnetically, and that the interaction is much larger than that of the corresponding monomer units.[1-3] The origin of the antiferromagnetic behavior has been ascribed to the superexchange interaction through the C=O group between Ag(II) ions.[1] They attempted to expand this study to polymers containing other paramagnetic ions. Rare earth metal ions Er(III) and Yb(III) were chosen instead of Ag(II) ions, because these ions have electrons in the f-orbital and accordingly are considered to be effective for the occurrence of magnetic interaction.[4] A weak ferromagnetic interaction was found in polyAOTPPEr(III)OH below 5K. A copolymer containing both CuTPP and VOTPP moieties, whose metal ions have d^9 and d^1 configurations, respectively,[5] was prepared. The temperature dependence of the magnetic susceptibility follows the Curie-Weiss law with θ=50K, indicating the existence of the ferromagnetic interaction between CuTPP and VOTPP moieties.

In this Chapter, we studied the magnetic behavior of the polymers containing paramagnetic metalloporphyrins of which the preparation were described in Chapter 2.

3,2. Experimental Section

3,2,1. Materials

Syntheses of $CuNH_2DPE$, $CuCH_3OCODPE$, $VONH_2DPE$, $VOCH_3OCODPE$, $MnClNH_2DPE$, $MnClCH_3OCODPE$, CuCuDPE, VOVODPE, MnMnDPE, CuMnDPE, VOMnDPE, polyCuAOMTPP, and polyVOAOMTPP were described in Chapter 2.

Iron (Fe), iron(III) oxide (Fe_2O_3), and iron(II,III) oxide (Fe_3O_4) were purchased from Nacalai tesque Co. and used without further purification.

3,2,2. Measurements

ESR measurements were carried out on a JEOL Model JES FE-1X and JES RE-2X ESR spectrometers with 100 kHz modulators at various temperature. A thermostat made by Scientific Instruments Co. was used for the measurements at 4.2 and 150K, and a thermostat made by JEOL Co. was used at 420K.

Gram magnetic susceptibility (χ_g) was determined by the Gouy method at room temperature using distilled water (χ_g=-0.72x10^{-6} cgsemu) as a standard. The temperature dependence of χ_g was determined by the Faraday method from 4.2 to 300K. Details of these measurements have been mentioned in the doctoral thesis of Xian Su Cheng.[6] Diamagnetic susceptibilities (χ_{dia}) for diphenyletioporphyrin compounds and polyMAOMTPPs were calculated by using Pascal's additive law with diamagnetic susceptibilities of NH_2DPE (-542x10^{-6} cgsemu) and TPP (-484x10^{-6}

cgsemu) which were estimated by the Gouy method, respectively. An apparent molar susceptibility (χ_A) and an effective magnetic moment were calculated from eq.(1) and (2), respectively.

$$\chi_A = \chi_g \times M_{w\ app} - \chi_{dia} \qquad (1)$$

$$\mu_{eff} = 2.83 \times (\chi_A T)^{0.5} \qquad (2)$$

where the apparent molecular weight $M_{w\ app}$ is the atomic weight of the metal divided by weight fraction of the metal in a compound, and T is the absolute temperature. In CuMnDPE and VOMnDPE, which have two kinds of metals in each compound, μ_{eff} were estimated for $Cu_{1.23}M\ n_1$ and $VO_{0.84}M\ n_1$ as one unit, respectively.

3,3. Results and Discussion

3,3,1. Magnetic Interactions of DPE Compounds

Polyamides based on diphenyletioporphyrin (DPE) were prepared to study a magnetic interaction through amide bond, and to obtain a ferrimagnet which is necessary to order two kinds of spins having different magnetic moments such as Cu and Mn, as shown in Figure 2 in Chapter 1.

3,3,1,a. Magnetic Behavior of CuCuDPE

ESR spectra of powders of $CuNH_2DPE$, $CuCH_3OCODPE$, and CuCuDPE at room temperature are shown in Figure 1. Sharp single lines having peak-to-peak widths of 5.8 mT appeared in the spectra of the monomers. While, a broader single line having a peak-to-peak width

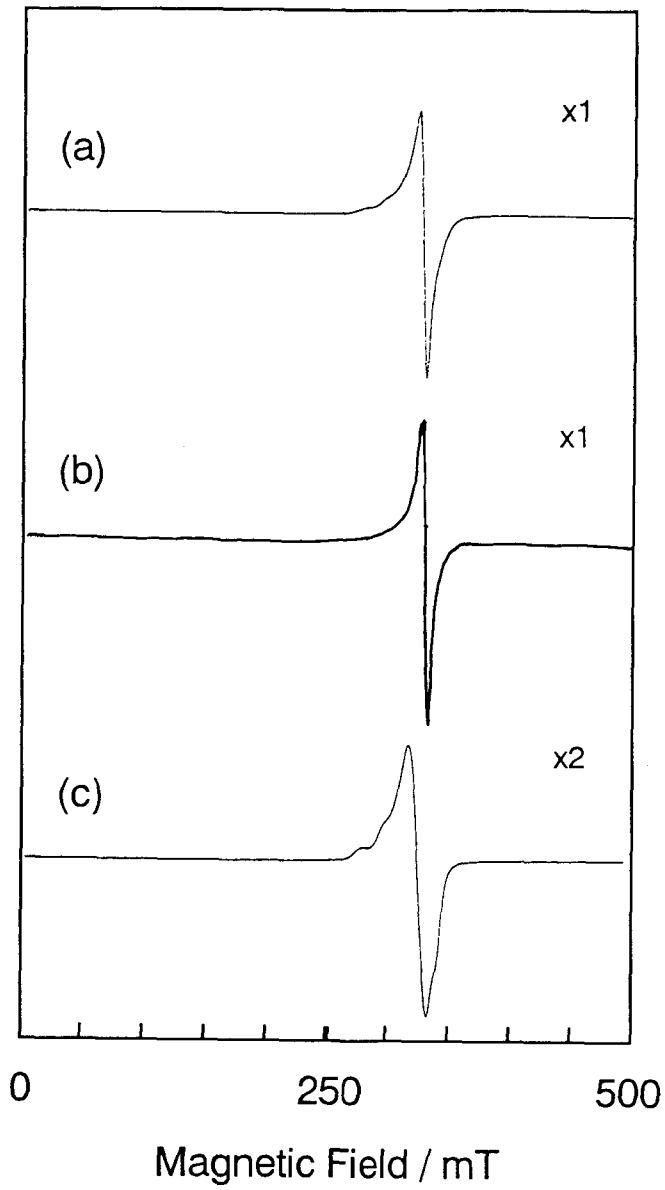

Figure 1 ESR spectra of powders of $CuNH_2DPE$ (a), $CuCH_3OCODPE$ (b), and CuCuDPE (c) at room temperature.

of 15.0 mT was observed in CuCuDPE. This finding suggests that the surroundings of the Cu(II) ion in CuCuDPE is different from that in the monomers and/or that an exchange interaction occurs between unpaired electrons of the Cu(II) ions in CuCuDPE.

Temperature dependence of an inverse magnetic susceptibility and a magnetic moment of CuCuDPE are shown in Figure 2-a. The magnetic moments in 70-300K region were almost constant having the values of 1.85 ± 0.02 Bohr magneton (B.M.) and those decreased with a decrease in temperature below 20K. This finding indicates that CuCuDPE has a weak antiferromagnetic interaction where the Weiss temperature, which estimated from the intercept of the abscissa of the inverse magnetic susceptibility, is -1.2K.

3,3,1,b. Magnetic Behavior of VOVODPE

ESR spectra of powders of $VONH_2DPE$, $VOCH_3OCODPE$, and VOVODPEDPE at room temperature are shown in Figure 3. The spectra of the monomers showed broad lines, and the absorption due to $g_{\perp}$ [7] was weaker than that due to $g_{/\!/}$.[7] On the other hand, the spectrum of VOVODPE showed sharper lines than the spectra of monomers, and the absorption due to $g_{\perp}$ was stronger than that due to $g_{/\!/}$. These findings suggest that the surroundings of the VO(II) ion in VOVODPE is different from that in the monomers and/or that an exchange interaction occurs between unpaired electrons of the VO(II) ions in VOVODPE.

Temperature dependences of an inverse magnetic susceptibility and a magnetic moment of VOVODPE are shown in Figure 2-b. The magnetic moment decreased with a decrease in temperature. This

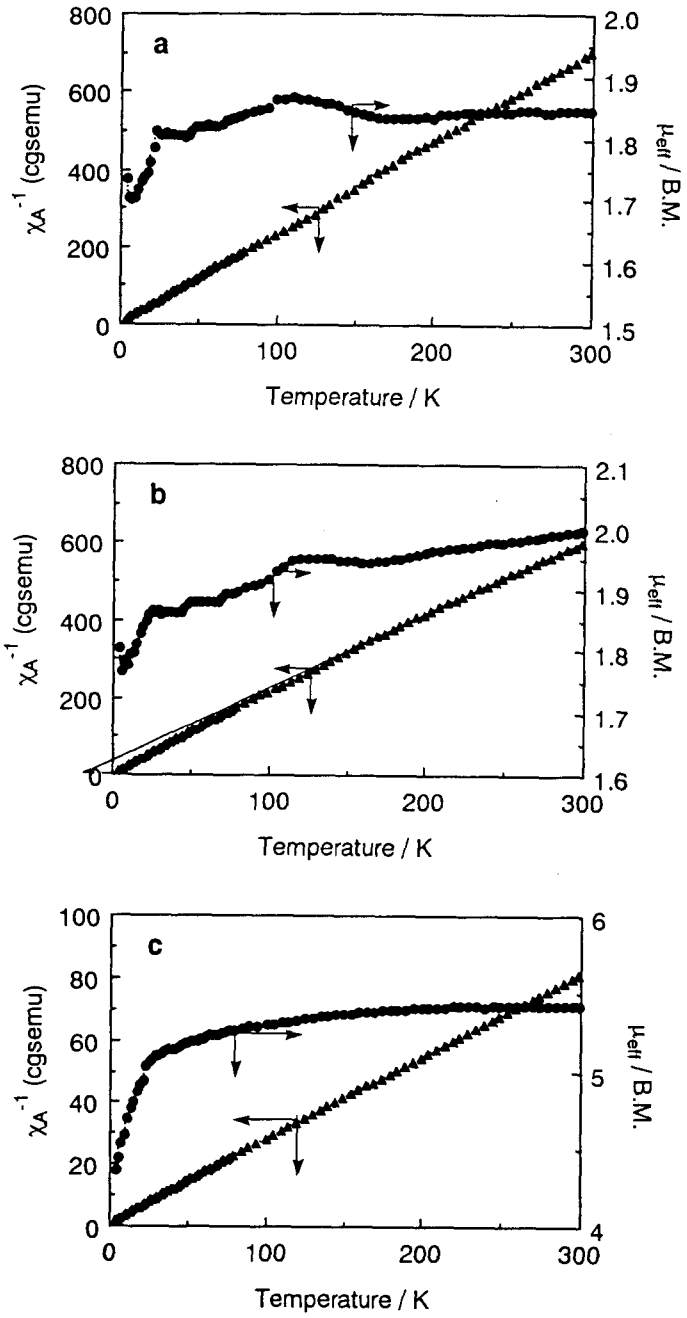

Figure 2 Temperature dependences of inverse magnetic susceptibilities and effective magnetic moments of CuCuDPE (a), VOVODPE (b), and MnMnDPE (c).

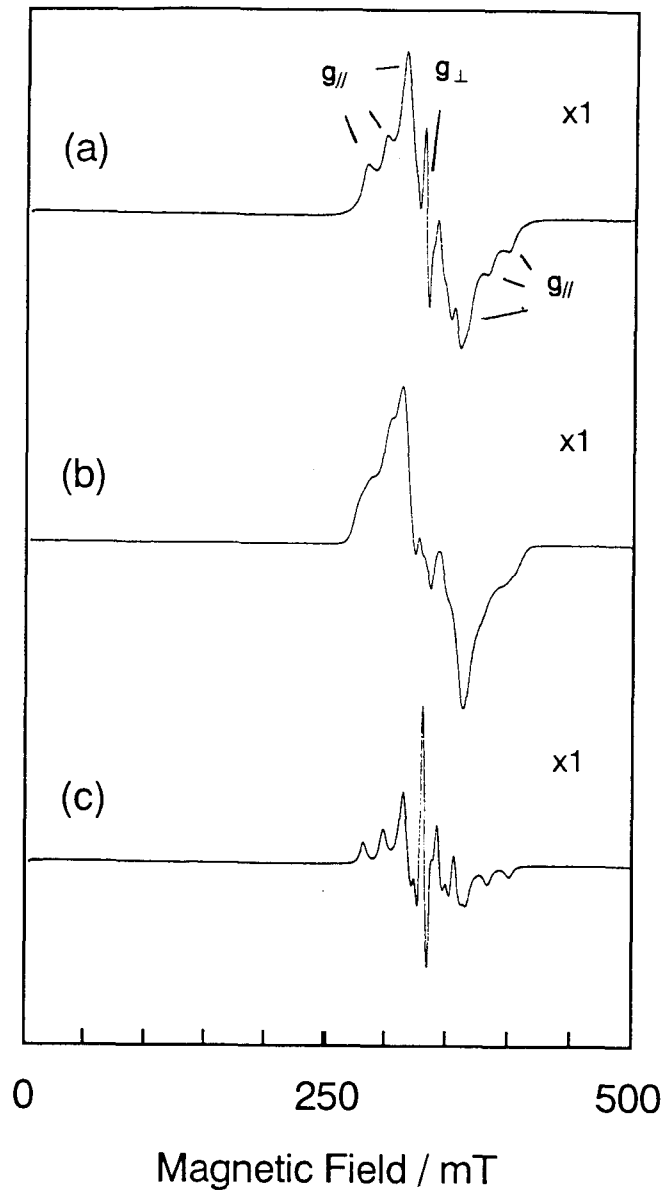

Figure 3 ESR spectra of powders of $VONH_2DPE$ (a), $VOCH_3OCODPE$ (b), and VOVODPE (c) at room temperature.

finding indicates that VOVODPE has antiferromagnetic interaction with the Weiss temperature of -15K.

3,3,1,c. Magnetic Behavior of MnMnDPE

ESR spectra of powders of $MnClNH_2DPE$, $MnClCH_3OCODPE$, and MnMnDPE at room temperature are shown in Figure 4. The spectral intensities of the monomers were much weaker than those of other monomers containing Cu or VO. This finding suggests that the Mn(III) ion in the monomers is in a low spin state, which is diamagnetic, and the ESR absorptions may be due to impurities such as other manganese complexes existing in the monomers. On the other hand, the spectral intensity of MnMnDPE was much higher than those of $MnClNH_2DPE$ and $MnClCH_3OCODPE$. The magnetic moment of MnMnDPE is 5.43 B.M. at 294K. Chlorine content of MnMnDPE (0.36%) was much smaller than those of monomers ($MnClNH_2DPE$, 3.86%: $MnClCH_3OCODPE$, 4.40%). These results suggest that a spin state and/or an oxidation number of the Mn ion in MnMnDPE are different from those of monomers.

Temperature dependence of an inverse magnetic susceptibility and a magnetic moment of MnMnDPE are shown in Figure 2-c. The magnetic moment decreased with a decrease in temperature. This finding indicates that MnMnDPE has weak antiferromagnetic interaction with the Weiss temperature of -5.3K.

3,3,1,d. Magnetic Behavior of CuMnDPE and VOMnDPE

ESR spectra of powders of CuMnDPE and VOMnDPE at room temperature are shown in Figure 5-a and 5-b, respectively. The ESR spectrum of CuMnDPE agreed with the sum of the spectra of CuCuDPE

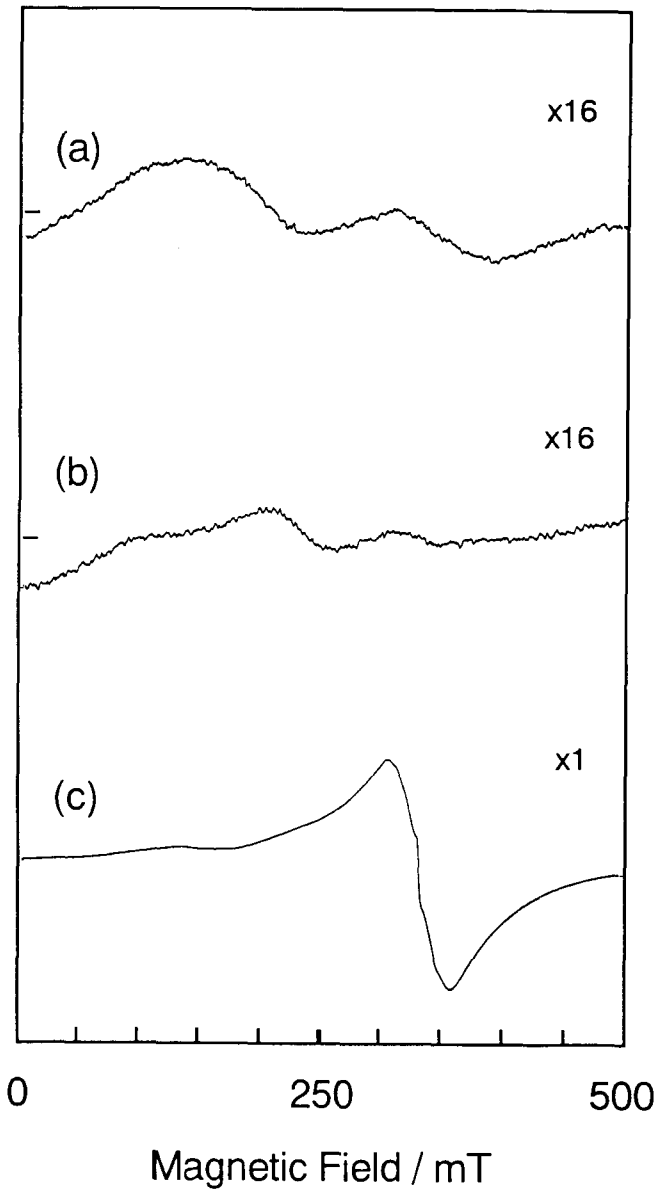

Figure 4 ESR spectra of powders of $MnClNH_2DPE$ (a), $MnClCH_3OCODPE$ (b), and MnMnDPE (c) at room temperature.

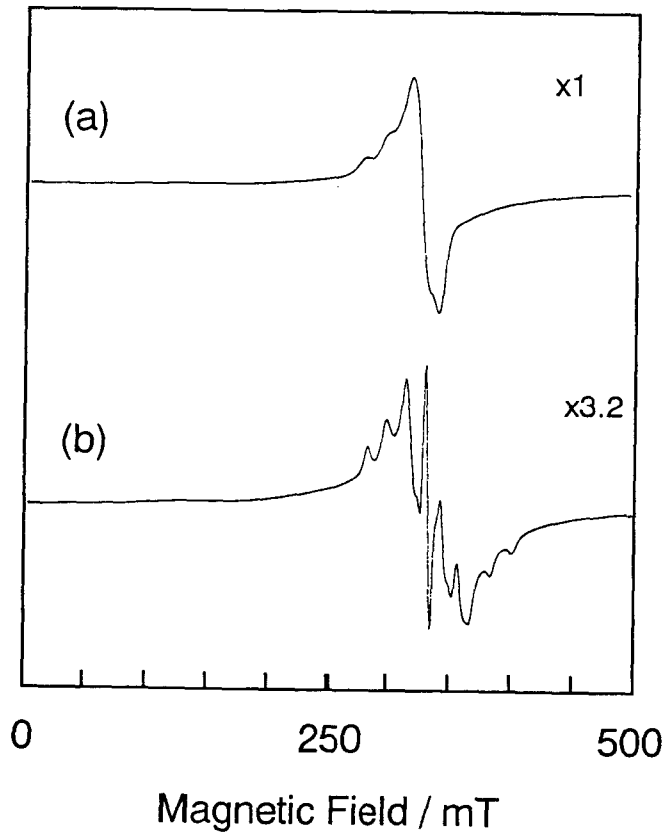

Figure 5 ESR spectra of powders of CuMnDPE (a) and VOMnDPE (b) at room temperature.

and MnMnDPE. Thus, the magnetic interaction between Cu and Mn ions may be almost zero. A similar result was obtained in VOMnDPE.

Temperature dependences of inverse magnetic susceptibilities and magnetic moments of CuMnDPE and VOMnDPE are shown in Figure 6-a, and 6-b, respectively. The magnetic moment of CuMnDPE decreased with a decrease in temperature. This finding indicates that CuMnDPE had weak antiferromagnetic interaction with the Weiss temperature of -6.0K. A similar result was obtained in VOMnDPE with the Weiss temperature of -5.5K.

These results of the magnetic behavior of DPE compounds show that a weak magnetic interaction through amide bond and/or through space occur, but that ferrimagnets are absent in CuMnDPE and VOMnDPE because the magnetic interactions are weak.

3,3,2. Magnetic Interactions of PolyCuAOMTPP and PolyVOAOMTPP

3,3,2,a. Magnetic Behavior of polyCuAOMTPP

ESR spectra of benzene solutions of CuAOMTPP and polyCuAOMTPP are shown in Figure 7. The spectrum of monomer showed hyper-fine structure (hfs) due to an interaction between an unpaired electron of Cu and four nitrogens of the porphyrin.[7c] On the contrary, the spectrum of the polymer showed a broad line without hfs. This finding suggests that the surroundings of the Cu(II) ion in the polymer is different from that in the monomer and/or that an exchange interaction occurs between unpaired electrons of the Cu(II) ions in the polymer.

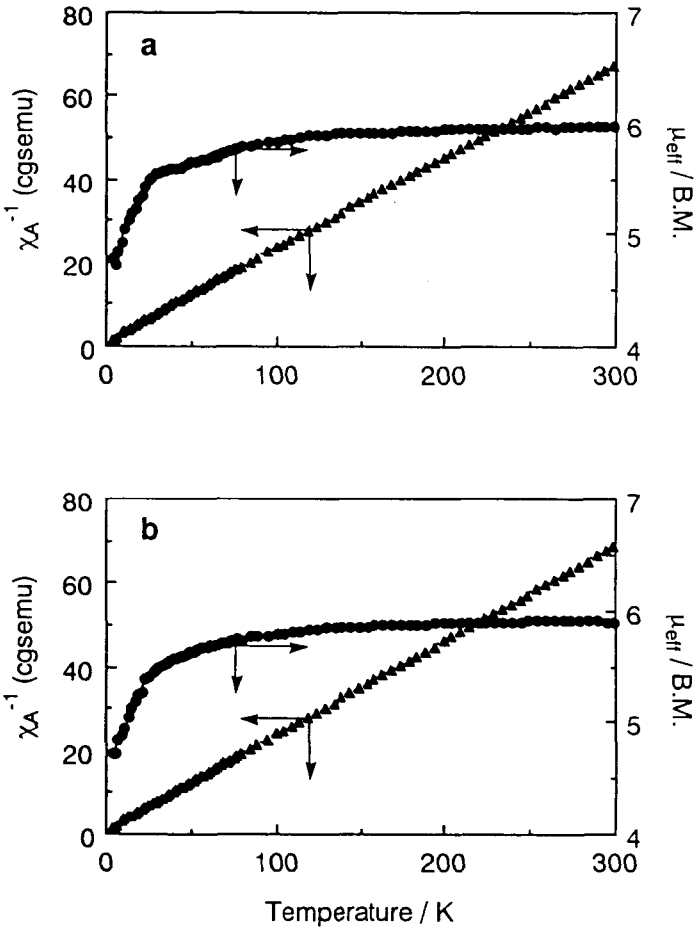

Figure 6 Temperature dependences of inverse magnetic susceptibilities and effective magnetic moments of CuMnDPE (a) and VOMnDPE (b).

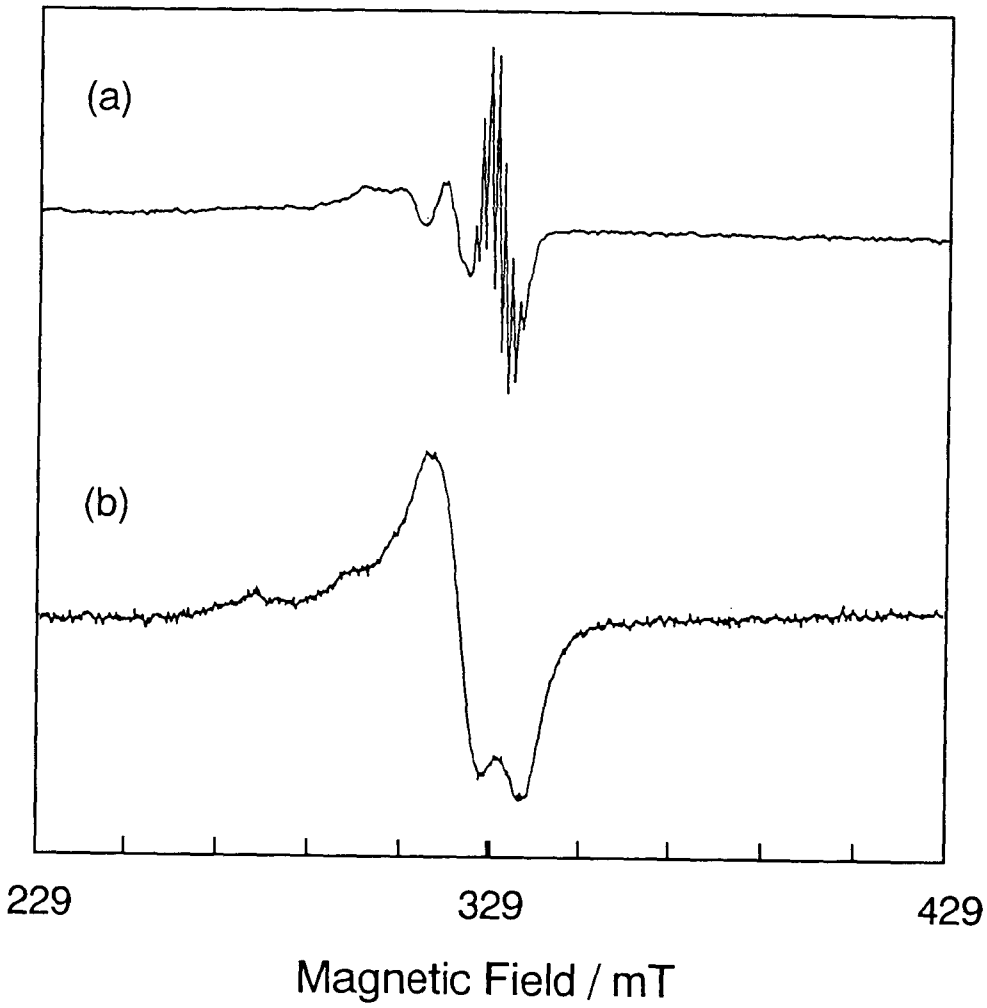

Figure 7 ESR spectra of CuAOMTPP and polyCuAOMTPP in benzene (1.3 mM) at room temperature.

Temperature dependence of an inverse magnetic susceptibility and a magnetic moment of polyCuAOMTPP is shown in Figure 8. The magnetic moment decreased with a decrease in temperature. This finding indicates that the polymer has antiferromagnetic interaction with the Weiss temperature of -38K. In the previous research in our laboratory, polyCuAOTPP had weak antiferromagnetic interaction with the Weiss temperature of -10K.[1] Thus, the magnetic interaction in the polyCuAOMTPP was stronger than that in the polyCuAOTPP. Since the distance from the main chain to the metal ion in polyCuAOMTPP is shorter than that in polyCuAOTPP, the distance between porphyrin moieties in polyCuAOMTPP may be shorter than that in polyCuAOTPP. Thus, the stronger magnetic interaction may result from the differences of the distance and/or the orientation between porphyrin moieties in their side chains.

3,3,2,b. Magnetic Behavior of polyVOAOMTPP

ESR spectra of benzene solutions of VOAOMTPP and polyVOAOMTPP are shown in Figure 9. The spectrum of the monomer showed isotropic eight sharp lines due to hfs of vanadium (I=7/2).[7] While, the spectrum of the polymer showed anisotropic lines with strong absorption of $g_{\perp}$. This finding, which is in agreement with the result for polyVOAOTPP in our laboratory,[6] suggests that the surroundings of the VO(II) ion in the polymer is different from that in the monomer and/or an exchange interaction occurs between unpaired electrons of the VO(II) ions bound to the side chain of the polymer.

Since a little magnetoactive part, which was responded to a

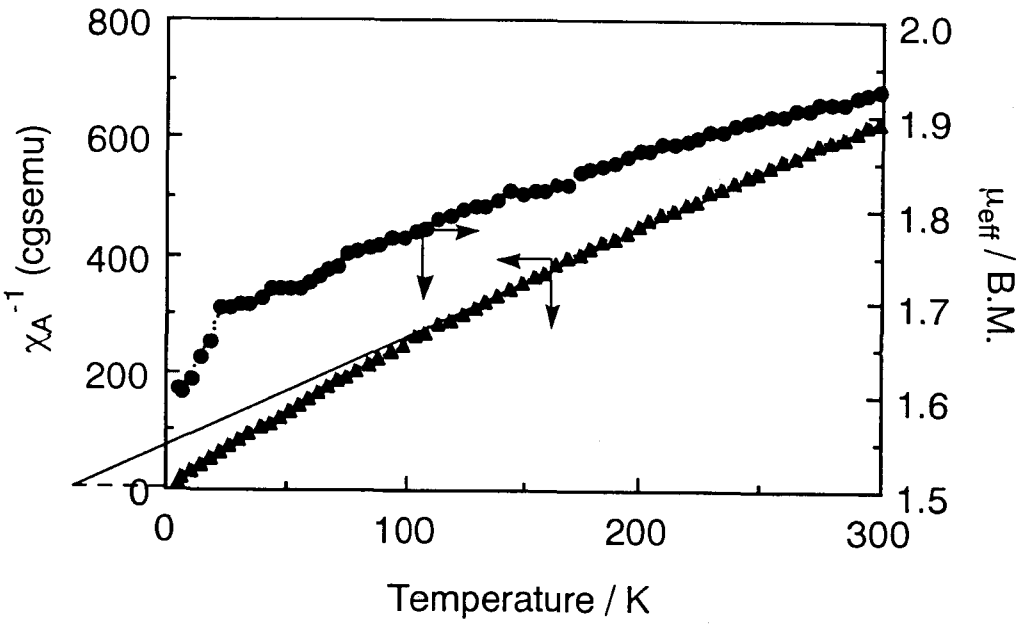

Figure 8 Temperature dependence of an inverse magnetic susceptibility and an effective magnetic moment of polyCuAOMTPP.

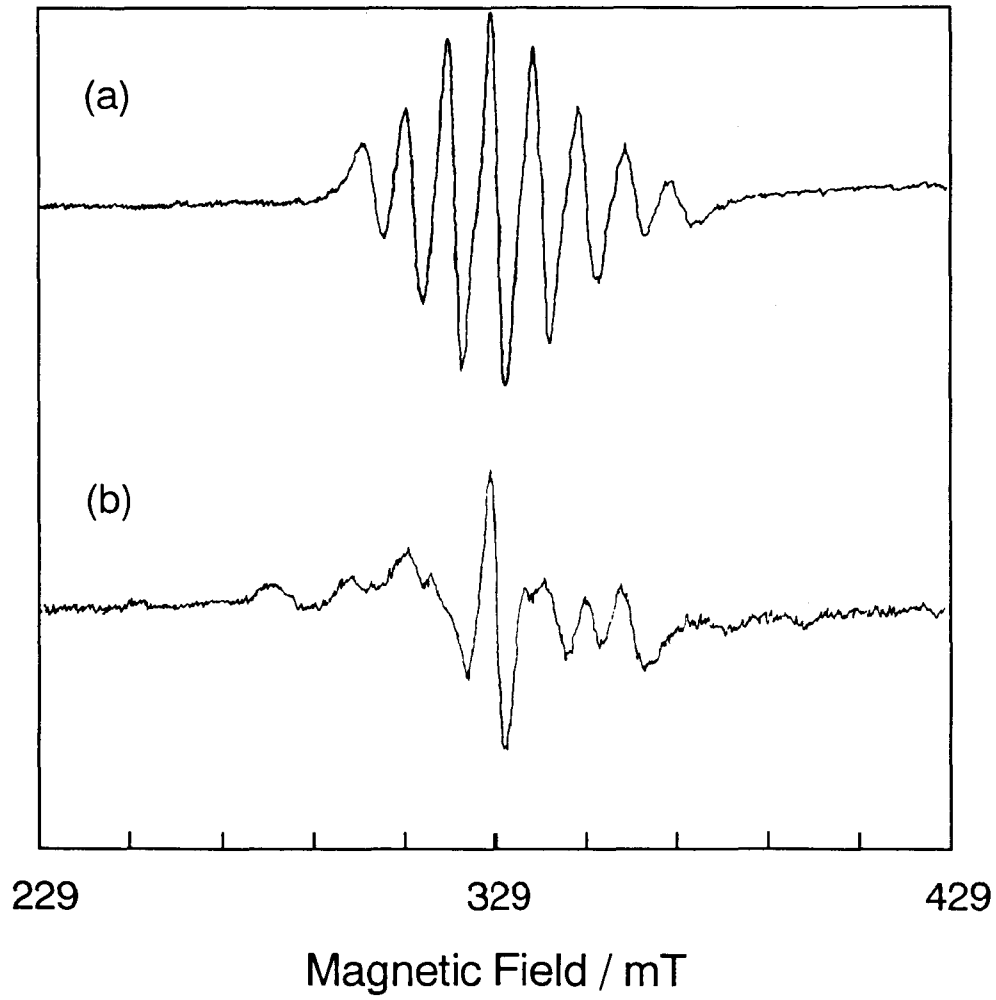

Figure 9 ESR spectra of VOAOMTPP and polyVOAOMTPP in benzene (1.3 mM) at room temperature.

magnetic field, existed in the powder of polyVOAOMTPP, polyVOAOMTPP was separated to the magnetoactive and magnetoinactive parts. ESR spectra of these parts are shown in Figure 10. The spectrum of the magnetoinactive part showed a signal in the 275-425 mT region due to paramagnetic VO(II) ion. On the other hand, the spectrum of the magnetoactive part showed the same signal of the magnetoinactive but superimposed on a broad signal in the whole magnetic field region. This finding indicates that the magnetoactive part comprised of the paramagnetic VO(II) ion and other magnetic sites.

ESR spectra of the magnetoactive part at 420, 150, and 4.2K are shown in Figure 11. The spectral intensities for the paramagnetic VO(II) ion (275-425 mT) decreased with an increase in the temperature, while those of the broad signal (0-500 mT), multiplied by a factor of 100, were almost independent of temperature. In order to compare the behavior of the magnetoactive part with that of a ferromagnet, ESR spectra of a powder of iron were measured at 420, 150, and 4.2K (Figure 12). The spectral intensities were almost independent of temperature similarly to the case of the magnetoactive part. These results suggest that the broad signal appeared in the ESR spectra of the magnetoactive part was not due to paramagnetic site, but may be due to a ferromagnet, which is produced by an ordering of paramagnetic species in the polymer or presence of a trace amount impurities. Since we could not carry out an elementary analysis for a contaminant such as iron in the magnetoactive part because of its small amount, we examined by ESR

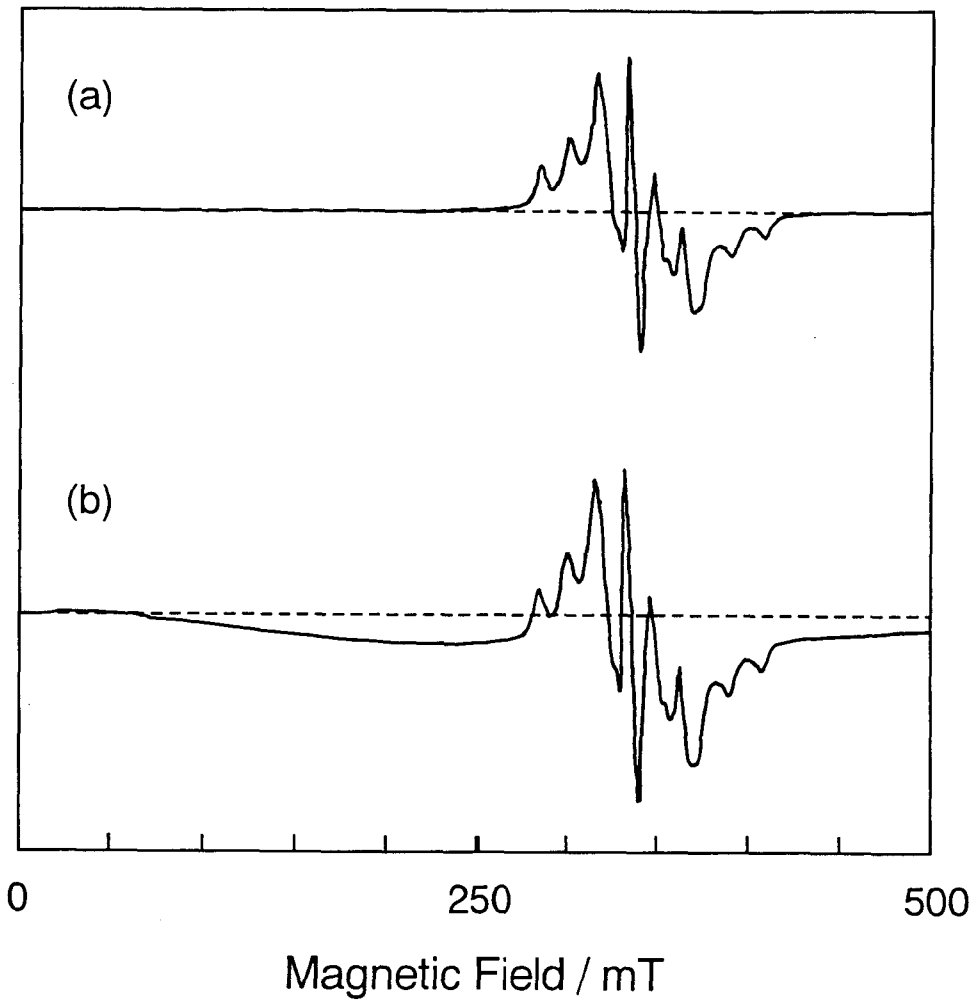

Figure 10 ESR spectra of powders of the magnetoinactive part (a) and the magnetoactive part (b) of polyVOAOMTPP at room temperature.

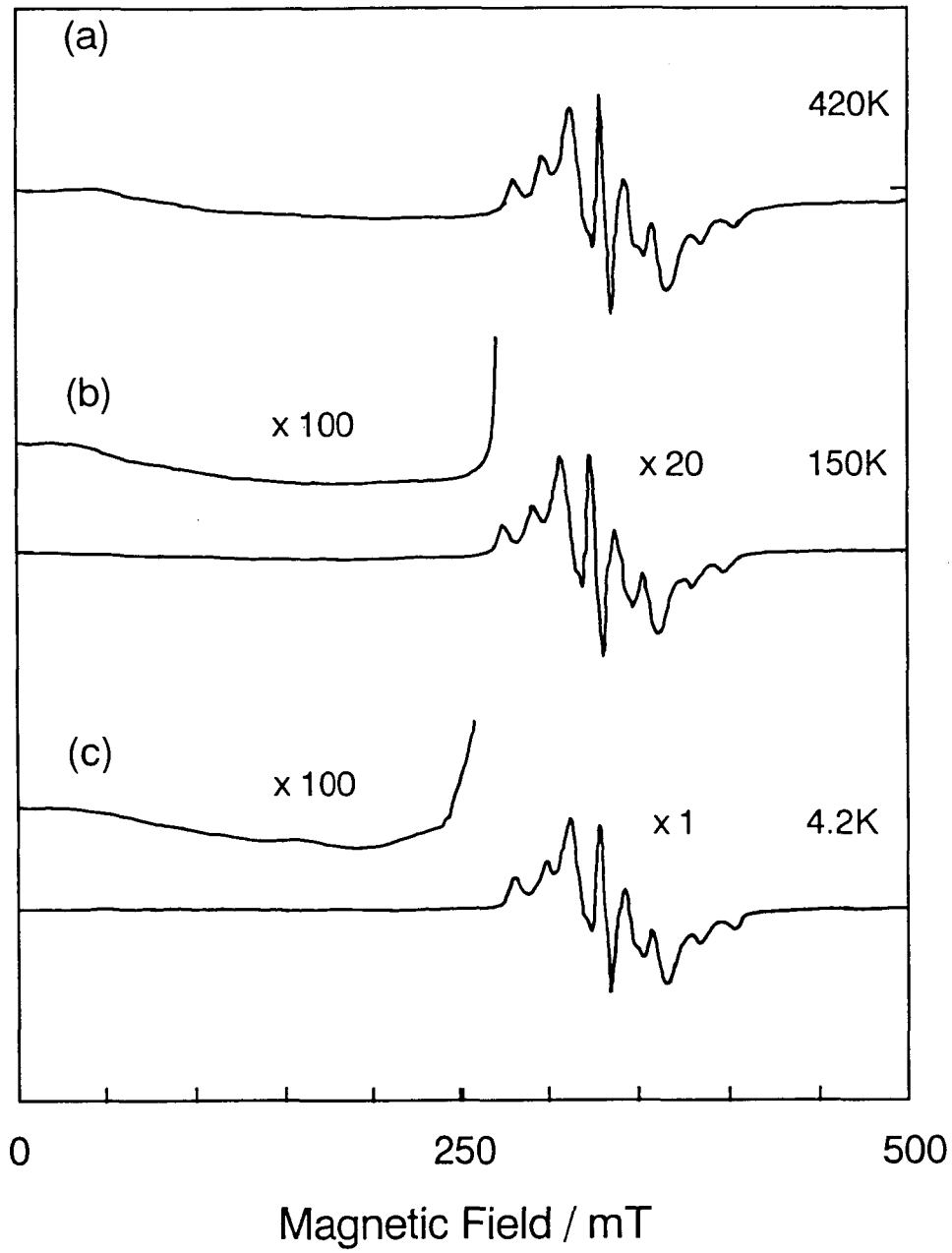

Figure 11 ESR spectra of powders of the magnetoactive part of polyVOAOMTPP at 420 (a), 150 (b), and 4.2K (c).

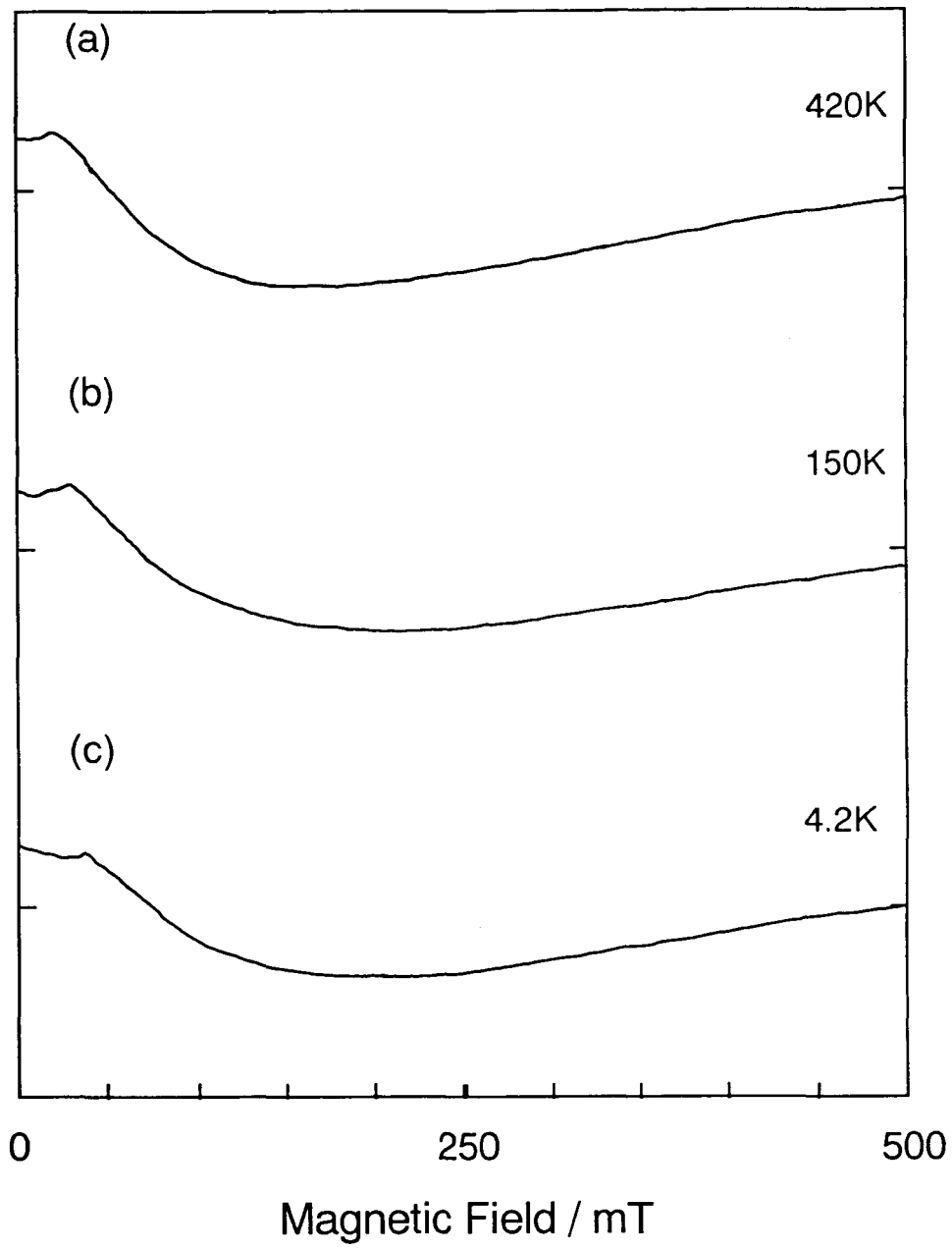

Figure 12 ESR spectra of a powder of iron at 420 (a), 150 (b), and 4.2K (c).

whether the magnetoactive part was due to the contaminant or not. ESR spectra of the powder of the magnetoactive part, iron, iron(III) oxide, and iron(II,III) oxide at room temperature were shown in Figure 13. The broad signal of the magnetoactive part was different from those of the iron compounds and could not be simulated by those. Accordingly, this finding suggests that the ferromagnetic behavior of polyVOAOMTPP is not due to contaminants involved in the polymer.

Temperature dependence of an inverse magnetic susceptibility and a magnetic moment of the magnetoinactive part of polyVOAOMTPP is shown in Figure 14. The magnetic moment increased with a decrease in temperature. It should be noted that the polymer has a ferromagnetic interaction with the Weiss temperature of +5K. In the previous research in our laboratory, polyVOAOTPP had antiferromagnetic interaction with the Weiss temperature of -170K.[6] This difference may result from the differences of the distance and/or the orientation between porphyrin moieties described above. It has been reported theoretically that a magnetic interaction between paramagnetic sites changes from antiferromagnetic to ferromagnetic by the orientation between the sites changing.[8] In this study, the distance and/or the orientation between porphyrin moieties in polyVOAOMTPP may be good enough to interact ferromagnetically. Furthermore, a small part of this polymer, which is the magnetoactive site, may be in the distance and/or in the orientation enough to form a ferromagnet.

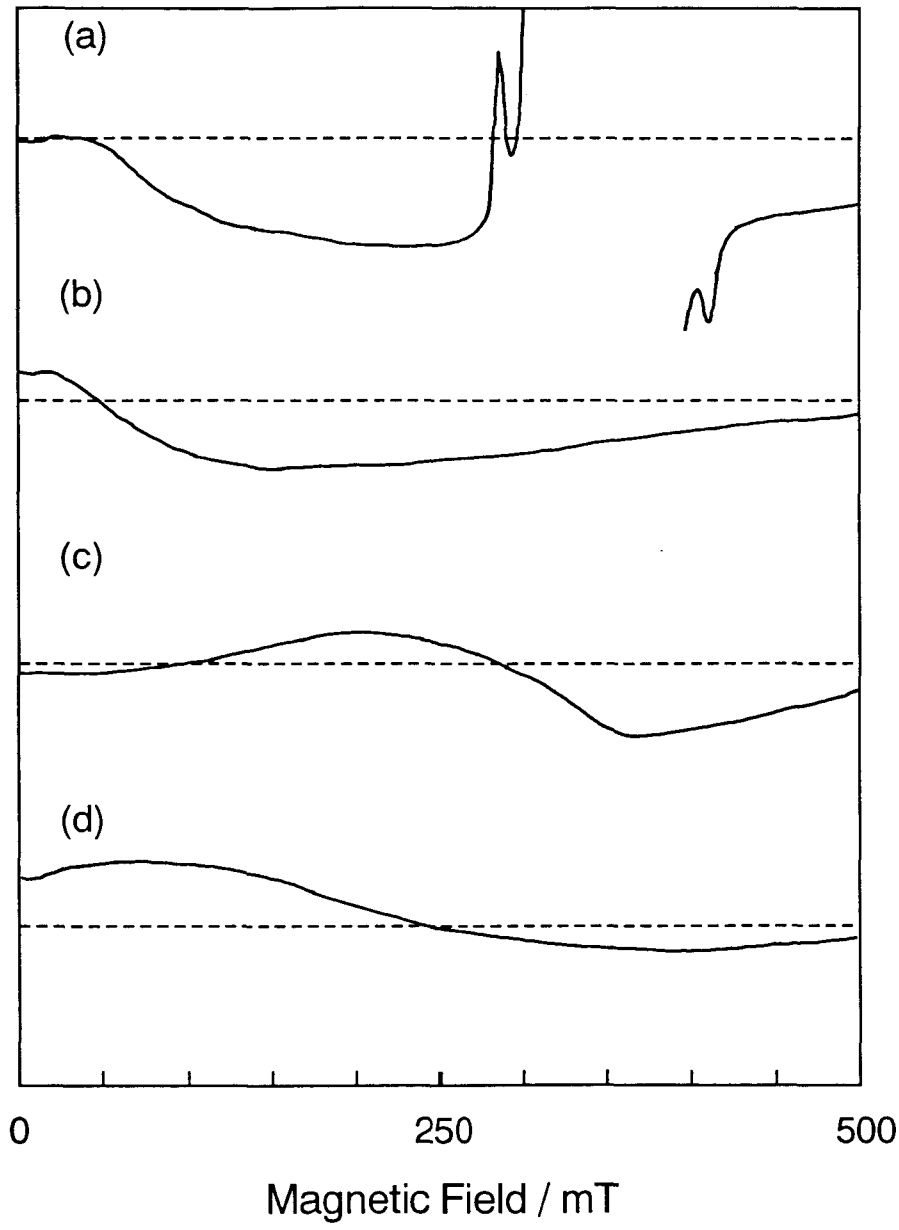

Figure 13 ESR spectra of powders of the magnetoactive part of polyVOAOMTPP (a), iron (b), iron(III) oxide (c), and iron(II,III) oxide (d) at room temperature.

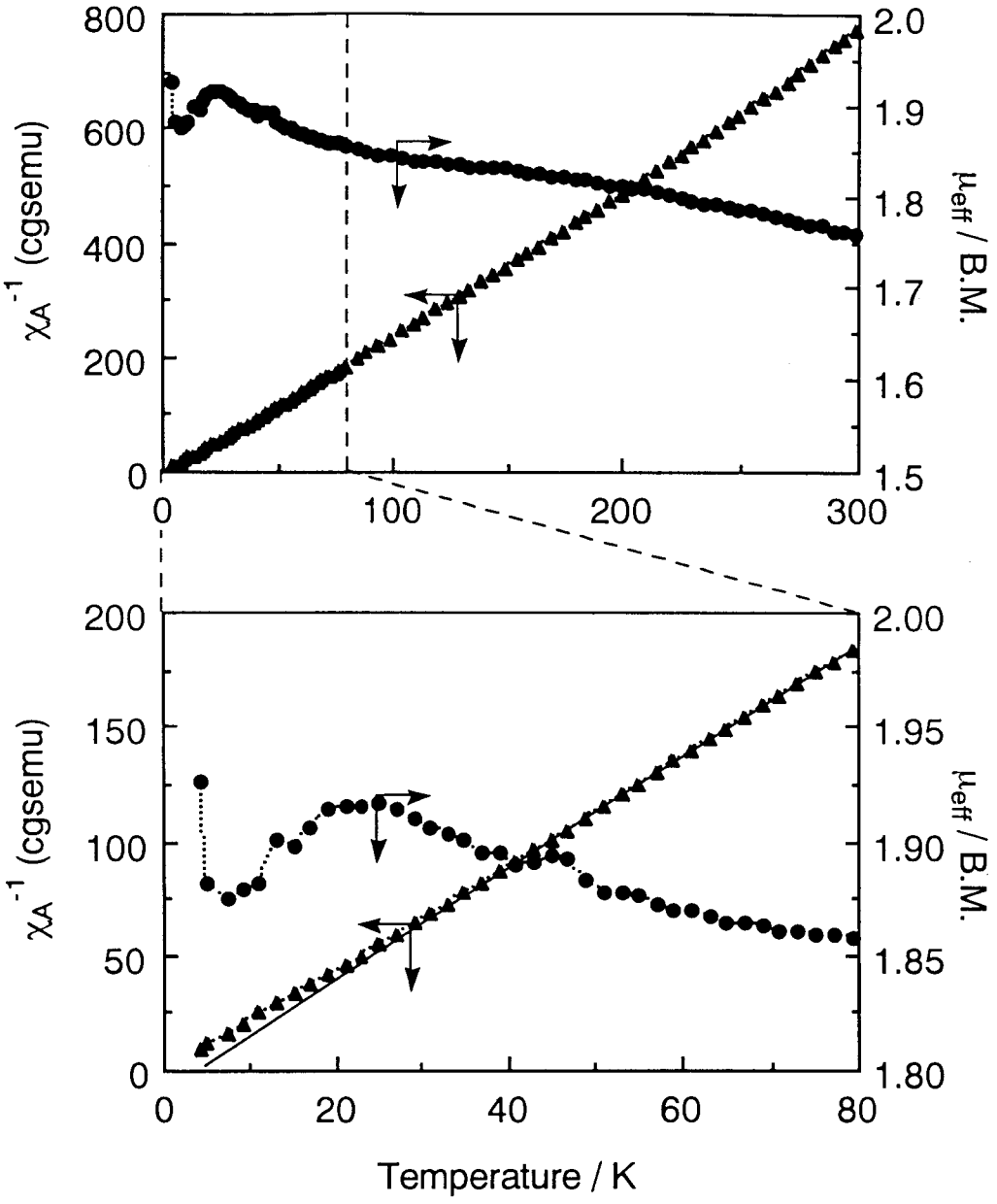

Figure 14 Temperature dependence of an inverse magnetic susceptibility and an effective magnetic moment of the magnetoinactive part of polyVOAOMTPP.

3.4. Conclusion

CuCuDPE, VOVODPE, MnMnDPE, CuMnDPE, and VOMnDPE had weak antiferromagnetic interactions through their amide bond and/or through space, but that ferrimagnets didn't exist in CuMnDPE and VOMnDPE because the magnetic interactions were weak.

PolyCuAOMTPP showed antiferromagnetic interaction with the Weiss temperature of -38K. This polymer had stronger magnetic interaction than polyCuAOTPP.

PolyVOAOMTPP had a small magnetoactive part. The ESR spectrum of the magnetoactive part contained a broad signal of which the intensity was almost independent of the temperature similar to behavior of a ferromagnet. Contaminants such as iron compound were not detected in the polymer. The magnetoinactive part showed a weak ferromagnetic interaction with the Weiss temperature of +5K. These results may be caused by the formation of a magnetic domain where the arrangement of the magnetic sites was good enough to interact magnetically.

References

1) Kamachi, M.; Akimoto, H.; Mori, W.; Kishita, M. *Polym. J.* **1984**, *16*, 23.

2) Kamachi, M.; Cheng, X. S.; Kida, T.; Kajiwara, A.; Shibasaka, M.; Nagata, S. *Macromolecules* **1987**, *20*, 2665.

3) Nozakura, S.; Kamachi, M. *Makromol. Chem. Suppl.* **1985**, *12*, 255.

4) Kamachi, M.; Cheng, X. S.; Nozakura, S. *Fifth Rare Earth Symposium.* (Tokyo, 1987), Preprints 2B05.

5) Kamachi, M.; Cheng, X. S.; Aota, H.; Mori, W.; Kishita, M. *Chem. Lett.* **1987**, 2331.

6) Cheng, X. S. Doctral Thesis, Osaka University, Osaka (1987).

7) (a) Kivelson, D.; Lee, S. K. *J. Chem. Phys.* **1964**, *41*, 1896. (b) Assour, J. M. *J. Chem. Phys.* **1965**, *43*, 2477. (c) Lin, W. C. Electron spin resonance and electronic structure of metalloporphyrins. In *The Porphyrins* ; Dolphin, D., Ed.; Academic Press: New York, 1979; Vol. IV, pp 355.

8) Iwamura, H. *Pure & Appl. Chem.* **1986**, *58*, 187.

Chapter 4

Photophysical Behavior of Compartmentalized ZnTPP

4.1. Introduction

Metalloporphyrins play an important role as functional groups in wide variety of biological systems. For instance, magnesiumchlorins act as sensitizers as well as redox chromophores in photosynthetic systems, while iron porphyrins act as catalytic centers in oxidases and catalases [1], electron carriers in cytochromes [2] and oxygen carriers in hemoglobins.[3]

The photophysical and photochemical properties of porphyrins have been studied intensively because of their usefulness as photosensitisers for transformation of solar energy into a storable form of energy. The possibility of using water soluble ZnTPP derivatives as a photosensitizer for the oxidation of water to oxygen in a photosystem that might serve as a generator of hydrogen has been well established.[4]

In recent years, Morishima et al.[5] have carried out a number of studies focussing on amphiphilic polyelectrolytes covalently tethered with functional groups. These systems are interesting because properties of the functional groups can be largely modified by the microenvironment provided by such polymers. If the content of hydrophobic units in an amphiphilic polyelectrolyte is sufficiently high, then the polymer may assume a micellelike structure in aqueous solution where the hydrophobic units form an interior domain surrounded by the charged outer layer [6]. The hydrophobic microdomain thus formed is "rigid" and "static" in nature as compared to dynamic nature of conventional surfactant micelles and vesicles.

When a small mole fraction of a hydrophobic functional group is covalently incorporated into such amphiphilic polyelectrolytes, the functional group is encapsulated in the hydrophobic domain and is forced to experience an unusual microenvironment [5a,7]: i.e., (1) the functional group is isolated or protected from the aqueous phase and placed in a nonpolar environment, (2) its molecular motions are highly restricted owing to the motional rigidity of the hydrophobic domain, and (3) electrostatic potential is exerted to the functional group by the changed outer layers.

Such unusual microenvironments for the compartmentalized functional group, unlike the conventional molecular assembly systems, may greatly change its physicochemical properties and chemical reactivities.

Morishima et al.[5] previously reported that photophysics and photochemistry of polycyclic aromatic chromophores such as phenanthrene and pyrene compartmentalized in amphiphilic polyelectrolytes were very much different from those in homogeneous solution. For example, fast electron transfer occurred from the compartmentalized photoexcited aromatics to methylviologen ionically bound on the surface of the microdomains, while back electron transfer was considerably slowed, and thus effective charge separation was achieved.[5a,7b]

We have chosen compartmentalized and non-compartmentalized ZnTPP as model systems and studied their photophysical behavior by absorption and emission spectroscopies.

4,2. Experimental Section

4,2,1. Materials

Syntheses of copolymer poly(A/ZnTPP) and terpolymers poly(A/La/ZnTPP), poly(A/Np/ZnTPP), and poly(A/Cd/ZnTPP) were described in Chapter 2. The content of the ZnTPP residue was limited to about 0.2 mol%, as shown in Table II in Chapter 2, to avoid chromophore-chromophore interactions.

5,10,15,20-Tetrakis(4-sulfonatophenyl)porphinatozinc (ZnTSPP) was prepared according to the method of Kalyanasundaram.[8] Crude ZnTSPP was purified by passing through a Sephadex LH-20 column with water as an eluent.

Water was doubly distilled. N,N-Dimethylformamide (DMF) was of spectroscopic grade.

4,2,2. Measurements

Absorption spectra were recorded on a Shimadzu UV-2100 spectrophotometer at room temperature.

Fluorescence spectra were recorded on a Shimadzu RF-5000 spectrofluorophotometer at room temperature. Absorbances of the sample solutions were adjusted to 0.050 at the absorption maximum of the Soret band at which wavelength the samples were excited.

Delayed emission spectra were recorded on a Shimadzu RF-502A spectrofluorometer with a phosphorescence attachment, including a cylindrical chopper operated at a frequency of 50Hz, at various temperatures. To control the temperature of the sample solutions, a n

optical cell with the sample solution was immersed in water in a Pyrex vessel prepared for this measurement, and water was circulated from a thermostat bath. Excitation wavelengths for the solutions were at the absorption maximum of the Soret band. Concentrations of the ZnTPP residues of the solutions were adjusted to 1 μM. The solutions were deaerated by bubbling with argon for 30 min.

Laser photolysis was performed by using a Q-switched Nd:YAG laser (Quantaray DCR-2) operated at second harmonic (120 mJ per flash at 532 nm with a 7-ns fwhm) at room temperature. An analyzing beam from a 150-W xenon arc lamp passing through a 430-nm cut-off filter (Toshiba Y-43) was set perpendicular to the laser beam. The details of the laser apparatus have been reported from our laboratory.[7a)] Concentrations of 10 and 100 μM of the ZnTPP residue aqueous solutions were used for the measurement of the transient absorption spectra in the regions from 430 to 550 nm and from 550 to 850 nm, respectively. The solutions were deaerated by bubbling with argon for 30 min.

4,3. Results and Discussion

4,3,1. Absorption and Fluorescence Spectra

Absorption spectra of the monomer and polymers in DMF solutions are shown in Figure 1-a. Poly(A/ZnTPP) was dissolved in DMF/water (9/1:v/v) because of poor solubility in DMF. All the compounds showed the Soret bands at ca.425 nm and the Q bands in the 500-700

nm region.[9] The absorption maxima of the Soret bands for all the polymers in DMF solutions were about the same as that of the monomer (ZnAATPP). Spectral profiles of the Soret bands for all the polymers closely resembled that of the monomer. This means that no electronic perturbations exist in the ZnTPP moieties in the polymers. Therefore, we assumed that molar extinction coefficients (ε) of ZnTPP moieties in the polymers were equal to that of the monomer (642000 $M^{-1} cm^{-1}$). The contents of the ZnTPP moieties in the polymers were calculated by using this value. The contents thus determined were listed in Table II in Chapter 2. The values of ε for the Soret and Q bands for the ZnTPP moieties in the polymers calculated on the basis of the ε value for the Soret band of the monomer are summarized in Table I. Although the absorption maxima of the Q bands of all the polymers were nearly equal to that of the monomer, the apparent ε values for the polymers were slightly different from that of the monomer. In the poly(A/ZnTPP) and poly(A/Np/ZnTPP) cases, new absorption bands appeared around 630 nm, which may be due to impurities generated by photooxidation[10] of the ZnTPP moieties in the process of polymerization and/or purification of the polymers. It was confirmed that free-base TPP, which can be generated by releasing the zinc ion from ZnTPP, was almost absent, because no absorption band (ε=18700 $M^{-1} cm^{-1}$ at 514 nm in benzene[4a]) around 515 nm due to free-base TPP was detected.

Absorption spectra of the polymers in aqueous solutions are shown in Figure 1-b and the values of ε are summarized in Table I.

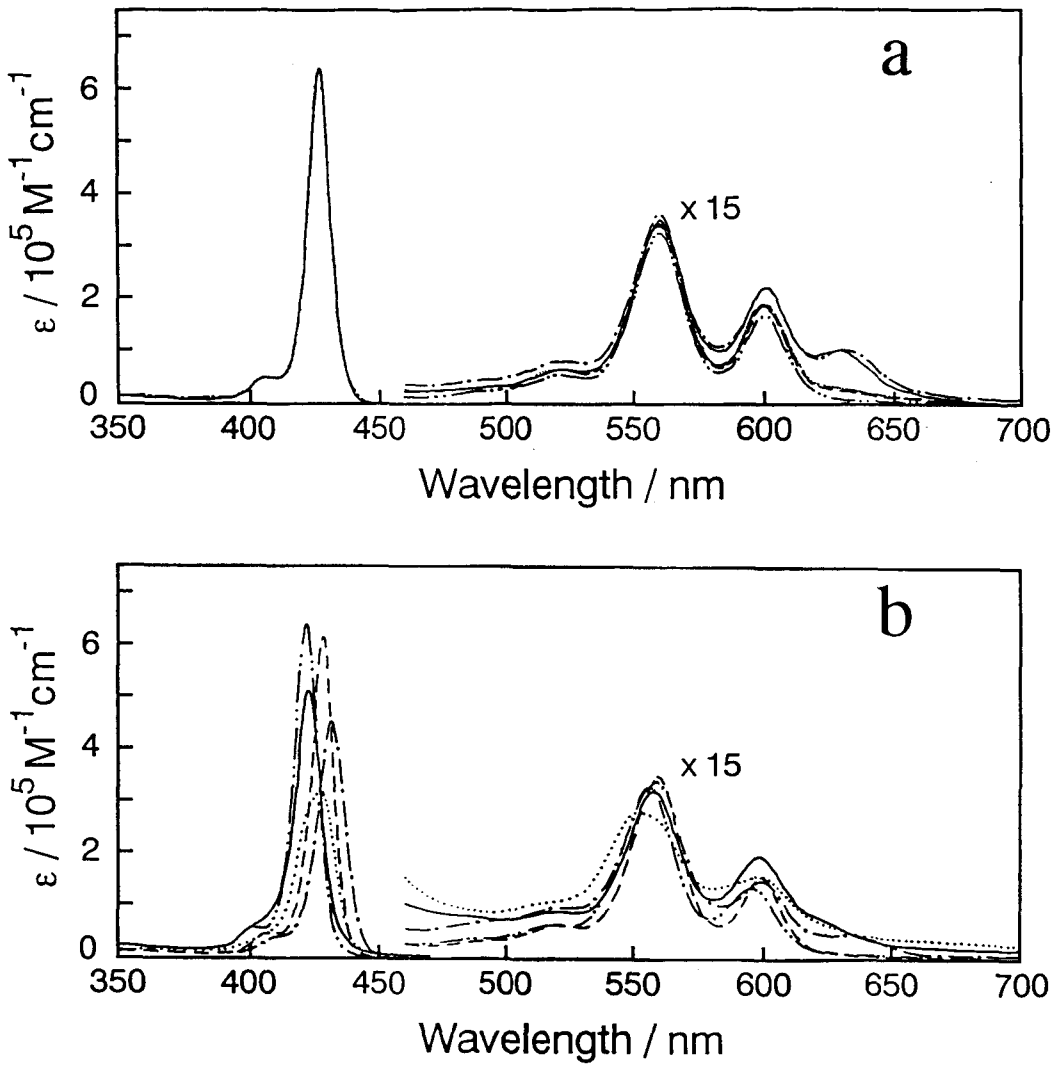

Figure 1. Absorption spectra of the terpolymers, the reference copolymer, ZnAATPP, and ZnTSPP: **a**, in DMF for the terpolymers and ZnAATPP and DMF/water (9/1 : v/v) for the reference copolymer; **b**, in water; — — —, poly(A/La/ZnTPP); —— • ——, poly(A/Np/ZnTPP); ·····, poly(A/Cd/ZnTPP); ————, poly(A/ZnTPP); —— • • ——, ZnAATPP in DMF and ZnTSPP in water.

Table I. Spectroscopic Data of the Monomer, Polymers, and ZnTSPP

	DMF solution ε/ $M^{-1}c\,m^{-1}$ (wavelength/nm)			aqueous solution ε/ $M^{-1}c\,m^{-1}$ (wavelength/nm)		
sample code	Soret	Q(1,0)	Q(0,0)	Soret	Q(1,0)	Q(0,0)
ZnAATPP	642000 (426.2)	21700 (559.6)	11100 (599.8)	——	——	——
poly(A/ZnTPP)	642000 [b] (426.6) [a]	23100 [a] (560.0) [a]	14700 [a] (600.2) [a]	514000 (422.0)	21600 (557.8)	13200 (597.8)
poly(A/La/ZnTPP)	642000 [b] (426.6)	22700 (559.4)	12500 (599.6)	618000 (427.8)	23300 (559.0)	10500 (598.4)
poly(A/Np/ZnTPP)	642000 [b] (427.0)	24000 (559.4)	14600 (600.2)	455000 (431.2)	22700 558.2)	10000 (598.8)
poly(A/Cd/ZnTPP)	642000 [b] (426.6)	22800 (559.4)	12500 (600.0)	321000 (427.4)	18700 (551.2)	10600 (598.2)
ZnTSPP	——	——	——	640000 (421.2)	22000 (555.6)	9100 (594.6)

[a] Solvent: DMF/water=9/1 (V/V).

[b] The molar extinction coefficient (ε) of the ZnTPP moieties in the polymers was assumed to be equal to ε of ZnAATPP in DMF solution.

Although absorption spectra in the region of the Soret bands in DMF solutions were almost the same among the polymers, those in aqueous solutions were quite different. The absorption maximum of the Soret band of the reference copolymer poly(A/ZnTPP) was almost equal to that of ZnTSPP, but the absorption maxima for the terpolymers were red-shifted by 5-10 nm from those of ZnTSPP and poly(A/ZnTPP). These findings indicate that the ZnTPP moieties in the terpolymers in aqueous solution exist in quite different microenvironments from that of the reference copolymer. The ZnTPP moieties in the terpolymers are expected to exist in hydrophobic domains of the terpolymers in aqueous solution, while those in the reference copolymer are exposed to the aqueous phase. It is to be noted that the absorption maxima and band profiles of the Soret absorption of the terpolymers are different for different hydrophobic groups in the terpolymers. In the Np terpolymer, the Soret band was most red-shifted, while in the Cd terpolymer, there was significant broadening of the absorption band in the Soret region with a concomitant decrease in the peak intensity. These observations imply that the microenvironments around the ZnTPP moieties are different for different hydrophobic groups in the terpolymers. The absorption maxima at the Q bands seem to be less sensitive to the microenvironments around the ZnTPP chromophores.

Fluorescence spectra of ZnTSPP and the co- and terpolymers in aqueous solutions are shown in Figure 2. The fluorescence band of poly(A/La/ZnTPP) and poly(A/Np/ZnTPP) resembled that of ZnTSPP, but the fluorescence of poly(A/Cd/ZnTPP) slightly differed from that

of ZnTSPP. This suggests that the surroundings of the ZnTPP moieties in poly(A/Cd/ZnTPP) are slightly different from those in the other terpolymers.

4,3,2. Transient Absorption Spectra

In Figure 3, time-resolved transient absorption spectra for poly(A/Cd/ZnTPP) were compared with those of poly(A/ZnTPP) in aqueous solution at room temperature. The spectra are assignable to the $T_n \leftarrow T_1$ absorption bands of the ZnTPP moieties by comparing with spectra reported for ZnTPP itself.[11] A striking observation was that the triplet absorption bands of the Cd terpolymer persisted for much longer time than those of the reference copolymer as is evident from Figure 3. Similarly persistent transient absorption spectra were observed for poly(A/La/ZnTPP) and poly(A/Np/ZnTPP).

The decay profiles of T_1 and the first-order plots for ZnTSPP and all the polymers monitored at 480 nm in DMF and aqueous solutions are shown in Figure 4. In aqueous solution, the decays for the terpolymers were much slower than that for the reference copolymer. The decays for the Cd and Np terpolymers and that of the reference copolymer approximately followed the first-order kinetics in aqueous solution, while there were portions of initial fast decay component in the La terpolymer. In DMF solution, on the other hand, decay rates for the terpolymers and the copolymer are not much different, although all the decays contained initial fast decay components. In particular, the copolymer showed a considerably larger fraction of initial fast decay component than the terpolymers did. These initial

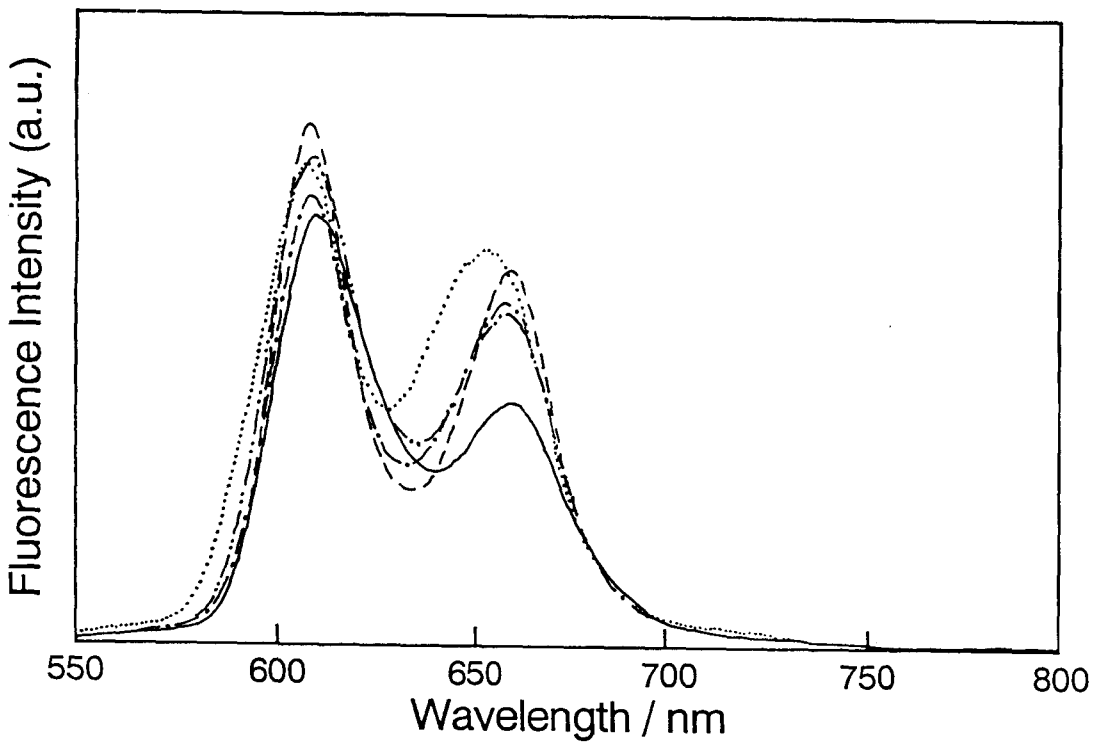

Figure 2. Fluorescence spectra of the terpolymers, the reference copolymer, and ZnTSPP in aqueous solution by excitation at the maxima of the Soret bands at room temperature: — — —, poly(A/La/ZnTPP); —— • ——, poly(A/Np/ZnTPP); ·····, poly(A/Cd/ZnTPP); ————, poly(A/ZnTPP); —— • • ——, ZnTSPP.

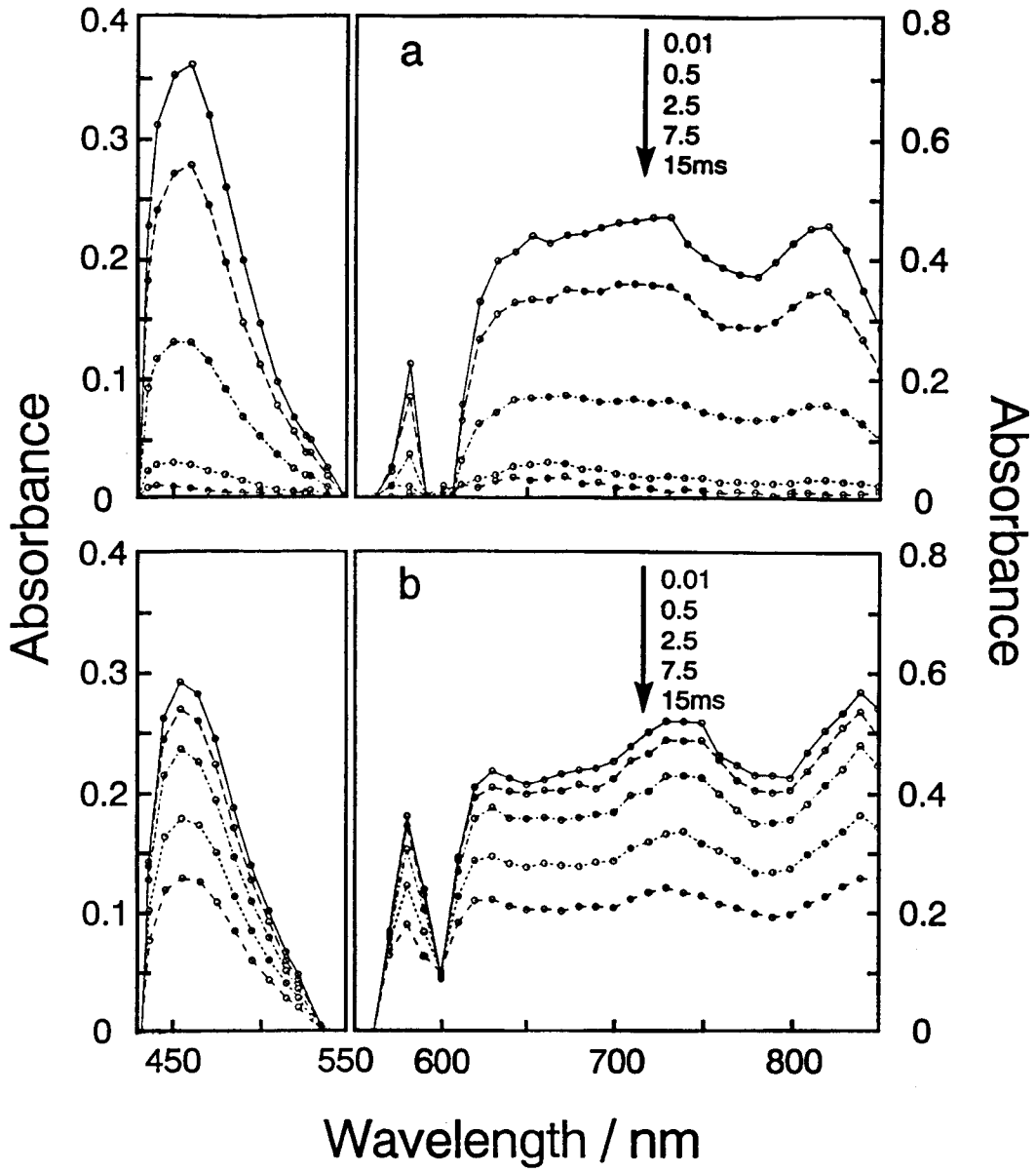

Figure 3. Comparison of time-resolved transient absorption spectra in aqueous solution at room temperature: **a**, poly(A/ZnTPP); **b**, poly(A/Cd/ZnTPP)

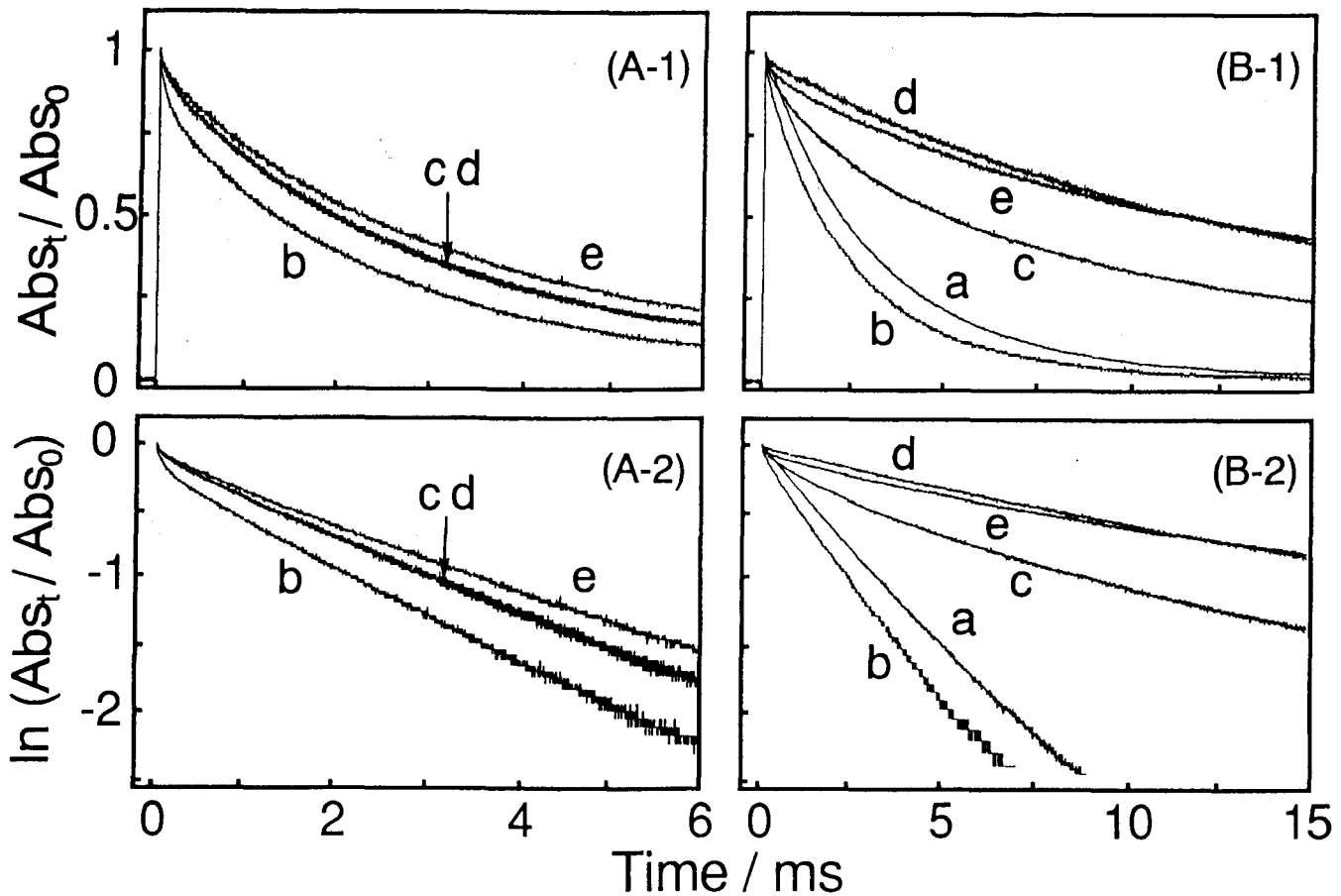

Figure 4. Decay profiles (A-1 and B-1) and the first-order plots (A-2 and B-2) of transient absorption monitored at 480 nm for ZnTSPP and all the polymers in DMF (A) and aqueous solution (B): **a**, ZnTSPP; **b**, poly(A/ZnTPP); **c**, poly(A/La/ZnTPP); **d**, poly(A/Np/ZnTPP); **e**, poly(A/Cd/ZnTPP): Abs_t and Abs_0 represent absorbances at time t and t=0, respectively.

fast decays are presumably due to T_1-T_1 annihilation.[12] In the reference copolymer in aqueous solution, both intramolecular and intermolecular charge repulsions prevent the ZnTPP moieties from encountering each other, thereby the triplet annihilation being prevented. In DMF, on the other hand, the triplet annihilation can occur because the charge repulsions are much weaker. Since each ZnTPP moiety is separately compartmentalized in the hydrophobic domains in the terpolymers in aqueous solution, the triplet annihilation is likely to be suppressed. In DMF, however, the terpolymers probably assume random coils in which the triplets may encounter each other within their lifetimes, thus leading to the triplet annihilation.

Another reason for the initial fast decay may be T_1 quenching by oxygen. We cannot rule out this possibility because the complete removal of oxygen from sample solutions is difficult. Even though this is the case, the triplet quenching by oxygen may be suppressed by steric protection in the compartmentalized ZnTPP systems.
Lifetimes of T_1 estimated from the slopes of the linear portions of the decay profiles shown in Figure 4 and initial absorbances immediately after laser excitation are summarized in Table II. Lifetimes of T_1 for the reference copolymer in water and in DMF were practically the same. In striking contrast, lifetimes for the terpolymers in water were much longer than those in DMF.

Triplet lifetimes of ZnTPP itself have been reported to be 1.19 and 1.25 ms in ethanol and toluene fluid solutions at 300K,

Table II. Initial Absorbances (Abs_0) and Lifetimes of Triplet Excited State (τ_t) for ZnTSPP and the Co- and Terpolymers

	DMF solution		aqueous solution	
sample code	Abs_0	τ_t/ms	Abs_0	τ_t/ms
poly(A/ZnTPP)	0.38 [a]	3.0 [a]	0.26	3.0
poly(A/La/ZnTPP)	0.42	3.7	0.45	12
poly(A/Cd/ZnTPP)	0.42	4.3	0.25	20
poly(A/Np/ZnTPP)	0.41	3.8	0.33	19
ZnTSPP			0.53	3.5

[a] Solvent: DMF/water=9/1 (V/V).

respectively,[13] while its phosphorescence lifetimes have been reported to be 25 and 26 ms in ethanol and toluene rigid glasses at 77K, respectively.[13] Thus the unusually long lifetimes observed in the present study for the terpolymers in aqueous solution at room temperature are due to a remarkable effect of the compartmentalization. The hydrophobic residues around the compartmentalized ZnTPP moieties serve not only as protection groups for the chromophores but also as a rigid microenvironment for

the chromophores similar to glass matrices at 77K even though the terpolymers are in fluid solution. In this context, the Cd and Np groups seem to be more effective than the La group to tightly wrap up the ZnTPP moieties in their hydrophobic domains.

4,3,3. Delayed Emission Spectra

The quantum yield of phosphorescence ϕ_p is given by [14]

$$\phi_p = \phi_{ST} k_p^0 \tau_T \qquad (1)$$

where ϕ_{ST} is the quantum yield of intersystem crossing, k_p^0 is the radiative rate of phosphorescence, and τ_T is the lifetime of the triplet excited state given by eq.(1). Studies to date [15] have revealed that zinc porphyrin generally shows only "prompt" fluorescence at room temperature in fluid solution, although it shows both fluorescence and phosphorescence in rigid glasses at 77K. If τ_T at room temperature is sufficiently long, there is a possibility that phosphorescence is observed even in a fluid solution at room temperature. Delayed emission spectra of ZnTSPP, the reference copolymer, and the terpolymers in aqueous solution at 25°C are shown in Figure 5. An interesting observation was that the terpolymers in deaerated aqueous solution showed delayed emissions, while ZnTSPP and poly(A/ZnTPP) showed no such delayed emissions. It is important to note that the delayed emission consisted of both phosphorescence above 700 nm and fluorescence below 700 nm. The delayed fluorescence was quenched by oxygen as sensitively as phosphorescence, indicating that the singlet excited state for the delayed fluorescence was generated from triplet excited state (T_1).

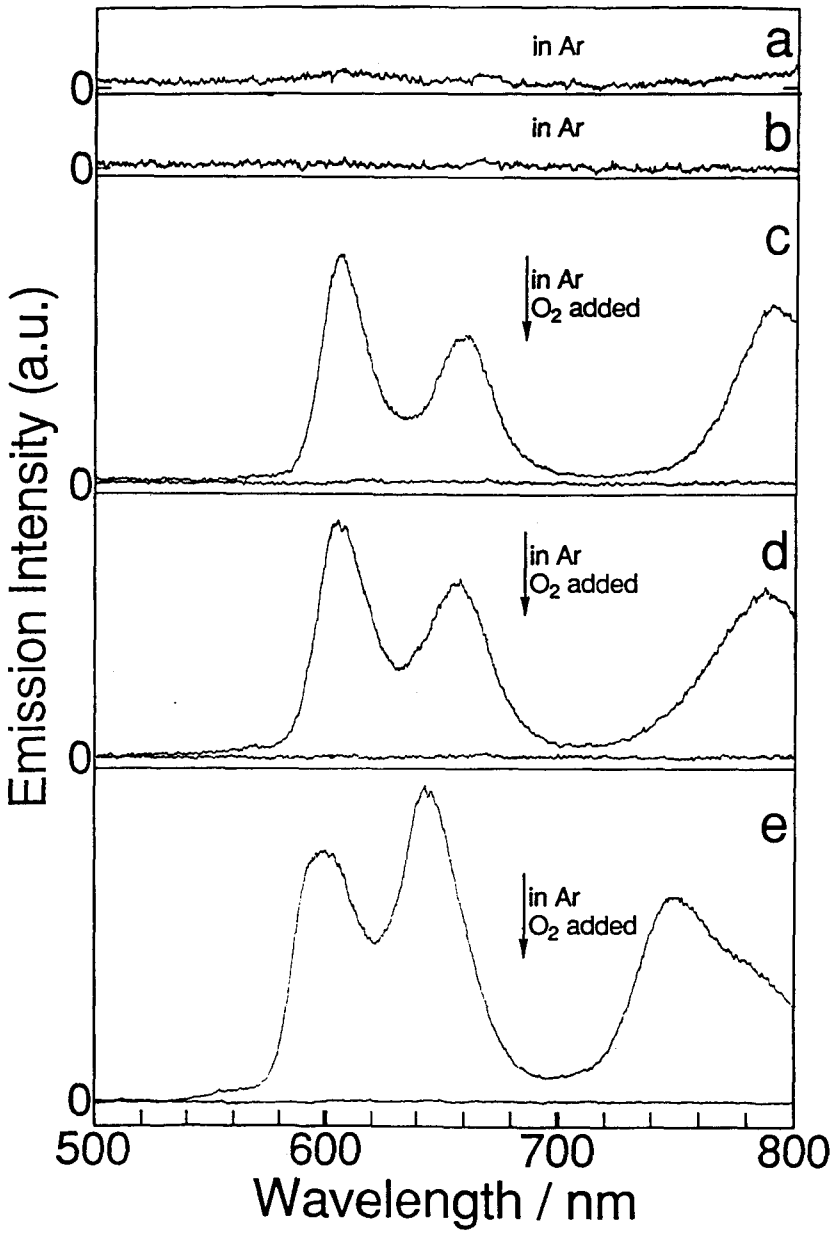

Figure 5. Delayed emission spectra for ZnTSPP and all the polymers in aqueous solution at 25°C observed at a delay time of 5 ms: **a**, ZnTSPP; **b**, poly(A/ZnTPP); **c**, poly(A/La/ZnTPP); **d**, poly(A/Np/ZnTPP); **e**, poly(A/Cd/ZnTPP).

In general, delayed fluorescence can be divided into two types [14]:

The first type is that T_1 is thermally popped back into S_1 (Thermally activated delayed fluorescence, TADF)

$$T_1 \xrightarrow{\text{heat}} S_1 \longrightarrow S_0 + h\nu\,(\text{fluorescence}) \quad (2)$$

The second type is that S_1 is generated resulting from triplet-triplet annihilation (T-T annihilation delayed fluorescence)

$$T_1 + T_1 \longrightarrow S_1 + S_0 \longrightarrow 2S_0 + h\nu\,(\text{fluorescence}) \quad (3)$$

Since no such T-T annihilation occurs in the terpolymers in aqueous solution, the delayed fluorescence observed in the present study may be TADF. In TADF, the emission intensity ratio of TADF to phosphorescence increases with an increase in temperature. Delayed emission spectra observed at various temperatures are shown in Figure 6. In fact, the delayed fluorescence intensity for all the terpolymers increased with an increase in temperature. On the contrary, the phosphorescence intensity decreased with an increase in temperature. Thus, this delayed fluorescence is attributed to TADF. The intensities of both TADF and phosphorescence for poly(A/La/ZnTPP) and poly(A/Np/ZnTPP) changed with temperature, but the spectral profiles remained unchanged. However, in the case of poly(A/Cd/ZnTPP), the spectral profiles significantly changed.

The activation free energy gap (ΔE) between T_1 and S_1 can be

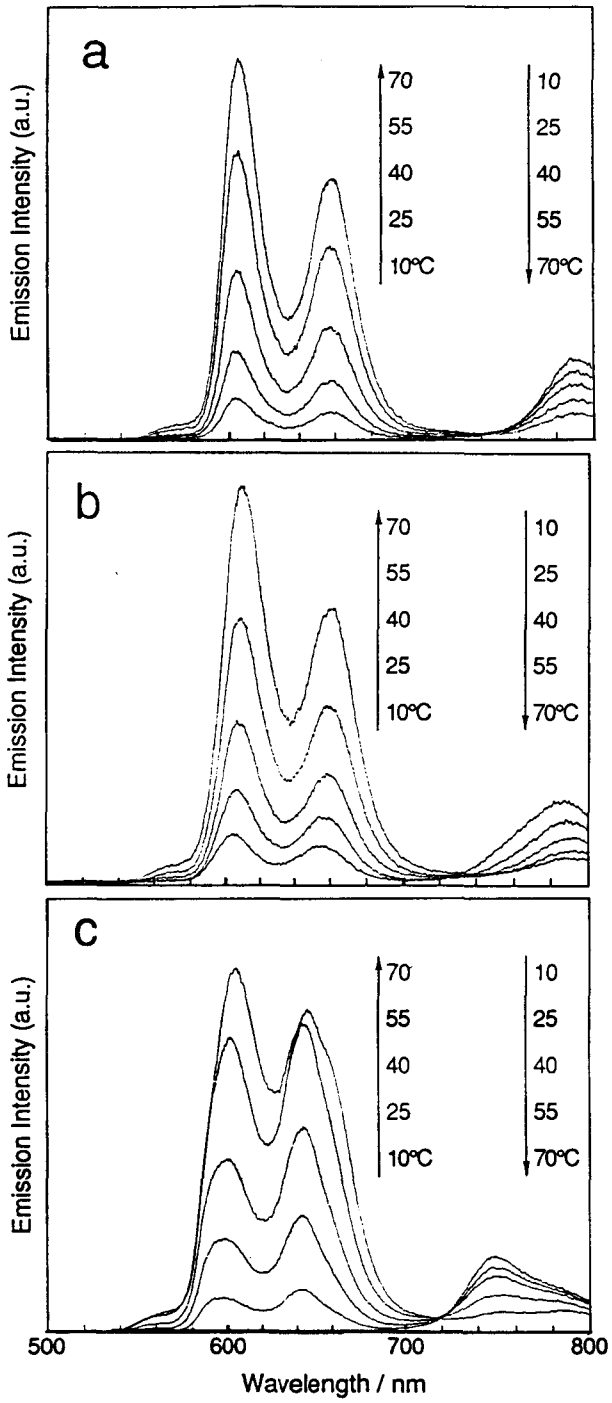

Figure 6. Delayed emission spectra of the terpolymers in deaerated aqueous solution recorded at varying temperatures: **a**, poly(A/La/ZnTPP); **b**, poly(A/Np/ZnTPP); **c**, poly(A/Cd/ZnTPP).

estimated by using following equations:

$$I_{TADF} = \phi_f k'_{isc} [T_1] \exp(-\Delta E / RT) \quad (4)$$

$$I_p = k_p [T_1] \quad (5)$$

then

$$I_{TADF} / I_p = (\phi_f k'_{isc} / k_p) \exp(-\Delta E / RT) \quad (6)$$

where I_{TADF} and I_p are the emission intensities of TADF and phosphorescence, respectively, ϕ_f is the quantum yield of fluorescence, k'_{isc} is the rate constant of intersystem crossing from T_1 to S_1, k_p is the radiative rate constant of phosphorescence, $[T_1]$ is the concentration of T_1, R is the gas constant, and T is the Kelvin temperature. Arrhenius' plots of for poly(A/La/ZnTPP) and poly(A/Np/ZnTPP) are shown in Figure 7. The ΔE values estimated from the slopes of the plots are 44.9 ± 0.8 kJ mol^{-1} for poly(A/La/ZnTPP) and 44.2 ± 0.8 kJ mol^{-1} for poly(A/Np/ZnTPP), but the ΔE value for poly(A/Cd/ZnTPP) was not able to be estimated because the spectral profiles changed when temperature was changed. On the basis of the emission maxima of fluorescence and phosphorescence, 607 and 790 nm for the poly(A/La/ZnTPP), and 608 and 786 nm for the poly(A/Np/ZnTPP), respectively, the energy gaps can be estimated to be 45.6 kJ mol^{-1} for poly(A/La/ZnTPP) and 44.5 kJ mol^{-1} for poly(A/Np/ZnTPP), being in fair agreement with the observed values.

Studies on TADF and phosphorescence at room temperature have only been reported for zinc, magnesium, and tin protoporphyrin IX dimethyl esters absorbed on filter papers.[16] To our best knowledge, we are the first to observe TADF of metalloporphyrins in

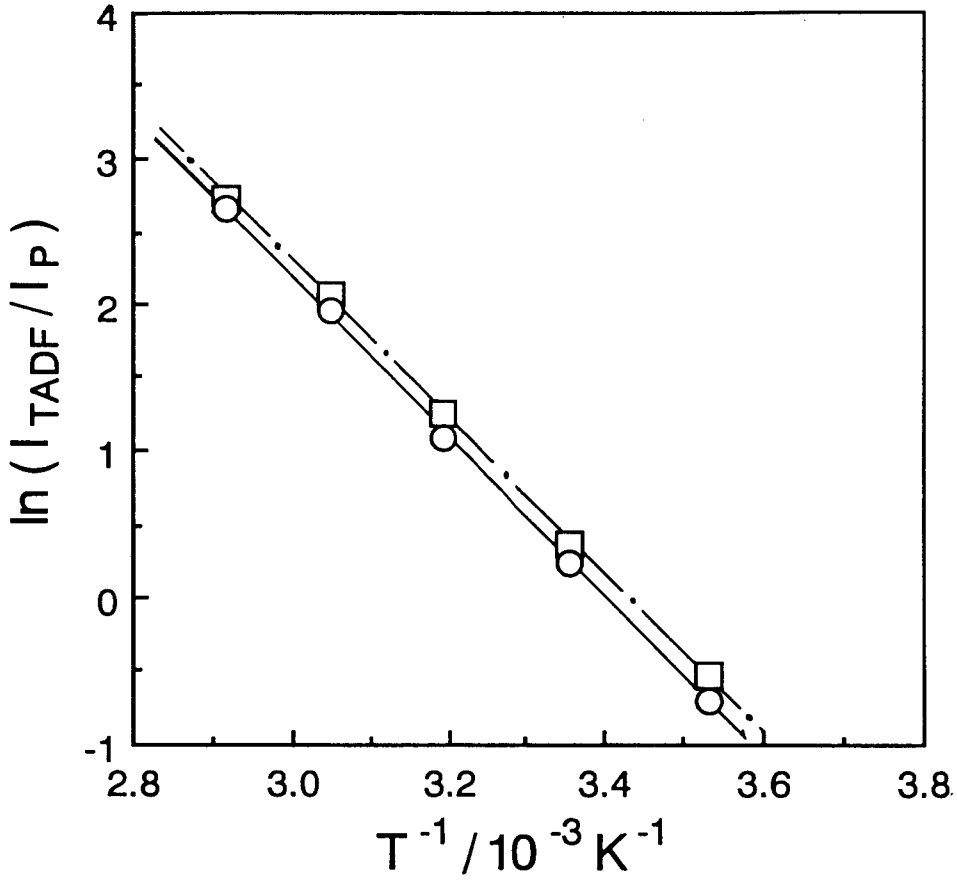

Figure 7. Plots of $\ln(I_{TADF} / I_P)$ against 1 / T for the terpolymers: ———○———, poly(A/La/ZnTPP); —• —□— • —, poly(A/Np/ZnTPP).

fluid solution at room temperature. This is a remarkable feature of the compartmentalized ZnTPP systems.

Spectroscopic features may be compared among the terpolymers in aqueous solution as follows:

(i) In absorption spectra, hypochromism and spectral broadening occurred only in poly(A/Cd/ZnTPP) (Figure 1).

(ii) In fluorescence spectra around 650 nm, spectral broadening occurred only in poly(A/Cd/ZnTPP) (Figure 2).

(iii) The spectral profiles of the delayed fluorescence (Figure 5) for poly(A/La/ZnTPP) and poly(A/Np/ZnTPP) were almost the same as those of the prompt fluorescence (Figure 2) at room temperature, but the profile of delayed fluorescence for poly(A/Cd/ZnTPP) was quite different from that of the prompt fluorescence.

(iv) Emission maxima for the phosphorescence of poly(A/La/ZnTPP) and poly(A/Np/ZnTPP) were about 790 nm, which was approximately equal to that for ZnTPP (781 nm),[17] but that of poly(A/Cd/ZnTPP) was considerably different (748 nm) (Figure 5) .

(v) In delayed emission spectra at various temperatures (Figure 6), the spectral profiles of both fluorescence and phosphorescence for poly(A/La/ZnTPP) at various temperatures were similar to those of poly(A/Np/ZnTPP) except intensities. However, in poly(A/Cd/ZnTPP), the ratio of emission intensities at 600 and 645 nm increased with increasing temperature, the spectral profiles of TADF gradually became to resemble the profile of prompt fluorescence, the emissions around 600 and 645 nm shifted to longer wavelength, and the ratio of emission intensities at 748 and 786 nm

decreased.

These spectral features for the Cd terpolymer is a reflection that the microenvironments around the ZnTPP moieties in the Cd domains are significantly different from those in the La and Np domains. Perhaps, packing densities of hydrophobic groups in the domains are different for different hydrophobic groups. In fact, in our laboratory, it has been recently revealed that Cd groups are much more densely packed in the domains than are La groups on the basis of the fact that photoisomerization of azobenzene moieties compartmentalized in the Cd domain is more suppressed than that in La domain.[5d)]

4.4. Conclusions

The ZnTPP chromophore was compartmentalized in the hydrophobic aggregate of the amphiphilic polyelectrolytes in aqueous solution.

Absorption maxima of the Soret band for the terpolymers in aqueous solution were longer than that for the reference copolymer because of differences in the environments around the ZnTPP moieties.

In absorption and fluorescence spectra, differences in the environments around the ZnTPP moieties were reflected on peak shift, hypochromism, and broadening effects.

Lifetimes of the triplet excited states for terpolymers in aqueous solution were very long because of the compartmentalization. Especially, the lifetimes for poly(A/Np/ZnTPP) and poly(A/Cd/ZnTPP)

were almost equal to the value of ZnTPP itself in glassy solid at 77K.

Phosphorescence and thermally activated delayed fluorescence were observed in the compartmentalized systems in fluid solution at room temperature.

Since all the hydrophobic groups used in this study consist of nearly equal numbers of the carbon atoms, degree of compartmentalization may depend on conformational rigidity of the hydrophobic groups.

References

1) Hewson, E.; Hager, L. P. Peroxidases, catalases, and chloroperoxidase. In *The Porphyrins*; Dolphin, D., Ed.; Academic Press: New York, 1979; Vol. VII, pp 295.

2) Ferguson-Miller, S.; Brautigan, D. L.; Margoliash, E. The electron transfer function of cytochrome c. In *The Porphyrins*; Dolphin, D., Ed.; Academic Press: New York, 1979; Vol. VII, pp 149.

3) Gibson, Q. H. The oxygenation of hemoglobin. In *The Porphyrins*; Dolphin, D., Ed.; Academic Press: New York, 1979; Vol. V, pp 153.

4) (a) Kalyanasundaram, K. *J. Chem. Soc., Faraday Trans. 2* **1983**, *79*, 1365. (b) Nahor, G. S.; Neta, P.; Hambright, P.; Thompson, Jr., A. N.; Harrimann, A. *J. Phys. Chem.* **1989**, *93*, 6181.

5) (a) Morishima, Y.; Tominaga, Y.; Kamachi, M.; Okada, T.; Hirata, Y.; Mataga, N. *J. Phys. Chem.* **1991**, *95*, 6027. (b) Morishima, Y.; Tominaga, Y.; Nomura, S.; Kamachi, M. *Macromolecules* **1992**, *25*, 861. (c) Morishima, Y. *Adv. Polym. Sci.* **1992**, in press. (d)

Morishima, Y.; Tsuji, M.; Kamachi, M.; Hatada, K. *Macromolecules* **1992**, *25*, 4406

6) (a) Morishima, Y.; Itoh, Y.; Nozakura, S. *Makromol. Chem.* **1981**, *182*, 3135. (b) Morishima, Y.; Kobayashi, T.; Nozakura, S. *J. Phys. Chem.* **1985**, *89*, 4081. (c) Morishima, Y.; Kobayashi, T.; Nozakura, S. *Polym. J.* **1989**, *21*, 267. (d) Guillet, J. E.; Rendall, W. A. *Macromolecules* **1986**, *19*, 224. (e) Guillet, J. E.; Wang, J.; Gu, L. *Macromolecules* **1986**, *19*, 2793.

7) (a) Morishima, Y.; Kobayashi, T.; Furui,T.; Nozakura, S. *Macromolecules* **1987**, *20*, 1707. (b) Morishima, Y.; Furui,T.; Nozakura, S.; Okada, T.; Mataga, N. *J. Phys. Chem.* **1989**, *93*, 1643.

8) Kalyanasundaram, K.; Grätzel, M. *Helv. Chim. Acta.* **1980**, *63*, 478.

9) Gouterman, M. Optical Spectra and Electronic Structure of Porphyrins and Related Rings. In *The Porphyrins*; Dolphin, D., Ed.; Academic Press: New York, 1978; Vol. III, pp 1.

10) Buchler, J. W. Synthesis and Properties of Metalloporphyrins. In *The Porphyrins*; Dolphin, D., Ed.; Academic Press: New York, 1978; Vol. I, pp 389.

11) Harriman, A. *J. Chem. Soc., Faraday Trans. 2* **1981**, *87*, 1281.

12) Frink, M. E.; Ferraudi, G. *Chem. Phys. Lett.* **1986**, *124*, 576.

13) Harriman, A.; Porter, G.; Searle, N. *J. Chem. Soc., Faraday Trans. 2* **1979**, *75*, 1515.

14) Turro, N. J. *Modern Molecular Photochemistry*; The Benjamin/Cummings Publishing: California, 1978.

15) Hopf, F. R.; Whitten, D. G. Chemical Transformations Involving Photoexcited Porphyrins and Metalloporphyrins. In *The*

Porphyrins; Dolphin, D., Ed.; Academic Press: New York, 1978; Vol. II, pp 161.

16) (a) Nishikawa, Y.; Hiraki, K.; Onoue, Y.; Nishikawa, K.; Yoshitake, Y.; Shigematsu, T. *Bunseki Kagaku* **1983**, *32*, E115. (b) Onoue, Y.; Hiraki, K.; Nishikawa, Y. *Bull. Chem. Soc. Jpn.* **1981**, *54*, 2633.

17) Quimby, D. J.; Longo, F. R. *J. Am. Chem. Soc.* **1975**, *97*, 5111.

Chapter 5

Photoinduced Electron Transfer from Compartmentalized ZnTPP to Methylviologen

5.1. Introduction

Zinc porphyrins can function as efficient sensitizers[1] for the photochemical production of hydrogen in aqueous solution by using methylviologen(MV^{2+}) as an electron acceptor. The reaction mechanism involved electron transfer from the triplet excited state of zinc porphyrin($^*ZnP$) to MV^{2+}, followed by the reduction of the oxidized form of the porphyrin (zinc porphyrin cation radical, $ZnP^{+}.$) by an irreversible redox couple such as ethylenediaminetetraacetic acid (EDTA)[2]:

$$^*ZnP + MV^{2+} \rightarrow ZnP^{+}. + MV^{+}..$$

$$ZnP^{+}. + EDTA \rightarrow ZnP + EDTA^{+}..$$

$$EDTA^{+}.. \rightarrow \text{products}$$

$$MV^{+}. + H_2O \rightarrow MV^{2+} + 1/2\ H_2 + OH^{-}$$

The formation of $ZnP^{+}.$ has been detected by the photochemical reaction of a reaction system which is composed of zinctetrapyridyl-methylporphyrin($ZnTMPyP^{4+}$) and MV^{2+}.[3] This detection is ascribable to a charge repulsion between $ZnTMPyP^{5+}.$ and $MV^{+}..$ On the contrary, no cation radical was detected by photochemical reaction of a reaction system of zinctetrasufonyl-phenylporphyrin ($ZnTSPP^{4-}$)-MV^{2+}, because a backward electron transfer occurred rapidly between $ZnTSPP^{3-}.$ and $MV^{+}..$[4]

Morishima et al.[5] showed that photophysical and photochemical behaviors of polycyclic aromatic chromophores such as phenanthrene and pyrene compartmentalized in amphiphilic polyelectrolyte were

much different from those in the corresponding homogeneous systems: fast electron transfer occurred from compartmentalized photoexcited aromatics to methylviologen while the back electron transfer was considerably slowed, and thus effective charge separation was achieved.

In this Chapter, the photoinduced electron transfer from ZnTPP compartmentalized in amphiphilic polyelectrolyte to MV^{2+} is studied. The energy potential diagram of ZnTPP-MV^{2+} system is shown in Figure 1.

5,2. Experimental Section

5,2,1. Materials

Syntheses of copolymer poly(A/ZnTPP) and terpolymers poly(A/La/ZnTPP), poly(A/Np/ZnTPP), and poly(A/Cd/ZnTPP) were described in Chapter 2.

Synthesis of ZnTSPP was described in Chapter 4.

Methylviologen (MV^{2+}) (Tokyo Kasei Co.) was purified by recrystallization from ethanol.

Water was doubly distilled.

5,2,2. Measurements

Absorption spectra were recorded on a Shimadzu UV-2100 spectrophotometer at room temperature. Concentrations of the ZnTPP residues in aqueous solutions were adjusted to 2 μM.

Fluorescence spectra were recorded on a Shimadzu RF-5000

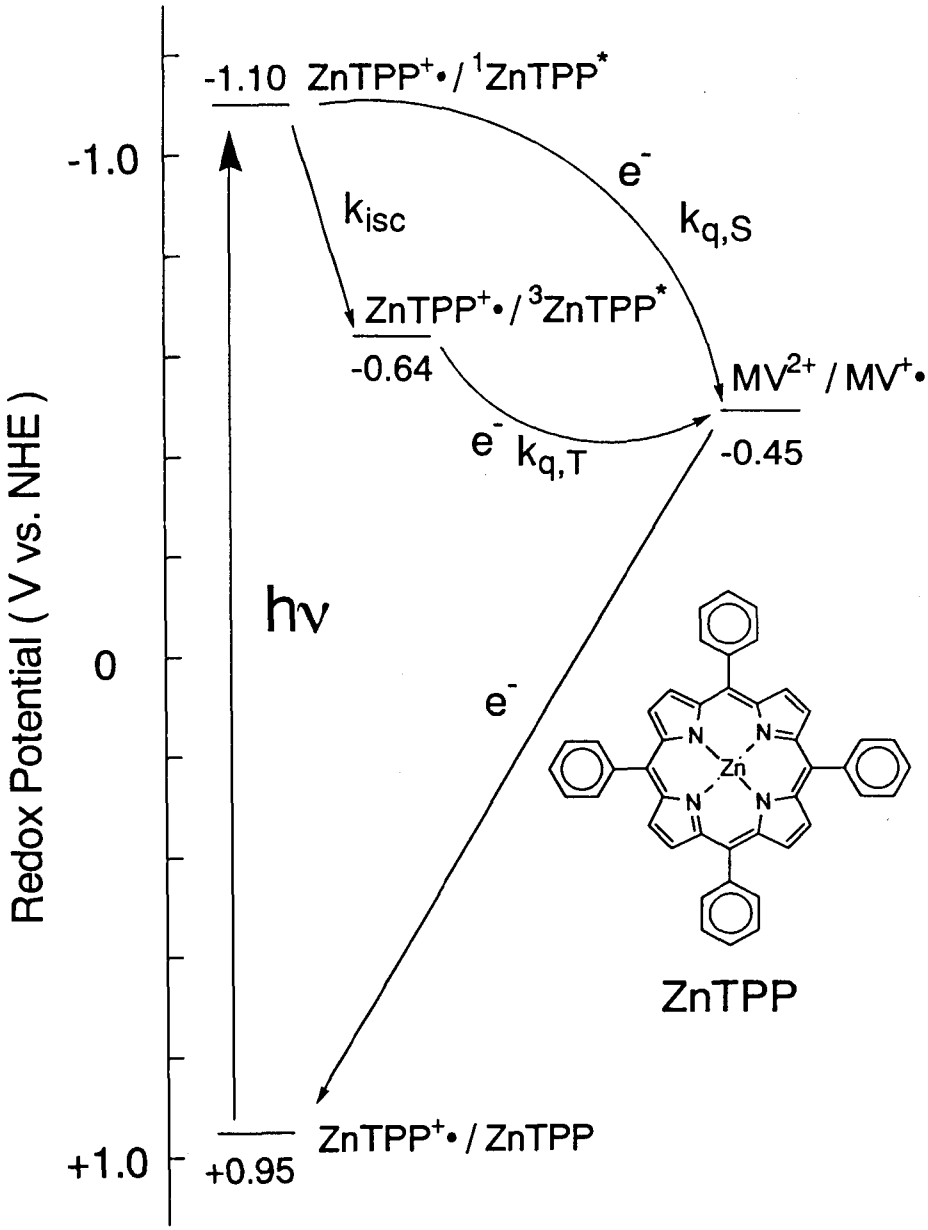

Figure 1. Energy level diagrams for ZnTPP and MV^{2+}.

spectrofluorophotometer at room temperature. Concentrations of the ZnTPP residues in aqueous solutions were adjusted to 2 μM. Excitation wavelength for the solutions was 563 nm.

Laser photolysis was performed as described in Chapter 4. A Toshiba KL-48 band-pass (480 nm) and a Toshiba Y-48 cut-off (480 nm) filters were placed between a 150-W xenon arc lamp (analyzing beam) and a sample cell for the measurement of the decay profiles of the $T_n \leftarrow T_1$ absorption of the ZnTPP residues at 480 nm. A Toshiba Y-43 cut-off filter (430 nm) was used in a similar manner for the measurement of time-resolved transient absorption spectra. Concentrations of 10 and 100 μM of the ZnTPP residues in aqueous solutions were used for the measurement of the decay profiles at 480 nm and time-resolved spectra, respectively. The solutions were deaerated by bubbling with argon for 30 min.

The concentrations of $ZnTPP^{+\cdot}$ were estimated from the time-resolved transient absorption spectra by using eq.(7) as follows. In the laser photolysis, a transient absorbance change (OD) at a given time and wavelength is given by

$$OD = \varepsilon_T [T_1] + \varepsilon_{ZnTPP^{+\cdot}} [ZnTPP^{+\cdot}] + \varepsilon_{MV^{+\cdot}} [MV^{+\cdot}] + \varepsilon_{S0}[S_0] - \varepsilon_{S0}[S_0]_0 \quad (1)$$

where ε_T, $\varepsilon_{ZnTPP^{+\cdot}}$, $\varepsilon_{MV^{+\cdot}}$, and ε_{S0} are the extinction coefficients of the lowest triplet excited state of ZnTPP moiety (T_1), $ZnTPP^{+\cdot}$, $MV^{+\cdot}$, and ground state of ZnTPP moiety (S_0) at a given wavelength, respectively, $[T_1]$, $[ZnTPP^{+\cdot}]$, $[MV^{+\cdot}]$, and $[S_0]$ are the concentrations of T_1, $ZnTPP^{+\cdot}$, $MV^{+\cdot}$, and S_0 at a given time, respectively. $[S_0]_0$ (=100 μM) is the initial concentration of S_0 given by

$$[S_0]_0 = [T_1] + [ZnTPP^{+}\cdot] + [S_0] \quad (2)$$

if we assume

$$[ZnTPP^{+}\cdot] = [MV^{+}\cdot] \quad (3)$$

then we obtain

$$OD = (\varepsilon_T - \varepsilon_{S0})\,[T_1] + (\varepsilon_{ZnTPP^{+}\cdot} + \varepsilon_{MV^{+}\cdot} - \varepsilon_{S0})\,[ZnTPP^{+}\cdot] \quad (4)$$

since absorbance of T_1 (OD_T) is given by

$$OD_T = (\varepsilon_T - \varepsilon_{S0})\,[T_1] \quad (5)$$

$$OD = OD_T + (\varepsilon_{ZnTPP^{+}\cdot} + \varepsilon_{MV^{+}\cdot} - \varepsilon_{S0})\,[ZnTPP^{+}\cdot] \quad (6)$$

OD_T at 650 nm is nearly equal to that at 800 nm (shown in Figure 3 in Chapter 4),

$$OD_{650} - OD_{800} \approx \{(\varepsilon_{ZnTPP^{+}\cdot} + \varepsilon_{MV^{+}\cdot} - \varepsilon_{S0})_{650} - (\varepsilon_{ZnTPP^{+}\cdot} + \varepsilon_{MV^{+}\cdot} - \varepsilon_{S0})_{800}\}\,[ZnTPP^{+}\cdot] \quad (7)$$

the values of $\varepsilon_{ZnTPP^{+}\cdot}$ and $\varepsilon_{MV^{+}\cdot}$ were approximately estimated from spectra reported in the literature to be 10000 [6] and 7700 $M^{-1}cm^{-1}$ [7] at 650 nm, and also to be 2100 $M^{-1}cm^{-1}$ [6] and practically zero [3b] at 800 nm, respectively. The values of ε_{S0} at 650 and 800 nm were determined to be 1000 and 300 $M^{-1}cm^{-1}$, respectively, by using absorption spectra shown in Fig. 1-b in Chapter 4.

5,3. Results and Discussion

5,3,1. Charge -Transfer Complexation

Absorption spectra of ZnTSPP, poly(A/ZnTPP), and poly(A/La/ZnTPP) in the region of the Soret band in the absence and presence of methylviologen (MV^{2+}) in aqueous solutions are shown in Figure 2. In the ZnTSPP and poly(A/ZnTPP) systems, in which ZnTPP moieties

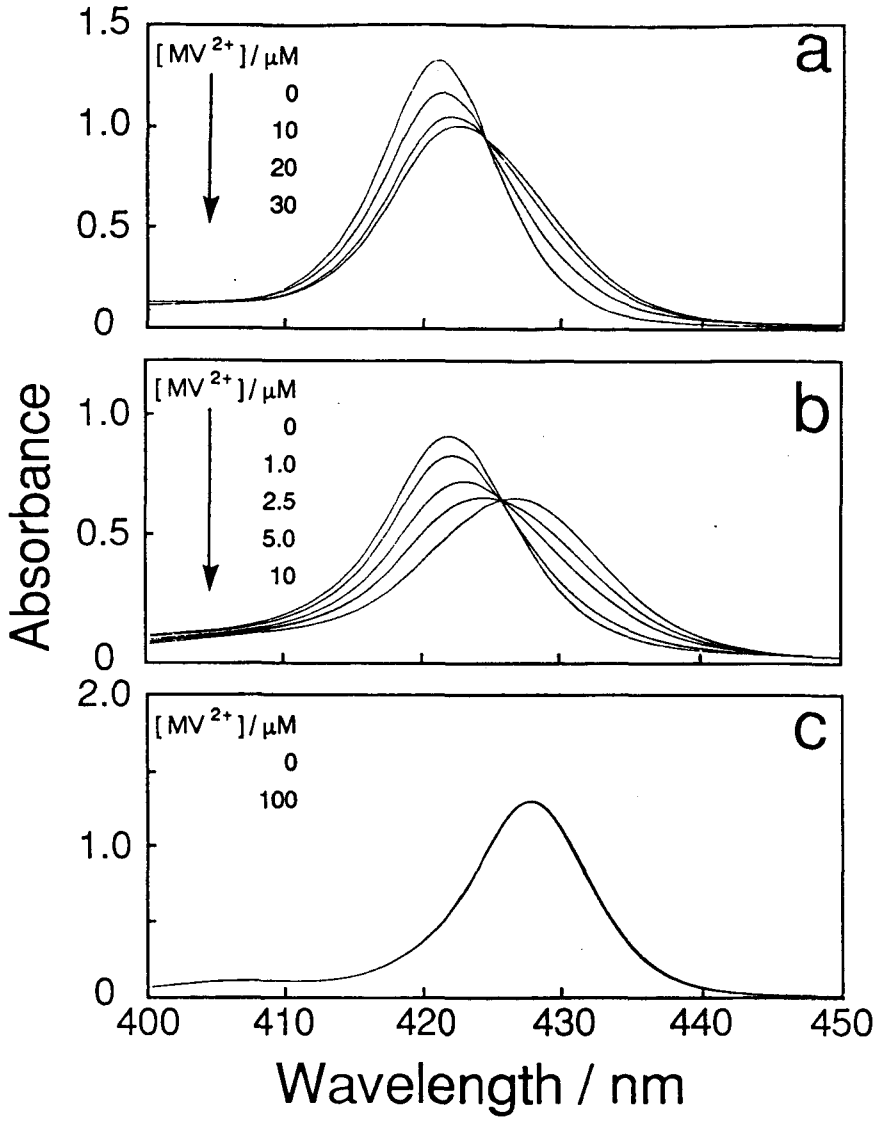

Figure 2. Absorption spectral changes of the aqueous solutions of ZnTSPP, poly(A/ZnTPP), and poly(A/La/ZnTPP) upon addition of various amounts of MV^{2+}: **a**, ZnTSPP; **b**, poly(A/ZnTPP); **c**, poly(A/La/ZnTPP); [ZnTPP](residue)=2 μM.

are exposed to the aqueous phase, the peaks shifted to longer wavelength with an increase in the concentration of MV^{2+}. However, in the poly(A/La/ZnTPP) system, in which ZnTPP moieties are compartmentalized by the hydrophobic groups, no such changes in spectral profile occurred although the concentration of added MV^{2+} was higher than those in the ZnTSPP and poly(A/ZnTPP) systems. The other terpolymer systems showed the same results as poly(A/La/ZnTPP). These findings indicate that the charge transfer (CT) complexation between the ZnTPP moiety and MV^{2+} occurs when the ZnTPP moieties are exposed to the aqueous phase, but not when they are compartmentalized in the terpolymers.

To estimate CT formation constants (K_{CT}) for the ZnTSPP and poly(A/ZnTPP) systems, Nash's plot (eq.8) was used [8].

$$1 / [\text{Acceptor}] = (1 / (1-A / A_0)) (K_{CT} - \alpha) - K_{CT};$$

$$\alpha = K_{CT} \varepsilon_C / \varepsilon_D \qquad (8)$$

where [Acceptor] is the concentration of the acceptor, A_0 and A are the absorbances in the absence and presence of the acceptor, and ε_C and ε_D are the extinction coefficients of the CT complex and the donor, respectively. These plots which were calculated from the absorption spectra in Figure 2 for ZnTSPP and the reference copolymer are shown in Figure 3. The K_{CT} values, estimated from the intercept of the ordinate, are listed in Table I. The values of K_{CT} for the reference copolymer was an order of magnitude larger than that for ZnTSPP. This is because the electrostatic interaction between MV^{2+} and the copolymer is larger than that between MV^{2+} and ZnTSPP. Although MV^{2+} may be bound to the surface of the microdomain in which the

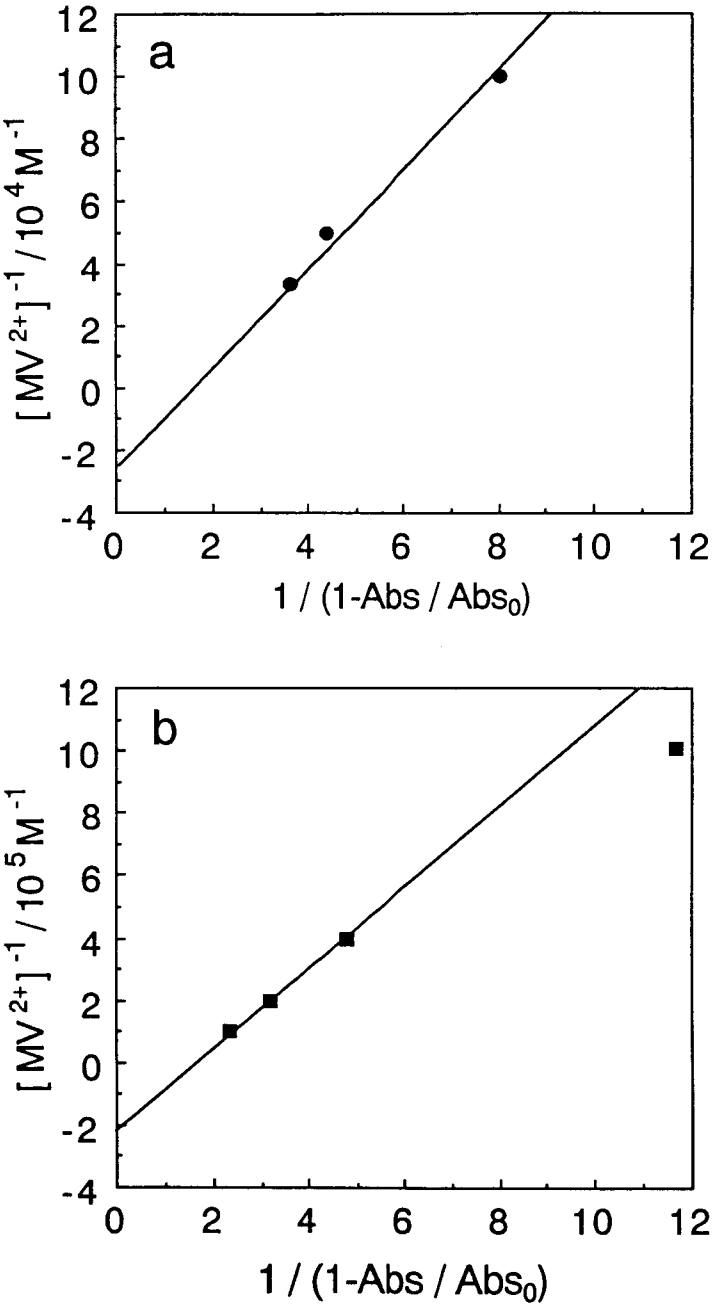

Figure 3. Nash's plots in aqueous solution: **a**, ZnTSPP; **b**, poly(A/ZnTPP).

Table I. Photochemical data for ZnTSPP and the Polymers with Methylviologen

sample code	K_{CT}/ M^{-1}	K_{SV}/ M^{-1} ($k_{q,S}$/ $M^{-1}s^{-1}$)[b]	$k_{q,T}$/ $M^{-1}s^{-1}$
ZnTSPP	2.5×10^4	3.2×10^4 (1.9×10^{13})	8.2×10^9
poly(A/ZnTPP)	2.3×10^5	3.4×10^5 (2.0×10^{14})	2.2×10^9
poly(A/La/ZnTPP)	___[a]	4.8×10^3 (2.8×10^{12})	2.2×10^9
poly(A/Np/ZnTPP)	___[a]	4.8×10^3 (2.8×10^{12})	7.4×10^8
poly(A/Cd/ZnTPP)	___[a]	2.1×10^3 (1.2×10^{12})	1.8×10^9

[a] No CT complexation was detected by absorption spectra.

[b] The apparent $k_{q,S}$ values were estimated from eq.(9) by using the lifetime of singlet excited state of ZnTSPP (1.7 ns).[10]

ZnTPP moieties are compartmentalized in the terpolymers, MV^{2+} cannot approach the ZnTPP moiety closely enough to form the CT complex because of steric hindrance of the compartmentalizing hydrophobic groups. These situations may be conceptually illustrated as shown in Figure 4.

5,3,2. Electron Transfer from the Singlet Excited State

Electron transfer (ET) quenching of the first singlet excited state (S_1) of the ZnTPP moiety is known to occur in the presence of MV^{2+}. To estimate the rate constant of the ET from S_1 ($k_{q,S}$) of the ZnTPP moiety to MV^{2+}, fluorescence quenching experiments were carried out. The fluorescence spectra for ZnTSPP, the reference copolymer, and the terpolymers in the absence and presence of MV^{2+} in aqueous solutions are shown in Figure 5. The Stern-Volmer equation is given by [9]

$$I_0 / I = 1 + K_{SV}[Q]; \quad K_{SV} = k_{q,S}\tau_0 \qquad (9)$$

where I_0 and I are the fluorescence intensities in the absence and presence of the quencher, respectively, K_{SV} is the Stern-Volmer constant, [Q] is the concentration of the quencher, and τ_0 is the lifetime of S_1 in the absence of the quencher. When CT complexes exist in the system, static quenching of fluorescence occurs. Then, the Stern-Volmer equation can be modified as

$$I_0 / I = (1 + K_{SV}[Q])(1 + K_{CT}[Q]) \qquad (10)$$

$$= 1 + (K_{CT} + K_{SV})[Q] + K_{CT}K_{SV}[Q]^2 \qquad (11)$$

if $[Q] << (1 / K_{SV}) + (1 / K_{CT})$,

then

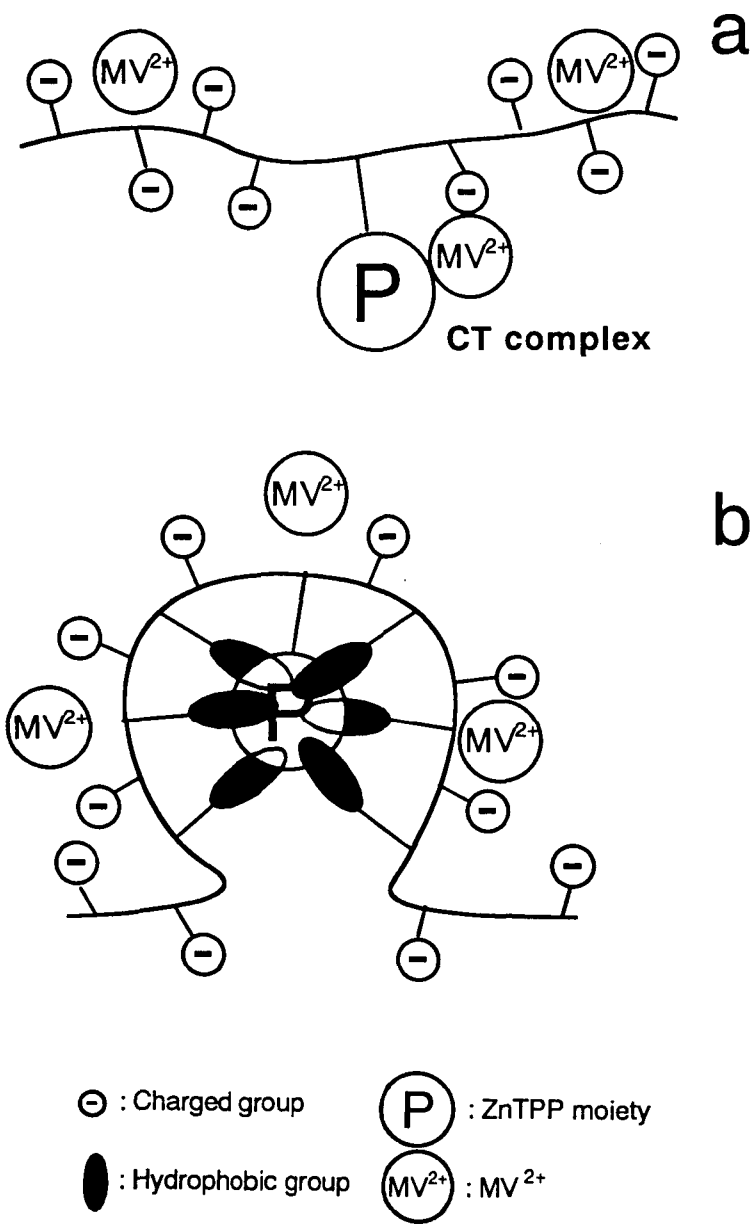

Figure 4. Conceptual illustrations of CT complexation of a ZnTPP moiety with MV^{2+}: **a**, the reference copolymer; **b**, the prohibition of the CT complexation for the terpolymers.

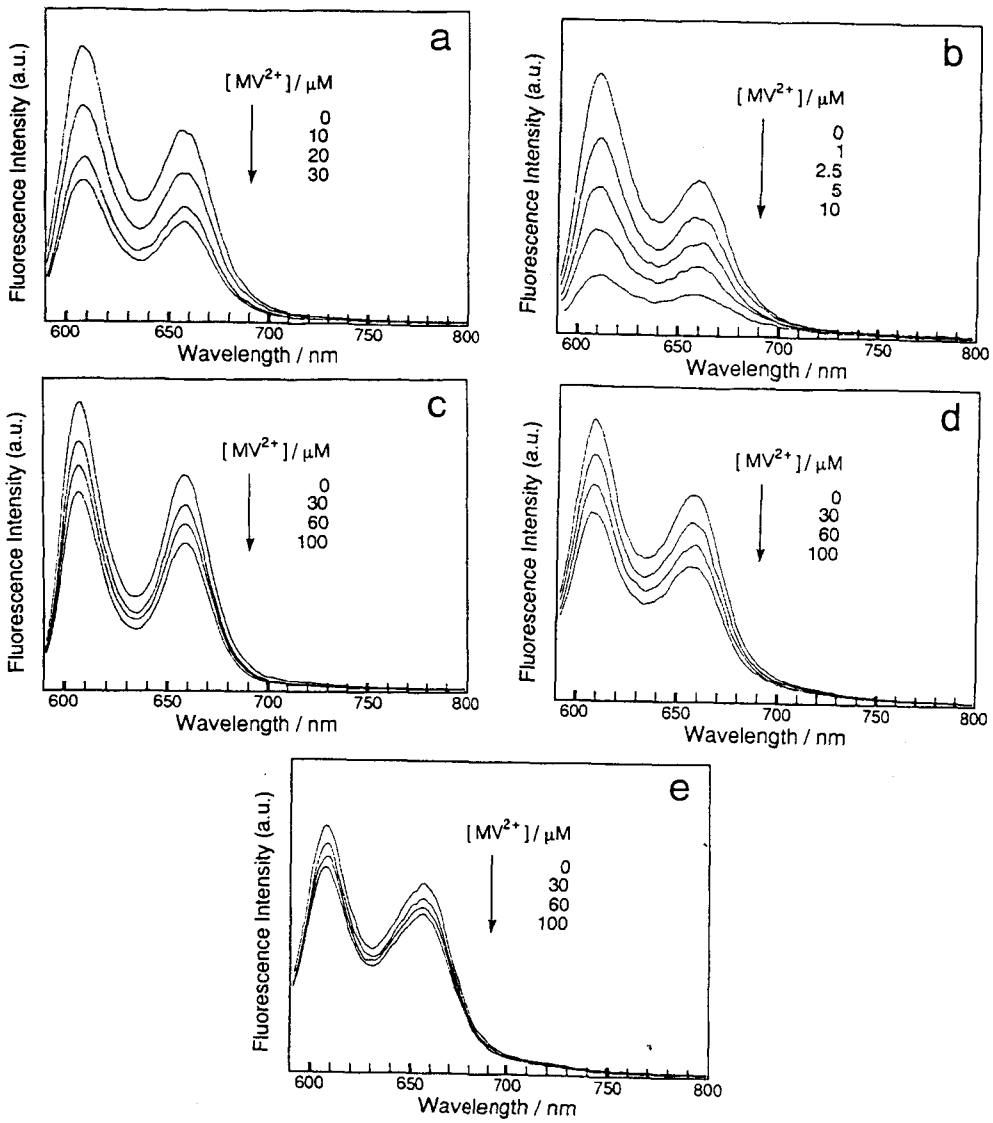

Figure 5. Fluorescence spectral changes of the aqueous solutions of ZnTSPP, the reference copolymer, and the terpolymers upon addition of various amounts of MV^{2+}: **a**, ZnTSPP; **b**, poly(A/ZnTPP); **c**, poly(A/La/ZnTPP); **d**, poly(A/Np/ZnTPP); **e**, poly(A/Cd/ZnTPP); [ZnTPP](residue)=2 μM; excitation wavelength, 563 nm.

$$I_0 / I \cong 1 + K'_{SV}[Q] \qquad (12)$$

where K'_{SV} (= K_{CT} + K_{SV}) is the apparent Stern-Volmer constant.

Stern-Volmer plots for ZnTSPP, the reference copolymer, and the terpolymers are shown in Figure 6. Since all the plots were nearly linear, the K_{SV} (or K'_{SV}) values were obtained from the slopes of the plots. For a rough estimation of apparent $k_{q,S}$ by using eq. (9), we used a literature value of the lifetime of S_1 of ZnTSPP in aqueous solution (τ_0=1.7ns).[10] These results are listed in Table I.

The ET processes in all the present systems are likely to be static in nature because of electrostatic interactions between MV^{2+} and each polymer or ZnTSPP. In fact, the apparent $k_{q,S}$ values were much larger than a diffusion-limititting rate constant (10^9-$10^{10}M^{-1}s^{-1}$).[9,11]

The K'_{SV} values for the reference copolymer and ZnTSPP are almost equal to the K_{CT} values. This suggests that most of the fluorescence quenching occurs by way of the CT complexation. The K_{SV} values for all the terpolymers were two orders of magnitude smaller than K'_{SV} for the reference copolymer. Since no CT complexes exist in the terpolymer systems, the fluorescence quenching can only occur by ET from S_1 of the compartmentalized ZnTPP moieties to MV^{2+}. The ET was suppressed in the order of lauryl ≅ naphthyl < cyclododecyl groups in the compartmentalized systems.

5,3,3. Electron Transfer from the Triplet Excited State

Time-resolved transient absorption spectra for poly(A/ZnTPP) and poly(A/Cd/ZnTPP) in the presence of MV^{2+} in aqueous solution are shown in Figure 7. These spectral profiles were similar to those of T_1

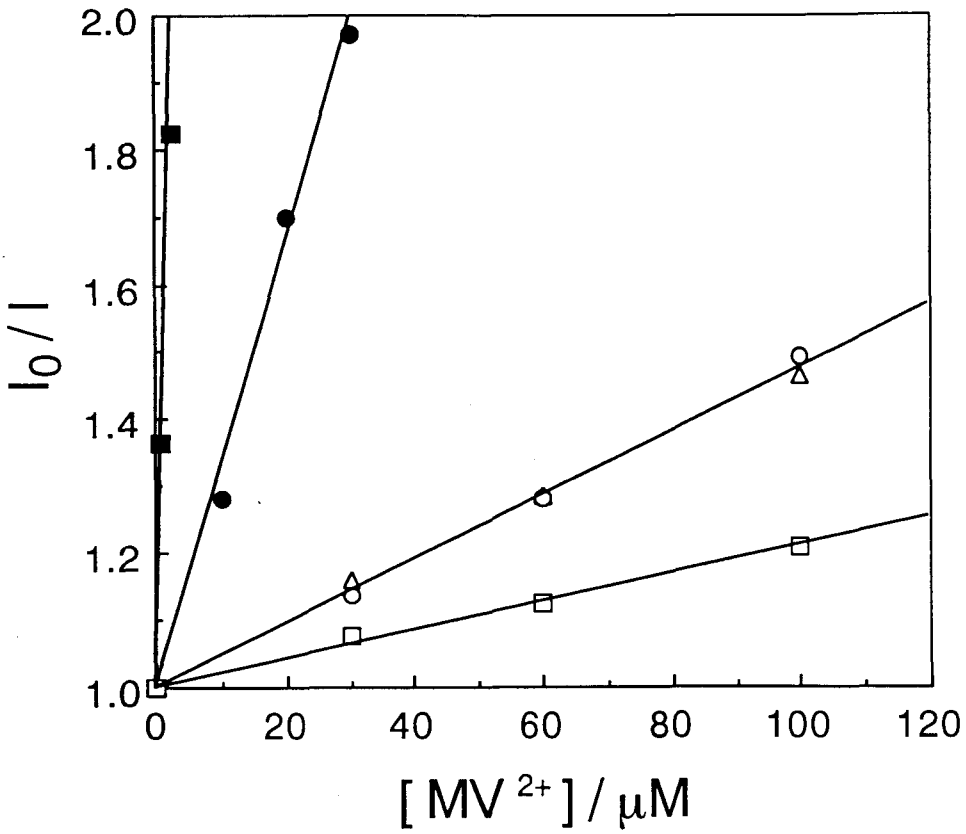

Figure 6. Stern-Volmer plots for the ZnTPP fluorescence quenching by MV^{2+} in aqueous solution: ●, ZnTSPP; ■, poly(A/ZnTPP); △, poly(A/La/ZnTPP); ○, poly(A/Np/ZnTPP); □, poly(A/Cd/ZnTPP).

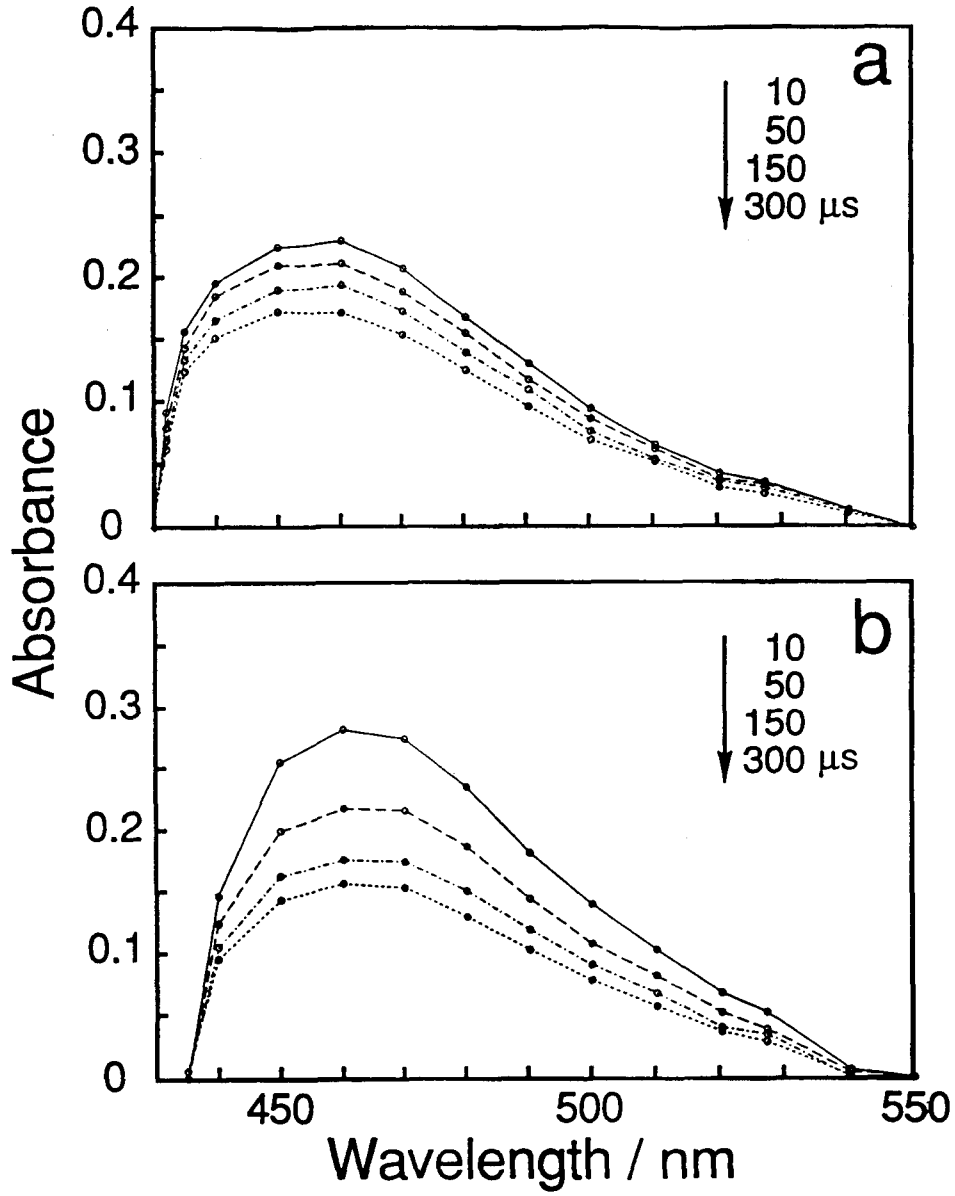

Figure 7. Time-resolved transient absorption spectra for poly(A/ZnTPP) and poly(A/Cd/ZnTPP) in the presence of MV^{2+} in aqueous solution: **a**, poly(A/ZnTPP) with 10 μM of MV^{2+}; **b**, poly(A/Cd/ZnTPP) with 30 μM of MV^{2+}; [ZnTPP](residue)=10 μM.

of the ZnTPP moiety in the absence of MV^{2+} (shown in Figure 3 in Chapter 4) but the decays of the absorbances were faster than that in the absence of MV^{2+}, indicating that ET occurred from T_1 of the ZnTPP moiety to MV^{2+}. To estimate the rate constant of the ET from T_1 ($k_{q,T}$) to MV^{2+}, the decay profiles of T_1 and the first-order plots for ZnTSPP and the polymers in the absence and presence of MV^{2+} in aqueous solutions monitored at 480 nm are shown in Figure 8. The rate constant $k_{q,T}$ is given by [9]

$$k_T = k_{0T} + k_{q,T}[Q] \qquad (13)$$

where k_T and k_{0T} are the rate constants of the decay of T_1 in the absence and presence of MV^{2+}, respectively, and [Q] is the concentration of MV^{2+}.

The first-order plots were not linear except for the ZnTSPP system. In Figure 9, k_T in the initial time region (up to 5 μs after laser excitation) are plotted as a function of $[MV^{2+}]$. The k_T values in the initial time region were used to avoid the contribution of the absorption due to $ZnTPP^+$. generated by the ET. The $k_{q,T}$ values obtained from the initial slopes of the plots are listed in Table I. The $k_{q,T}$ value for the reference copolymer system was almost equal to those for the terpolymer systems but smaller than that for ZnTSPP. The ET from T_1 may occur dynamically because the lifetime of T_1 is extremely long as described in Chapter 4. In the terpolymer systems, the order of $k_{q,T}$ was naphthyl < cyclododecyl < lauryl systems. This order doesn't agree with the order of K_{SV}. In the poly(A/Np/ZnTPP) system, k_T was proportional to $[MV^{2+}]$. But, this was not the case in other terpolymer systems. The initial fast

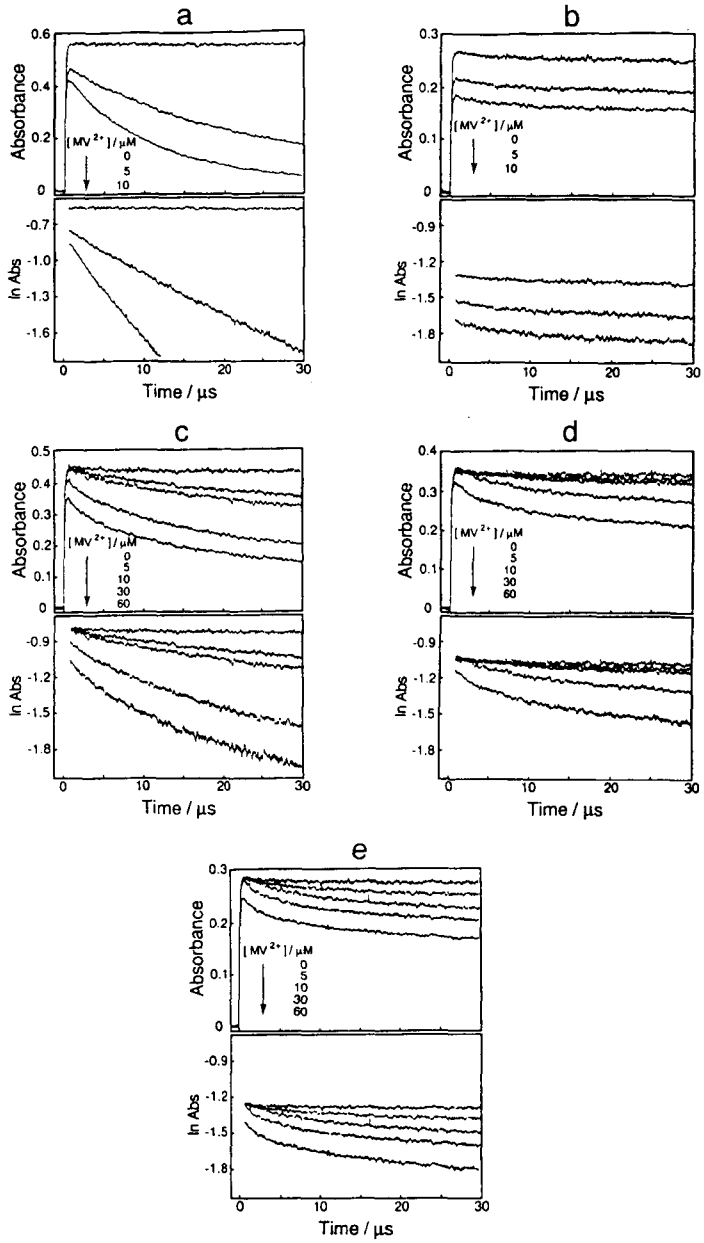

Figure 8. Decay profiles and the first-order plots of transient absorption monitored at 480 nm for ZnTSPP and all the polymers in the absence and presence of MV^{2+} in aqueous solution: **a**, ZnTSPP; **b**, poly(A/ZnTPP); **c**, poly(A/La/ZnTPP); **d**, poly(A/Np/ZnTPP); **e**, poly(A/Cd/ZnTPP); [ZnTPP](residue)=10 μM.

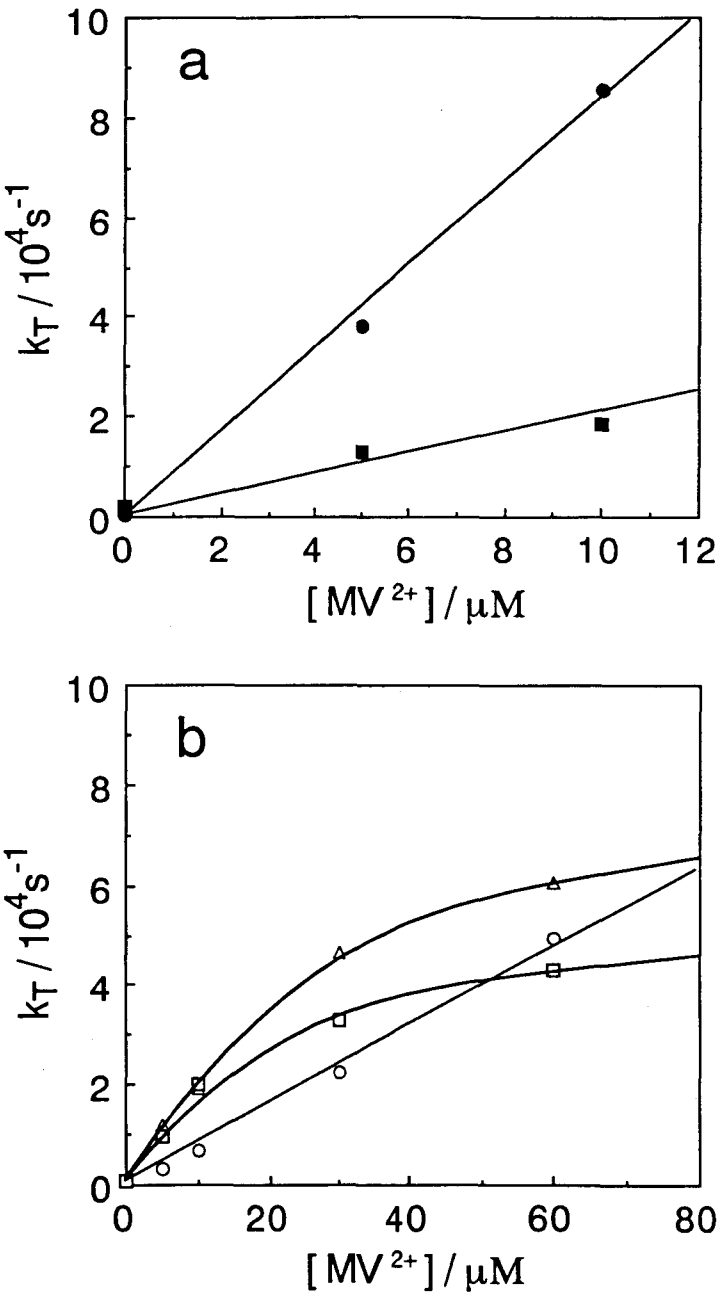

Figure 9. Plots of k_T of the ZnTPP moiety against $[MV^{2+}]$: ●, ZnTSPP; ■, poly(A/ZnTPP); △, poly(A/La/ZnTPP); ○, poly(A/Np/ZnTPP); □, poly(A/Cd/ZnTPP).

quenching in the region of low [MV^{2+}] in the poly(A/Cd/ZnTPP) system may occur at ZnTPP sites not sufficiently compartmentalized. The apparent $k_{q,T}$ estimated from the initial slope for poly(A/Np/ZnTPP) was smaller than that of poly(A/Cd/ZnTPP). It should be noted that the order of k_T at 60 μM of [MV^{2+}] was cyclododecyl < naphthyl < lauryl groups. This order agrees with the order of K_{SV}. ET may occur from T_1 to the nearest-situated MV^{2+}. If the nearest site to a compartmentalized ZnTPP moiety, where MV^{2+} can be bound, is already occupied by a MV^{2+} species, an excess of MV^{2+} may not contribute any more to the ET. This explains the finding that k_T was not proportional to [MV^{2+}] in the poly(A/La/ZnTPP) and poly(A/Cd/ZnTPP) systems. However, we cannot explain the reason why k_T is proportional to [MV^{2+}] in the poly(A/Np/ZnTPP) system.

5,3,4. Accumulation of Photoproducts

Time-resolved transient absorption spectra for the reference copolymer and the terpolymers in the presence of MV^{2+} in aqueous solution are shown in Figure 10. In the copolymer system, absorbances were very weak in the microsecond time region. On the other hand, in the terpolymer systems absorbances persisted for a few milliseconds. The absorptions are due to $ZnTPP^{+\cdot}$, [6], $MV^{+\cdot}$, [7], and T_1 of the ZnTPP moieties. It can be seen from Figure 10 that backward ET from $MV^{+\cdot}$ to $ZnTPP^{+\cdot}$ was suppressed owing to the compartmentalization of the ZnTPP moiety, and accumulations of $ZnTPP^{+\cdot}$ and $MV^{+\cdot}$ occurred. These results are consistent with the

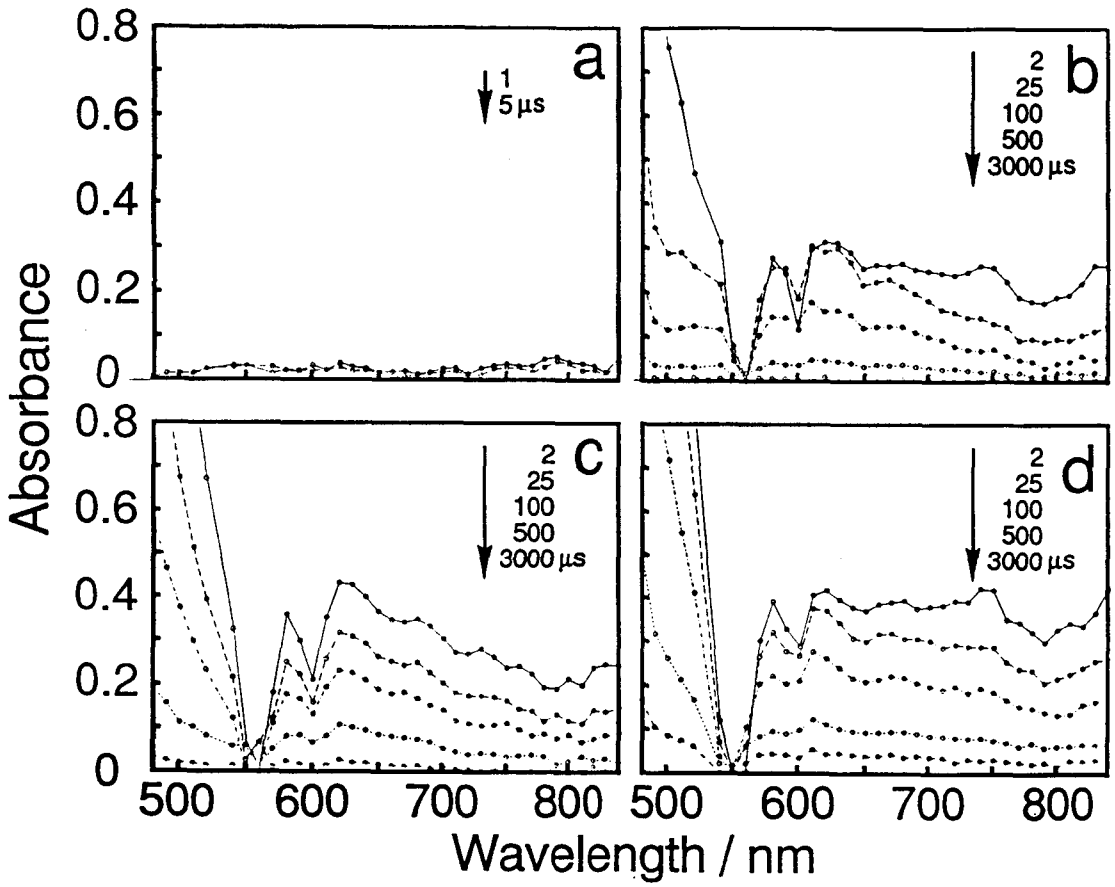

Figure 10. Time-resolved transient absorption spectra of the reference copolymer and the terpolymers in the presence of MV^{2+} in aqueous solution: **a**, poly(A/ZnTPP); **b**, poly(A/La/ZnTPP); **c**, poly(A/Np/ZnTPP); **d**, poly(A/Cd/ZnTPP); [ZnTPP](residue)=100 μM; $[MV^{2+}]$=5 mM.

previous studies in our laboratory using phenanthrene and pyrene as chromophores [5a,5b,12]. Such accumulations of the photoproducts in the ZnTPP terpolymer-MV^{2+} systems may be qualitatively explained in a similar manner as the previous studies of our laboratory.[5a,5b,12]

According to a kinetic model reported for photoinduced ET in the compartmentalized chromophore systems,[5b] forward and backward ET and charge escape may occur as follows:

$$^{S}ZnTPP \,//\, MV^{2+}(MV^{2+}) \xrightarrow{h\nu} {}^{S}ZnTPP^{*} \,//\, MV^{2+}(MV^{2+}) \quad (14)$$

$$^{S}ZnTPP^{*} \,//\, MV^{2+}(MV^{2+}) \xrightarrow{k_{isc}} {}^{T}ZnTPP^{*} \,//\, MV^{2+}(MV^{2+}) \quad (15)$$

$$^{S}ZnTPP^{*} \,//\, MV^{2+}(MV^{2+}) \xrightarrow{k_{q,S}} {}^{S}[ZnTPP^{+}. \,//\, MV^{+}.(MV^{2+})] \quad (16)$$

$$^{T}ZnTPP^{*} \,//\, MV^{2+}(MV^{2+}) \xrightarrow{k_{q,T}} {}^{T}[ZnTPP^{+}. \,//\, MV^{+}.(MV^{2+})] \quad (17)$$

$$^{S}[ZnTPP^{+}. \,//\, MV^{+}.(MV^{2+})] \xrightarrow{k_{b1,S}} {}^{S}ZnTPP \,//\, MV^{2+}(MV^{2+}) \quad (18)$$

$$^{T}[ZnTPP^{+}. \,//\, MV^{+}.(MV^{2+})] \xrightarrow{k_{b1,T}} {}^{S}ZnTPP \,//\, MV^{2+}(MV^{2+}) \quad (19)$$

$$^{S}[ZnTPP^{+}. \,//\, MV^{+}.(MV^{2+})] \xrightarrow{k_{d,S}} {}^{S}[ZnTPP^{+}. \,//\, MV^{2+}(MV^{+}.)] \quad (20)$$

$$^{T}[ZnTPP^{+}. \,//\, MV^{+}.(MV^{2+})] \xrightarrow{k_{d,T}} {}^{T}[ZnTPP^{+}. \,//\, MV^{2+}(MV^{+}.)] \quad (21)$$

$$^{S}[ZnTPP^{+}. \,//\, MV^{2+}(MV^{+}.)] \xrightarrow{k_{b2,S}} {}^{S}ZnTPP \,//\, MV^{2+}(MV^{2+}) \quad (22)$$

$$^{T}[ZnTPP^{+}\cdot\ //\ MV^{2+}(MV^{+}\cdot)] \xrightarrow{k_{b2,T}} {}^{S}ZnTPP\ //\ MV^{2+}(MV^{2+}) \qquad (23)$$

Here, S and T represent singlet and triplet states, respectively, $ZnTPP//MV^{2+}$ represents a pair of a compartmentalized ZnTPP moiety and the nearest-situated MV^{2+} species, and MV^{2+} designated in parentheses represents a MV^{2+} species located most closely to the MV^{2+} species in the $ZnTPP//MV^{2+}$ pair. Photoinduced ET would occur from a singlet excited ZnTPP moiety ($^{S}ZnTPP^{*}$) and a triplet excited ZnTPP moiety ($^{T}ZnTPP^{*}$) to the nearest-situated MV^{2+} (steps 16 and 17). Primary ion-pair states thus produced may undergo fast charge recombinations (steps 18 and 19) or charge escapes (steps 20 and 21). The kinetic model assumes that the charge escapes occur via an electron exchange between $MV^{+}\cdot$ and MV^{2+} bound side-by-side on the surface of the hydrophobic microdomain.[5a,13] If the charge escapes take place via steps 20 and 21, backward ET (steps 22 and 23) would be slowed depending on separation between $ZnTPP^{+}\cdot$ and the $(MV^{+}\cdot)$ sites. Free energy gaps ($-\Delta G^{0}$) for the forward ET from S_1 to MV^{2+} (step 16) and from T_1 to MV^{2+} (step 17) are 0.65 and 0.19 eV, respectively. The $-\Delta G^{0}$ value for the backward ET (steps 18, 19, 22, and 23) is 1.40 eV. Therefore, the backward ET in the singlet-ion pairs may be comparable to or faster than forward ET. The backward ET in the triplet-ion pairs (steps 19 and 23) should be slower than that in the singlet-ion pairs (steps 18 and 22) because the backward ET in the triplet-ion pairs are spin-forbidden. Therefore, the charge escape from the singlet-ion pairs (step 20) may be difficult to occur, whereas that from the triplet-ion pairs (step 21)

may occur more easily than charge recombination (step 19) . Hence, the backward ET (step 23) can be slowed. These situations may be conceptually illustrated as shown in Figure 11.

In Figure 10, the spectral profiles are different for different hydrophobic groups in the terpolymers when compared 2 μs after laser excitation. This is because of differences in the relative ratios of $ZnTPP^{+\cdot}$, $MV^{+\cdot}$, and T_1 of ZnTPP in the sample solutions after the laser excitation. The time profiles of the concentrations of $ZnTPP^{+\cdot}$ estimated from the difference in absorbances at 650 and 800 nm are shown in Figure 12. The maximum of the transient concentration of $ZnTPP^{+\cdot}$ in the poly(A/La/ZnTPP) system was 8 μM which corresponds to 8% of the initial concentration of the ZnTPP residue, while those in the poly(A/Np/ZnTPP) and poly(A/Cd/ZnTPP) systems were 11 and 5%, respectively. In the poly(A/La/ZnTPP) system, $ZnTPP^{+\cdot}$ completely decayed at 1.5 ms after excitation, while, in the poly(A/Np/ZnTPP) and poly(A/Cd/ZnTPP) systems, significant amounts of $ZnTPP^{+\cdot}$ remained at 3 ms. It should be noted that, in the latter systems, no significant decay of $ZnTPP^{+\cdot}$ were observed after 1 ms.

5.4. Conclusions

The CT complexation was completely suppressed by the compartmentalization of the ZnTPP moieties in the terpolymers.
The ET from S_1 of the ZnTPP moiety to MV^{2+} for the compartmentalized systems were two orders of magnitude slower

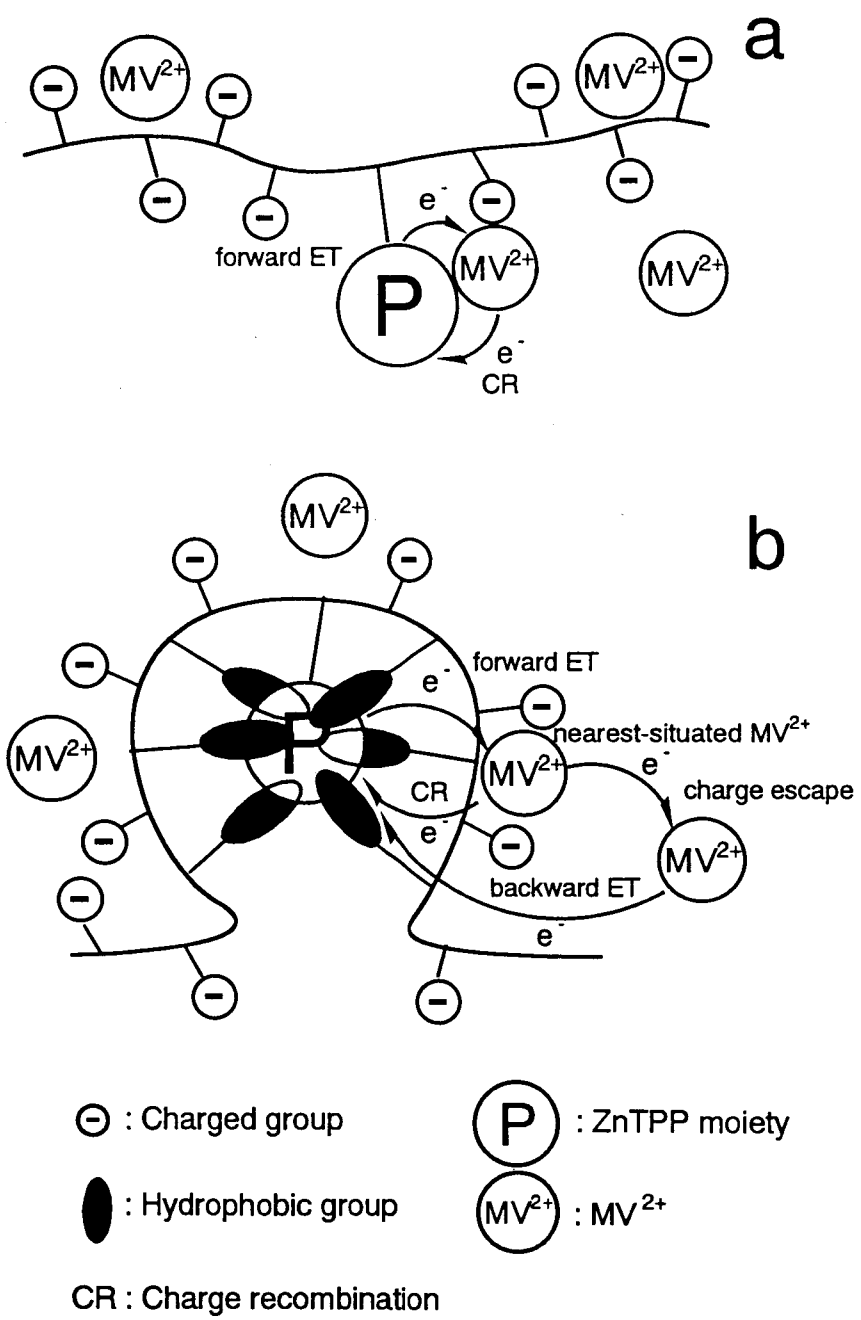

Figure 11. Conceptual illustration of ET and charge escape in ZnTPP-MV^{2+} system; **a**, the reference copolymer; **b**, the terpolymers

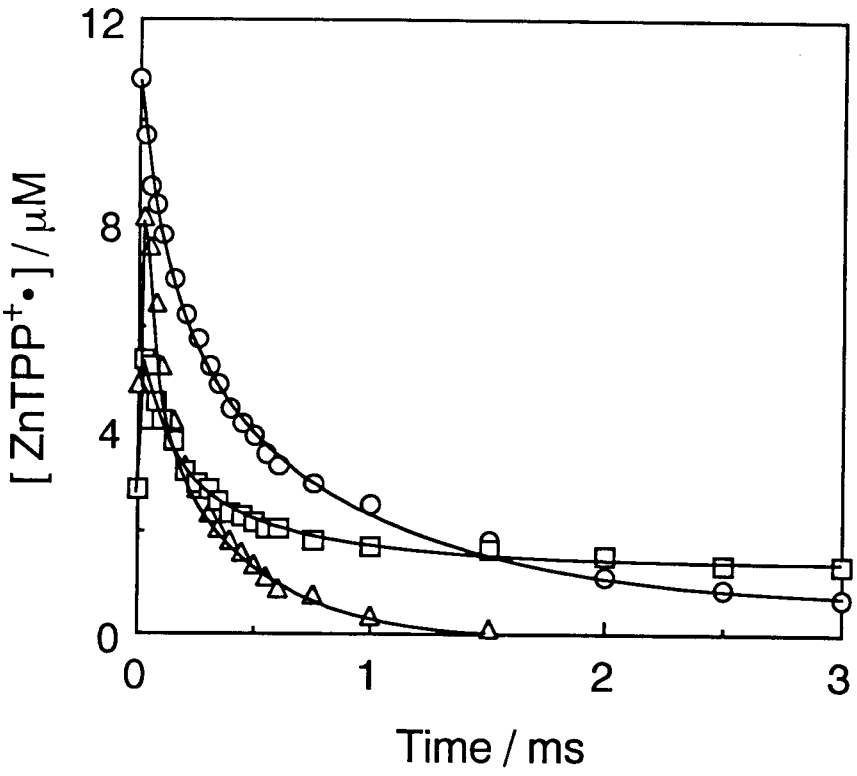

Figure 12. Decay profiles of $ZnTPP^{+\bullet}$ moieties calculated from transient absorption spectra of the terpolymer-MV^{2+} systems: △, poly(A/La/ZnTPP); ○, poly(A/Np/ZnTPP); □, poly(A/Cd/ZnTPP)..

than that for the reference copolymer system because of the steric hindrance of the compartmentalizing hydrophobic groups.

The apparent rate constants of the ET from T_1 of the ZnTPP moiety to MV^{2+} ($k_{q,T}$) for the terpolymer systems were almost equal to that for the reference copolymer but were smaller than that for ZnTSPP.

The accumulation of $ZnTPP^{+\cdot}$ was observed as a result of the compartmentalization. The naphthyl and cyclododecyl groups were effective to accumulate $ZnTPP^{+\cdot}$, in which cases $ZnTPP^{+\cdot}$ persisted for several milliseconds.

References

1) (a) Seely, G. R. *Photochem. Photobiol.* **1978**, *27*, 639. (b) Felton, R. H. Primary Redox Reactions of Metalloporphyrins. In *The Porphyrins* ; Dolphin, D., Ed.; Academic Press: New York, 1978; Vol. V, pp 53. (c) Harriman, A.; Richoux, M.-C. *J. Photochem.* **1981**, *15*, 335.

2) Richoux, M.-C.; Harriman, A. *J. Chem. Soc., Faraday Trans. 1* **1982**, *78*, 1873.

3) (a) Harriman, A.; Porter, G.; Richoux, M.-C. *J. Chem. Soc., Faraday Trans. 2* **1981**, *77*, 833. (b) Harriman, A.; Porter, G.; Richoux, M.-C. *J. Chem. Soc., Faraday Trans. 2* **1982**, *78*, 1955.

4) (a) Harriman, A.; Richoux, M.-C. *J. Photochem.* **1980**, *14*, 253. (b) Harriman, A.; Richoux, M.-C. *J. Chem. Soc., Faraday Trans. 2*

1980, *76*, 1618.

5) (a) Morishima, Y.; Furui,T.; Nozakura, S.; Okada, T.; Mataga, N. *J. Phys. Chem.* **1989**, *93*, 1643. (b) Morishima, Y.; Tominaga, Y.; Kamachi, M.; Okada, T.; Hirata, Y.; Mataga, N. *J. Phys. Chem.* **1991**, *95*, 6027.

6) Fajer, J.; Borg, D. C.; Forman, A.; Dolphin, D.; Felton, R. H. *J. Am. Chem. Soc.* **1970**, *92*, 3451.

7) Watanabe, T.; Honda, K. *J. Phys. Chem.* **1982**, *86*, 2617.

8) Nash, C. P. *J. Phys. Chem.* **1960**, *64*, 950.

9) Turro, N. J. *Modern Molecular Photochemistry* ; The Benjamin / Cummings Publishing: California, 1978.

10) Kalyanasundaram, K. *J. Chem. Soc., Faraday Trans. 2* **1983**, *79*, 1365.

11) Calvert, J. G; Pitts, J. N. Jr. *Photochemistry* ; John Wiley and Sons: New York 1966.

12) Morishima, Y.; Kobayashi, T.; Furui,T.; Nozakura, S. *Macromolecules* **1987**, *20*, 1707.

13) (a) Gauliello, J. G.; Ghosh, P. K.; Bard, A. J. *J. Am. Chem. Soc.* **1985**, *107*, 3027. (b) Atherton, S. J.; Tsuka, K.; Wilkins, R. G. *J. Am. Chem. Soc.* **1986**, *108*, 3380. (c) Takuma, K.; Sakamoto, T.; Nagamura, T.; Matsuo, T. *J. Phys. Chem.* **1981**, *85*, 619. (d) Matsuo, T.; Sakamoto, T.; Takuma, K.; Sakura, K.; Ohsaka, T *J. Phys. Chem.* **1981**, *85*, 1277. (e) Matsuo, T. *Pure & Appl. Chem.* **1982**, *54*, 1693.

Chapter 6

Photoinduced Electron Transfer from Compartmentalized ZnTPP to a Sulfonium Salt

6,1. Introduction

To accumulate $ZnTPP^{+\cdot}$ by photoinduced electron transfer reaction, the compartmentalization was very effective as described in Chapter 5. In compartmentalized ZnTPP-MV^{2+} system, $ZnTPP^{+\cdot}$ persisted for several milliseconds. In order to accumulate $ZnTPP^{+\cdot}$ more effectively and for a longer time, an irreversible electron acceptor was used in place of MV^{2+}.

Onium cations, especially diaryliodonium and triarylsulfonium, are used as photoinitiator of both radical and cationic polymerizations.[1] Electron transfer sensitized photolysis of onium sults have been studied by DeVoe et al.[2] These cations cleave themselves irreversibly at ca. 200ps after accepting an electron.[2] Moreover, the redox potential of the triarylsulfonium cations can be changed by changing their leaving groups.[3]

In this Chapter, we describe the photoinduced electron transfer from the compartmentalized ZnTPP to one of the triarylsulfonium salt, phenylmethylphenacylsulfonium p-toluenesulfonate (PMPS), studied by ESR in addition to the similar procedures as described in Chapter 5. The reaction mechanism of this system is shown in Scheme I.

6,2. Experimental Section

6,2,1. Materials

Syntheses of a copolymer poly(A/ZnTPP) and terpolymers poly(A/La/ZnTPP), poly(A/Np/ZnTPP), and poly(A/Cd/ZnTPP) were

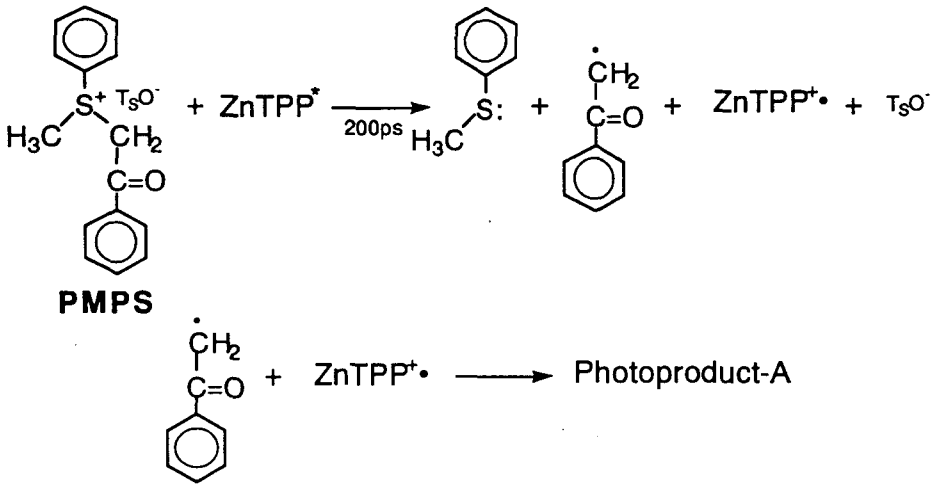

Scheme I

described in Chapter 2.

Synthesis of ZnTSPP was described in Chapter 4.

PMPS was prepared according to the literature.[3] Anal. Calcd for $C_{22}H_{22}S_2O_4$: C,63.74; H,5.35%. Found: C,63.40; H,5.51%. The half-peak reduction potential ($E_{p/2}$) was -0.60 V vs SCE in acetonitrile.

Water was doubly distilled.

6,2,2. Measurements

Absorption spectra and fluorescence spectra were measured, and laser photolysis was performed in the same manner as described in Chapter 5.

The poly(A/Cd/ZnTPP)-PMPS system was irradiated with 550 nm light for 3 min using a 500-W xenon arc lamp in combination with a monochrometer (Japan Spectroscopic CT-10). The concentrations of

the ZnTPP residues and PMPS were adjusted to 50 μM and 10 mM, respectively. The solution was deaerated by bubbling with argon for 30 min.

ESR was measured on a JEOL Model JES FE-1X and JES RE-2X ESR spectrometers with 100 kHz modulation at room temperature. Steady-state visible light was irradiated at the sample solutions by using a 1-kW high-pressure mercury lamp combined with Toshiba O-54, IRA-25S, ND-25, and ND-50 filters ($540 < \lambda < 700$ nm). G-values were estimated by comparing with the third (g=2.033) and fourth (g=1.981) lines of MnO. Decay profiles of $ZnTPP^{+\cdot}$ generated by irradiation of the polymer-PMPS systems for 1 min were monitored at 333.9 mT (peak top). The concentrations of the ZnTPP residues and PMPS were adjusted to 100 μM and 10 mM, respectively. The solutions were deaerated by bubbling with argon for 30 min.

Photoinduced radical polymerizations of acrylamide initiated by the radicals generated from PMPS were performed as follows. An aqueous solution containing poly(A/Cd/ZnTPP) (50 μM of the ZnTPP residues), 6.7 mM of PMPS, and 10 % (w/w) of acrylamide was deaerated by bubbling with argon for 30 min. The solution was irradiated with ten laser pulses with stirring, and then allowed to stand for 5 min in the dark. This cycle was repeated five times. Finally, the solution was allowed to stand for 30 min in the dark after irradiating final ten laser pulses. The solution was poured into methanol to precipitate polyacrylamide. The polymer was washed with methanol and dried for 6 h under reduced pressure at 100°C.

6,3. Results and Discussion

6,3,1. Charge-Transfer Complexation

Absorption spectra of ZnTSPP, poly(A/ZnTPP), and poly(A/La/ZnTPP) in the region of the Soret band in the absence and presence of PMPS in aqueous solution are shown in Figure 1. In the ZnTSPP and poly(A/ZnTPP) systems, in which ZnTPP moieties are exposed to the aqueous phase, the peaks shifted to longer wavelength with an increase in the concentration of PMPS. However, in the poly(A/La/ZnTPP) system, in which ZnTPP moieties were compartmentalized by the hydrophobic groups, no such changes in spectral profile occurred although the concentration of added PMPS was higher than those in the ZnTSPP and poly(A/ZnTPP) systems. The other terpolymers showed the same results as poly(A/La/ZnTPP). These findings indicate that the charge transfer (CT) complexation between ZnTPP and PMPS occurs when the ZnTPP moieties are exposed to the aqueous phase, but not when they are compartmentalized in the terpolymers. This is consistent with the MV^{2+} case as described in Chapter 5.

CT formation constants (K_{CT}) for the ZnTSPP and poly(A/ZnTPP) systems were estimated using Nash's plots (eq.(8) in Chapter 5) (Figure 2). These plots were calculated from the absorption spectra in Figure 1 for ZnTSPP and the reference copolymer. The K_{CT} values, estimated from the intercept of the ordinate, are listed in Table I. The values of K_{CT} for the reference copolymer were two orders of magnitude larger than that for ZnTSPP. This is because the

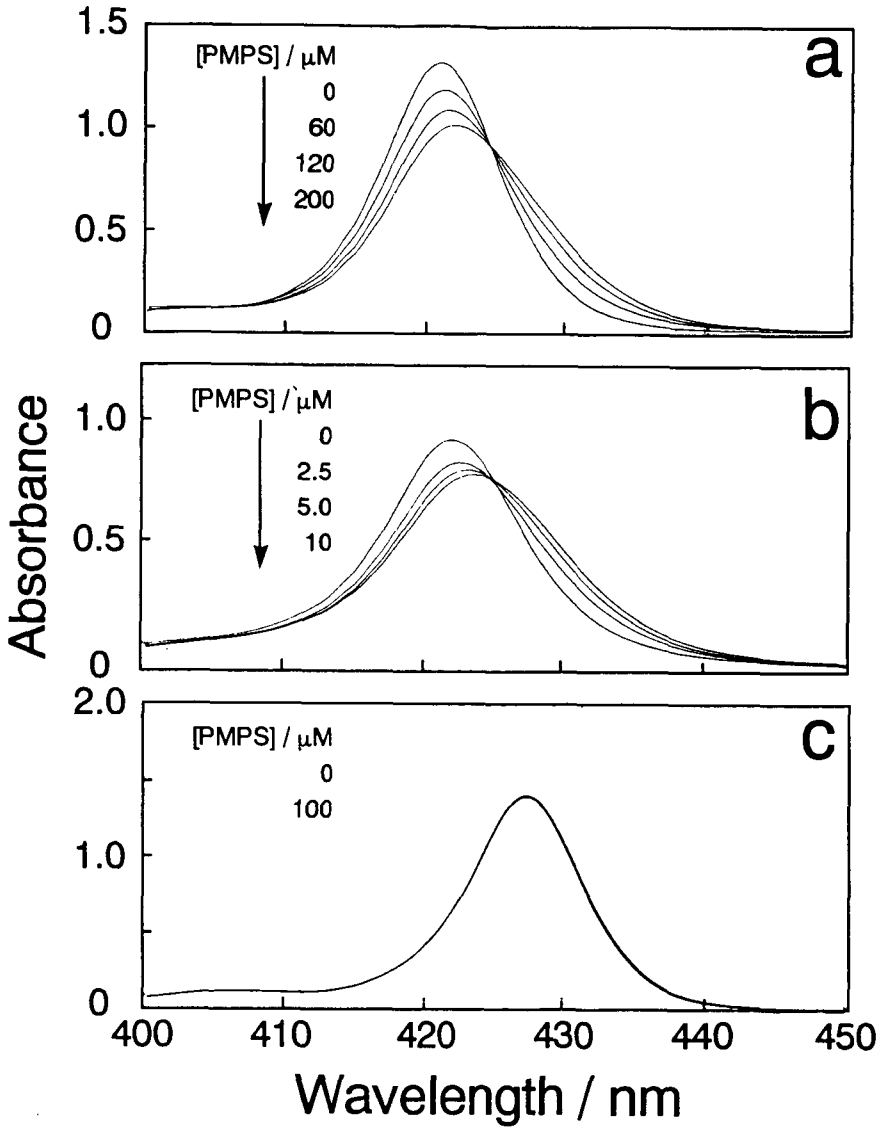

Figure 1. Absorption spectral changes for the aqueous solutions of ZnTSPP, poly(A/ZnTPP), and poly(A/La/ZnTPP) upon addition of various amounts of PMPS: **a**, ZnTSPP; **b**, poly(A/ZnTPP); **c**, poly(A/La/ZnTPP); [ZnTPP](residue)=2 μM.

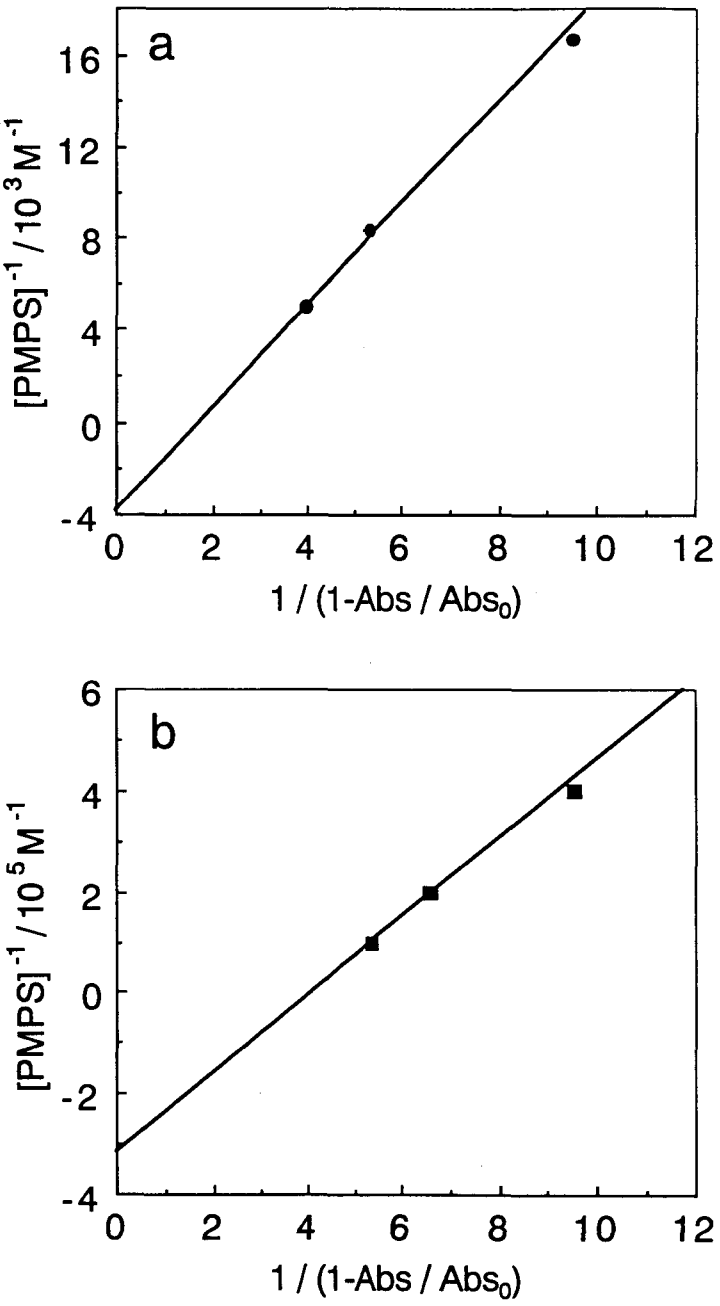

Figure 2. Nash's plots in aqueous solution: **a**, ZnTSPP; **b**, poly(A/ZnTPP).

Table I. Photochemical data for ZnTSPP and the Polymers with PMPS

sample code	K_{CT}/ M^{-1}	K_{SV}/ M^{-1} ($k_{q,S}$/ $M^{-1}s^{-1}$)[b]	$k_{q,T}$/ $M^{-1}s^{-1}$
ZnTSPP	3.7×10^3	1.6×10^3 (9.4×10^{11})	1.5×10^7
poly(A/ZnTPP)	3.2×10^5	7.5×10^4 (4.4×10^{13})	1.4×10^8
poly(A/La/ZnTPP)	___[a]	___[c]	3.8×10^6
poly(A/Np/ZnTPP)	___[a]	___[c]	3.8×10^6
poly(A/Cd/ZnTPP)	___[a]	___[c]	1.1×10^6

[a] No CT complexation was detected by absorption spectra.

[b] The apparent $k_{q,S}$ values were estimated from eq.(9) given in Chapter 5 by using the lifetime of singlet excited state of ZnTSPP (1.7 ns) [4].

[c] Fluorescence was not quenched.

electrostatic interaction between PMPS and the copolymer is larger than that between PMPS and ZnTSPP. Although PMPS may be bound to the surface of the microdomain of the terpolymers in which the ZnTPP moieties are compartmentalized, PMPS cannot approach the ZnTPP moiety closely enough to form the CT complex because of steric hindrance of the compartmentalizing hydrophobic groups.

6,3,2. Electron Transfer from the Singlet Excited State

To estimate the rate constant ($k_{q,S}$) for ET from S_1 (first singlet excited state) of the ZnTPP moiety to PMPS, fluorescence quenching experiments were carried out in the same manner as described in Chapter 5. The fluorescence spectra of ZnTSPP, the reference copolymer, and poly(A/La/ZnTPP) in the absence and presence of PMPS in aqueous solution are shown in Figure 3. Fluorescence quenching occurred in ZnTSPP and poly(A/ZnTPP) systems, but no fluorescence quenching occurred in poly(A/La/ZnTPP) system, although a high concentration of PMPS (10 mM) was employed. Similar results were obtained for the poly(A/Np/ZnTPP) and poly(A/Cd/ZnTPP) systems. These findings indicate that the ET from S_1 of ZnTPP moieties to PMPS occurs when the ZnTPP moieties are exposed to the aqueous phase, but not when they are compartmentalized in the terpolymers. As described in Chapter 5, fluorescence of the ZnTPP moieties in the terpolymers was quenched by MV^{2+}. Free energy gap ($-\Delta G$) for the ET from the S_1 of ZnTPP to PMPS (0.74 eV) is close to that to MV^{2+} (0.66 eV). A difference in the fluorescence quenching between PMPS and MV^{2+} may be due to a

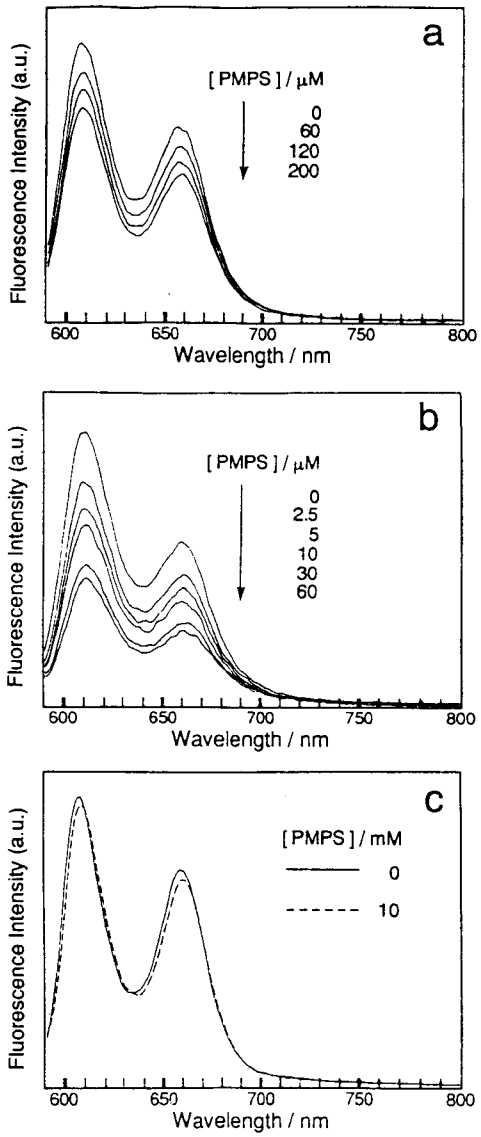

Figure 3. Fluorescence spectral changes of aqueous solution upon addition of various amounts of PMPS: **a**, ZnTSPP; **b**, poly(A/ZnTPP); **c**, poly(A/La/ZnTPP); [ZnTPP](residue)=2 μM; excitation wavelength, 563 nm.

difference in electrostatic interactions and/or a difference in orbitals which accept electrons from the S_1 of the ZnTPP moiety. Since the hydrophobic microdomains of the terpolymers are surrounded by polyanion segments, MV^{2+} (dication species) would electrostatically interact more strongly with the microdomains than PMPS (monocation species). Furthermore, ET may occur to the π^*-orbital of MV^{2+}, while it may occur to the σ^*-orbital of PMPS. These may be the reasons why ET to PMPS was slower than that to MV^{2+}.

Stern-Volmer plots for ZnTSPP and the reference copolymer are shown in Figure 4. Since the plots were nearly linear, K_{SV} (or K'_{SV}) values were obtained from the slopes of the plots in the same manner as described in Chapter 5. For a rough estimation of apparent $k_{q,S}$ by using eq. (9) in Chapter 5, we used a literature value of the lifetime of S_1 of ZnTSPP (τ_0=1.7ns).[4] These results are listed in Table I. The values of K_{SV} for the PMPS systems were an order of magnitude smaller than those for the MV^{2+} systems.

6,3,3. Electron Transfer from the Triplet Excited State

Time-resolved transient absorption spectra for poly(A/ZnTPP) and poly(A/Cd/ZnTPP) in the presence of PMPS in aqueous solutions are shown in Figure 5. The spectral profiles at 10 μs after laser pulse were similar to those of T_1 (first triplet excited state) of the ZnTPP moieties in the absence of PMPS (Figure 3 in Chapter 4) but the decays of the absorbances were faster than that in the absence of PMPS, indicating that ET occurred from T_1 of the ZnTPP moiety to PMPS. The decay profiles of T_1 and the first-order plots for ZnTSPP

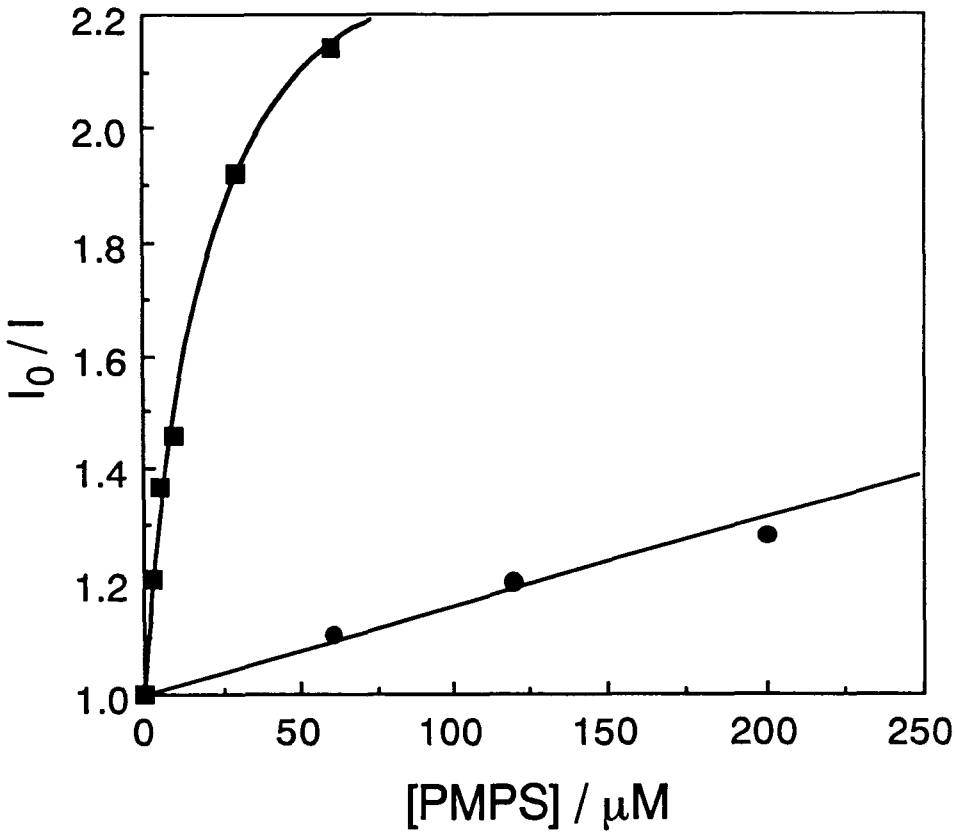

Figure 4. Stern-Volmer plots for the ZnTPP fluorescence quenching by PMPS in aqueous solution: ●, ZnTSPP; ■, poly(A/ZnTPP).

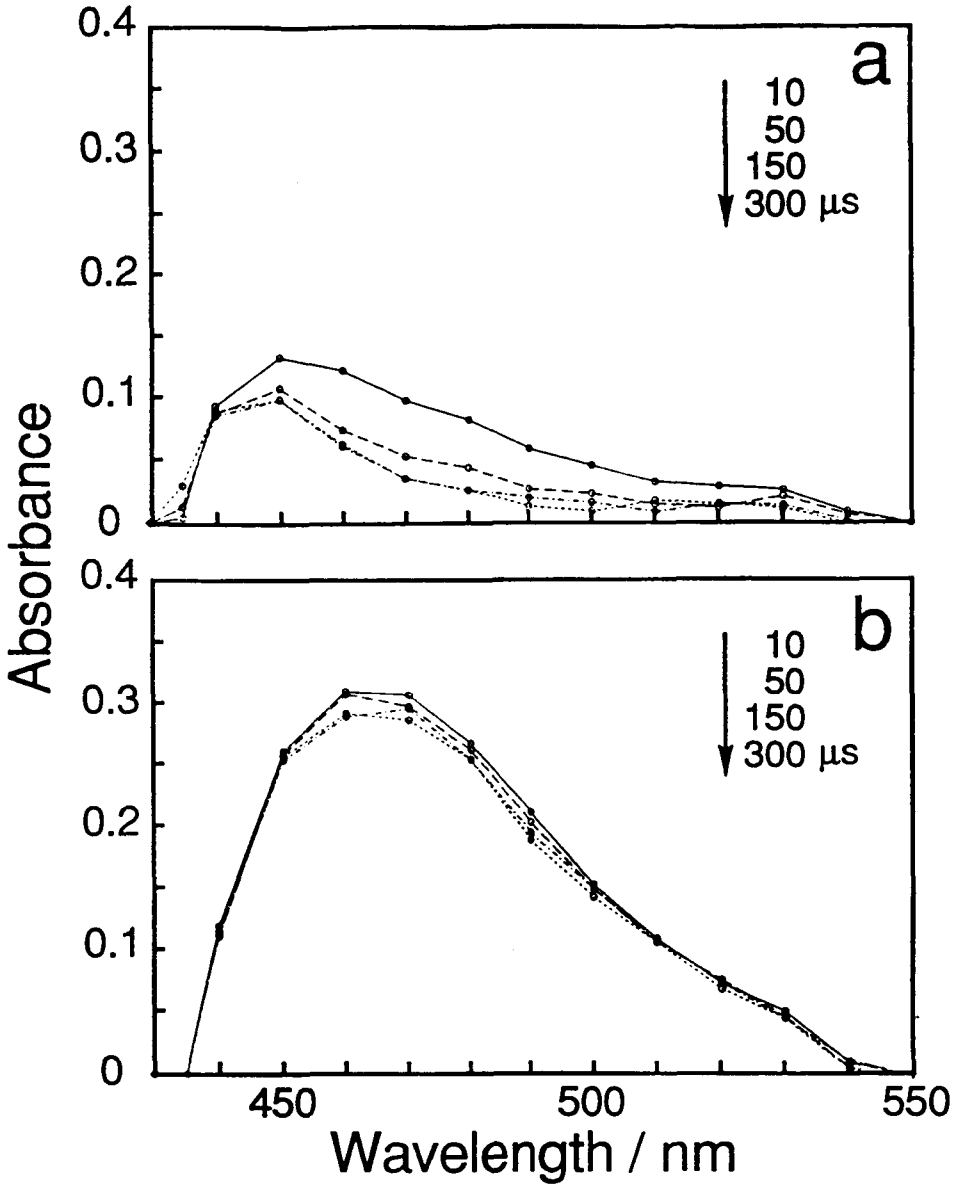

Figure 5. Time-resolved transient absorption spectra in the presence of 100 μM of PMPS in aqueous solution: **a**, poly(A/ZnTPP); **b**, poly(A/Cd/ZnTPP); [ZnTPP](residue)=10 μM.

and the polymers in the absence and presence of PMPS in aqueous solution monitored at 480 nm are shown in Figure 6. The rate constant of the ET from T_1 ($k_{q,T}$) to PMPS was estimated in the same manner as described in Chapter 5. In Figure 7, k_T values in the initial time region (up to 20 μs for ZnTSPP and the reference copolymer and 100 μs for the terpolymers after laser excitation) were plotted as a function of [PMPS]. The k_T values in the initial time region were used to avoid the contribution of the absorption due to $ZnTPP^{+\cdot}$ generated by the ET. The $k_{q,T}$ values obtained from the initial slopes of the plots are listed in Table I. The $k_{q,T}$ values for the terpolymer systems were two orders of magnitude smaller than that for the reference copolymer system. This result indicates that the compartmentalization of the ZnTPP moiety suppresses the ET from T_1 to PMPS. Although ET from S_1 to PMPS could not be observed in the terpolymer systems, ET from T_1 to PMPS occurred, because the lifetime of T_1 is seven orders of magnitude longer than that of S_1 in the terpolymer systems.

6,3,4. Accumulation of Photoproducts

Initial photoproducts generated by photoinduced ET from the excited ZnTPP moiety to PMPS are $ZnTPP^{+\cdot}$, sulfide, and a radical fragment from PMPS (Scheme I). A stable photoproduct (represented as Photoproduct-A), which is generated by the reaction between the $ZnTPP^{+\cdot}$ moiety and the fragment radical, may exist in the ZnTPP-PMPS system (Scheme I).

Time-resolved transient absorption spectra for the reference

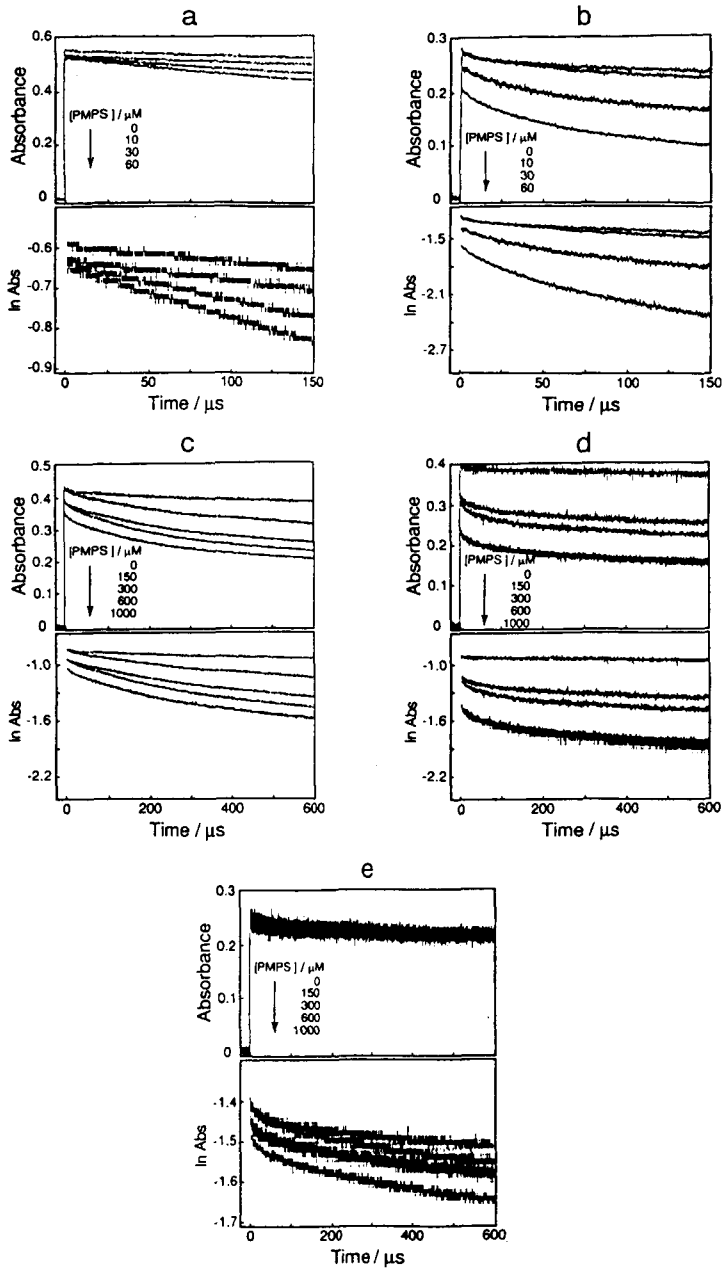

Figure 6. Decay profiles and the first-order plots of transient absorption monitored at 480 nm for ZnTSPP and all the polymers in the absence and presence of PMPS in aqueous solution: **a**, ZnTSPP; **b**, poly(A/ZnTPP); **c**, poly(A/La/ZnTPP); **d**, poly(A/Np/ZnTPP); **e**, poly(A/Cd/ZnTPP); [ZnTPP](residue)=10 μM.

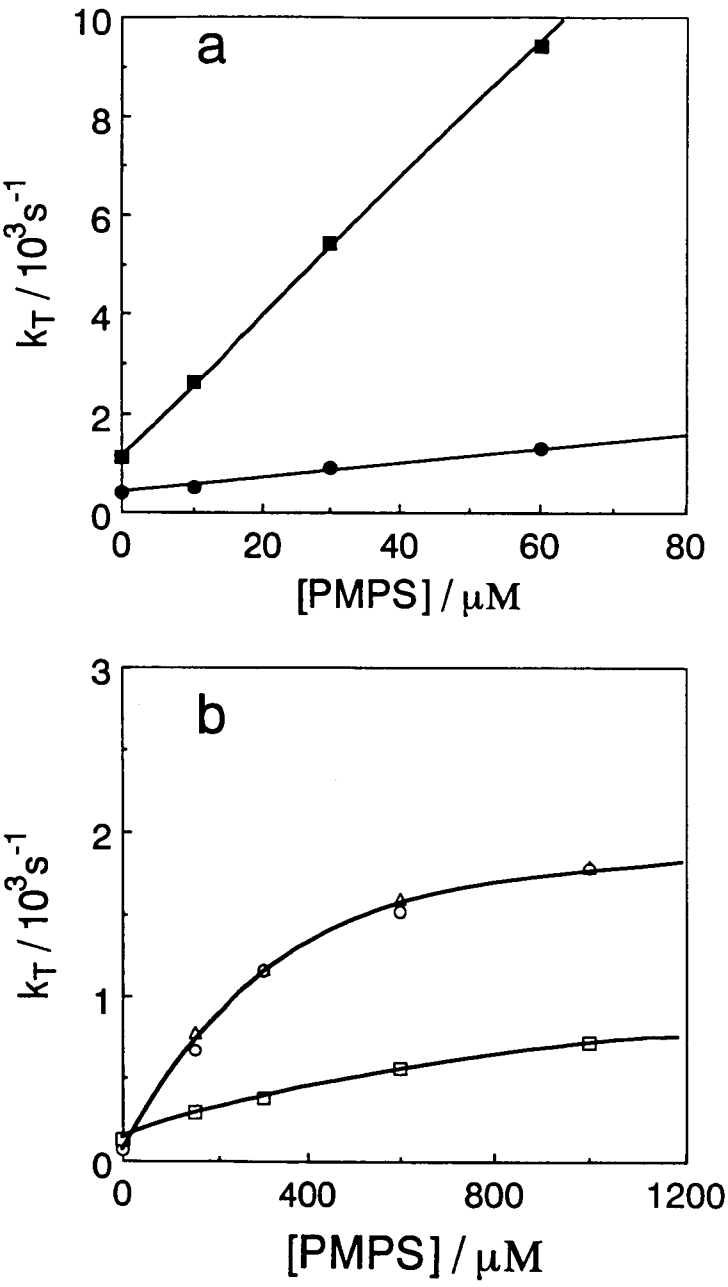

Figure 7. Plots of k_T for the ZnTPP moiety against [PMPS]: ●, ZnTSPP; ■, poly(A/ZnTPP); △, poly(A/La/ZnTPP); ○, poly(A/Np/ZnTPP); □, poly(A/Cd/ZnTPP).

copolymer and the terpolymers in the presence of PMPS in aqueous solution are shown in Figure 8. In the reference copolymer system (Fig.8-a), absorbances in the region from 610 to 750 nm were small and decayed in the 50 μs -150 ms time region after laser excitation. This result suggests that T_1 and/or $ZnTPP^{+\cdot}$ moieties existed in this system even though the concentrations of these species were low. On the other hand, absorbances in the region from 750 to 840 nm were larger than those in the region from 610 to 750 nm and the intensity remained almost constant in this time region. The spectral profiles in the 750-840 nm region were not similar to the absorption bands of either T_1 [5] or $ZnTPP^{+\cdot}$.[6] These differences in the spectra may be caused by absorption of Photoproduct-A. In the terpolymer systems, spectral profiles were different for different times after laser pulse and for different hydrophobic groups. These spectra may be due to absorptions of T_1, $ZnTPP^{+\cdot}$, and Photoproduct-A. Absorbances due to T_1 of the ZnTPP moieties were almost zero at 25 ms after laser pulse in the poly(A/La/ZnTPP) system and 150 ms after laser pulse in poly(A/Np/ZnTPP) and poly(A/Cd/ZnTPP) systems because these times were much longer than the lifetimes of T_1 described in Chapter 4. The spectral profiles at these time regions resembled the absorption spectrum of $ZnTPP^{+\cdot}$ itself generated by an electrochemical procedure [6] except a region over 800 nm.

Absorption spectra of poly(A/Cd/ZnTPP) in the presence of PMPS in aqueous solution before irradiation of visible light and standing for 15 s and 30 min in the dark, after irradiation for 3 min, are shown in Figure 9-a. The absorption band of the ZnTPP moiety around 550 nm

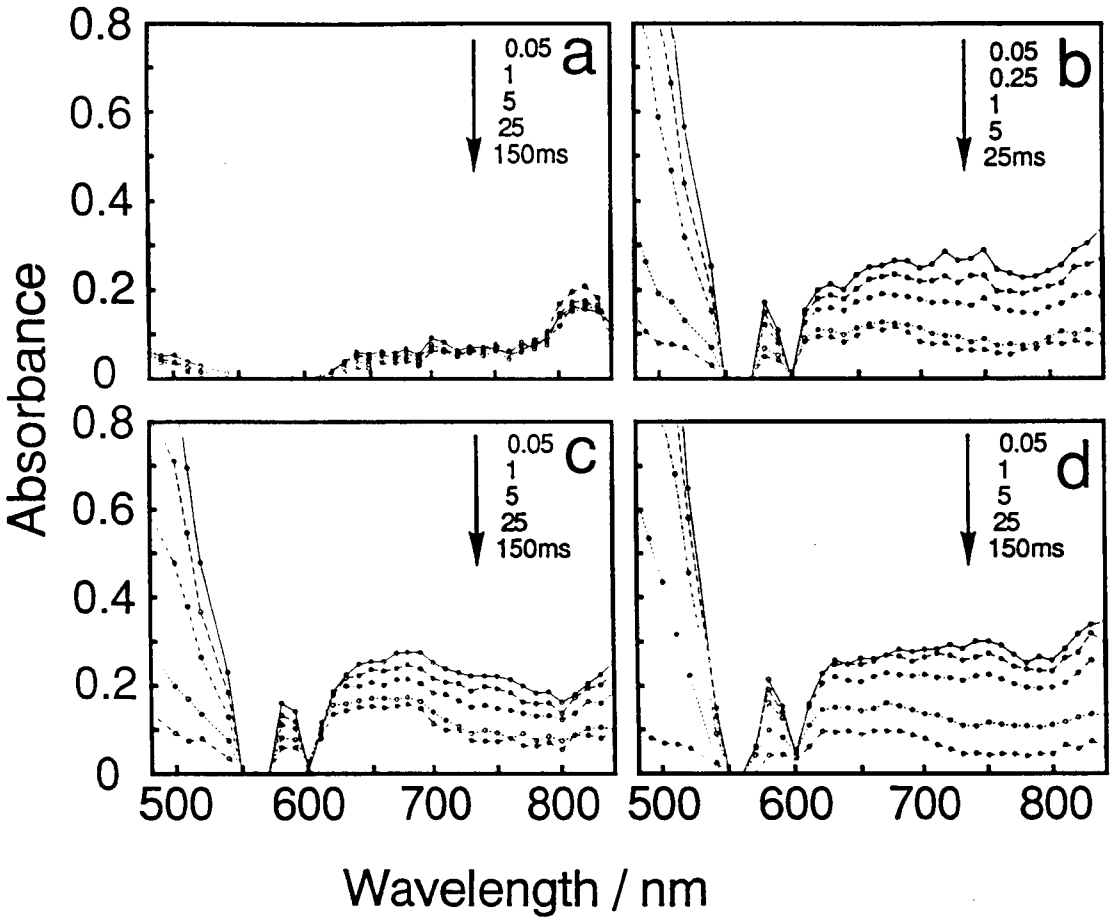

Figure 8. Time-resolved transient absorption spectra of the reference copolymer and the terpolymers in the presence of PMPS in aqueous solution: **a**, poly(A/ZnTPP); **b**, poly(A/La/ZnTPP); **c**, poly(A/Np/ZnTPP); **d**, poly(A/Cd/ZnTPP); [ZnTPP](residue)=100 μM; [PMPS]=10 mM.

decreased and a new broad absorption band peaking at about 815 nm appeared after irradiation. The spectral profile of the new absorption band around 800 nm resembled the transient absorption bands in the reference copolymer-PMPS system shown in Fig.8-a.

A difference absorption spectrum between the absorption spectra at 30 min and 15 s after irradiation is shown in Figure 9-b. In the 630-800 nm region, the difference absorption spectrum was assigned to the absorption of $ZnTPP^{+\cdot}$ moieties by comparing with spectra reported for $ZnTPP^{+\cdot}$ itself generated by an electrochemical procedure.[6] Furthermore, in the 500-630nm region, the absorption due to the $ZnTPP^{+\cdot}$ moieties decayed during a period from 15 s to 30 min, while the ground state of the ZnTPP moieties was , in turn, regenerated. Figure 9-a shows isosbestic points appearing at 544 and 573 nm, suggesting that the $ZnTPP^{+\cdot}$ moieties are completely converted back to the ZnTPP moieties.

The new absorption band at 815 nm may be due to Photoproduct-A. The structure of Photoproduct-A may be an isoporphyrin derivative because the spectral profile is similar to that of isoporphyrin.[7] Differences in the spectral profiles in the wavelength region between the transient absorption spectra of the terpolymer systems (Figure 8-b,c,d) and that of $ZnTPP^{+\cdot}$ itself[6] may be due to the isoporphyrin derivatives.

The $ZnTPP^{+\cdot}$ moiety may decay *via* two different reactions, i.e, the reaction between the $ZnTPP^{+\cdot}$ moiety and the carbon radical to generate Photoproduct-A (Scheme I), and the reaction by which the $ZnTPP^{+\cdot}$ moiety is converted to the ground state of ZnTPP moiety.

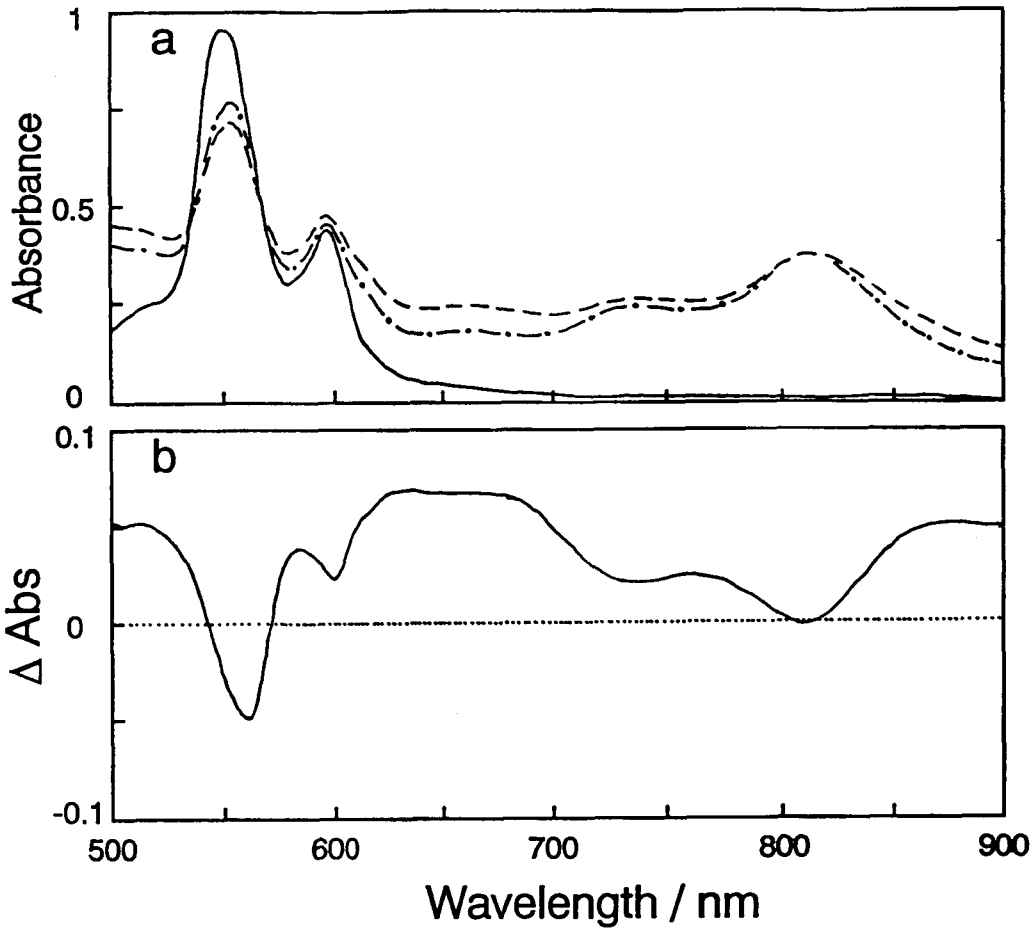

Figure 9. (**a**) Absorption spectra of poly(A/Cd/ZnTPP) in the presence of PMPS in aqueous solution before irradiation (——), and after standing in the dark for 15 s (— — —) and 30 min (—• —) after steady-state light irradiation for 3 min at 500 nm. (**b**) Difference absorption spectrum between the absorption spectrum after standing in the dark for 30 min and that for 15 s: [ZnTPP](residue) = 50 μM; [PMPS] = 10 mM.

The former may occur only immediately after photoinduced ET because the carbon radical is short-lived. We cannot explain what an electron donor is for the latter reaction.

6,3,5. ESR Studies of The Photoproducts

ESR spectra under irradiation of steady-state visible light at the polymers in the presence of PMPS in aqueous solution are shown in Figure 10. In the compartmentalized ZnTPP systems, all the ESR spectra showed no hyper-fine structures (hfs) with a line width of 4.9 gauss. These spectra agreed with that of $ZnTPP^{+\cdot}$ itself in the glassy state at 77K reported by Wolberg et al.[8] The $ZnTPP^{+\cdot}$ itself has shown hfs due to eight equivalent *ortho* hydrogens on the phenyl group in liquid solution at room temperature.[8,9] This result suggests that four phenyl groups of the $ZnTPP^{+\cdot}$ moieties in the terpolymers cannot rotate freely because of steric hindrance of the surrounding hydrophobic groups in the compartment. A difference in the ESR spectra of $ZnTPP^{+\cdot}$ itself between in liquid and glassy phases [8] has been explained in the same manner. On the other hand, intensity of the ESR spectrum of the poly(A/ZnTPP)-PMPS system was much weaker than those of the terpolymer systems. The hfs caused by delocalization of a radical on phenyl hydrogens [8,9] could not be detected because of the small intensity of ESR signal.

For all the polymer-PMPS systems no ESR signal due to the carbon radical generated from PMPS (Scheme I) could be detected. This suggests that the reactivity of the carbon radical is high, and the concentrations of the radical are too low to be detected by the ESR

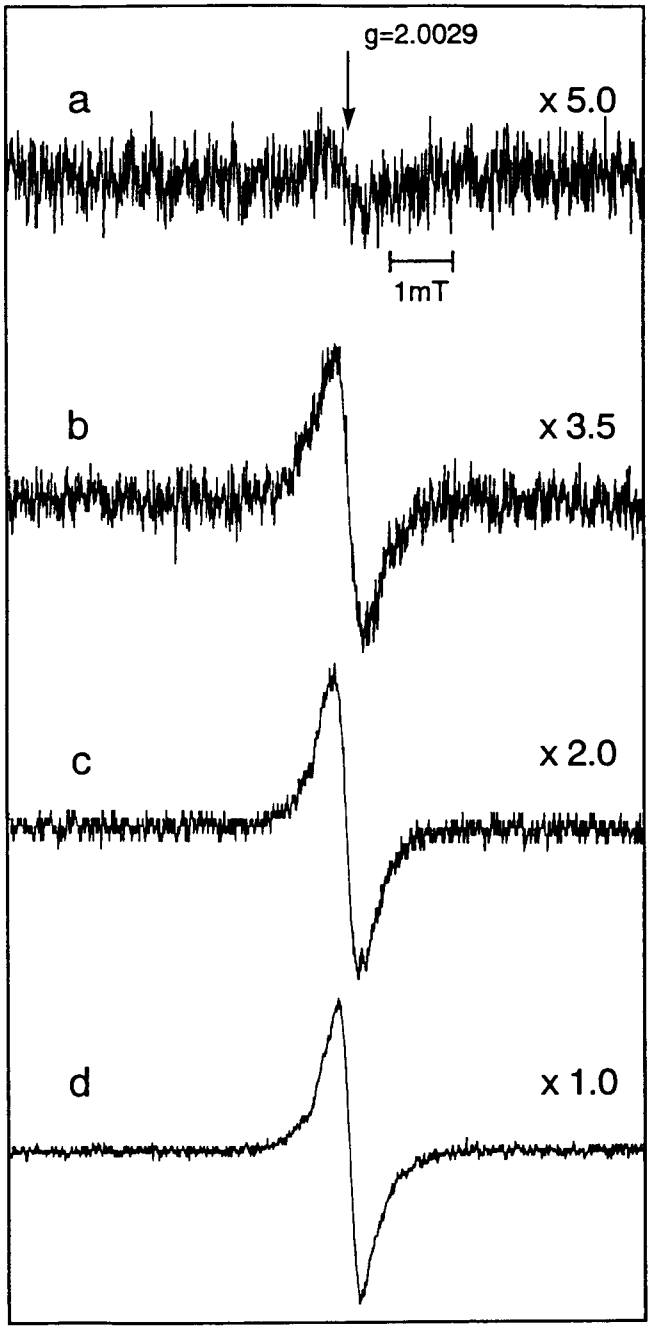

Figure 10. ESR spectra under irradiation of steady-state visible light for the polymers in the presence of PMPS in aqueous solution: **a**, poly(A/ZnTPP); **b**, poly(A/La/ZnTPP); **c**, poly(A/Np/ZnTPP); **d**, poly(A/Cd/ZnTPP); [ZnTPP](residue)=100 μM; [PMPS]=10 mM.

measurement in aqueous solution at room temperature.

Figure 11 shows ESR spectra for poly(A/Cd/ZnTPP) in the presence of PMPS under irradiation of steady-state visible light and 45 min after irradiation was stopped. The spectral profile in the dark, 45 min after finish off irradiation, agreed with that under irradiation except intensity. The spectral intensity at the peak top (333.9 mT) is proportional to the concentration of the $ZnTPP^{+\cdot}$ moiety. Figure 12 shows decay profiles monitored at 333.9 mT for the $ZnTPP^{+\cdot}$ moieties produced by irradiation of steady-state visible light for 1 min in the polymer-PMPS systems in aqueous solution. Half-lives of the $ZnTPP^{+\cdot}$ moieties in the polymers are listed in Table II. The initial concentration of the $ZnTPP^{+\cdot}$ in the reference copolymer system was much lower than those in the terpolymer systems and the half-life was shorter. The half-life of the reference copolymer system (7 s) was close to half-life of $ZnTSPP^{+\cdot}$ (6 s) reported by Neta et al.[10] On the other hand, in the terpolymer systems, the initial concentrations and the half-lives of the $ZnTPP^{+\cdot}$ moieties depended on the compartmentalizing hydrophobic groups. The half-lives for poly(A/Np/ZnTPP) and poly(A/Cd/ZnTPP) systems were much longer than those for ZnTSPP, the reference copolymer, and poly(A/La/ZnTPP) systems. It should be noted that 45% of the initial concentration of the $ZnTPP^{+\cdot}$ moieties in poly(A/Cd/ZnTPP) existed at 20 min after irradiation was stopped.

6,3,6. Photoinduced Radical Polymerization

Results of photoinduced radical polymerizations of acrylamide

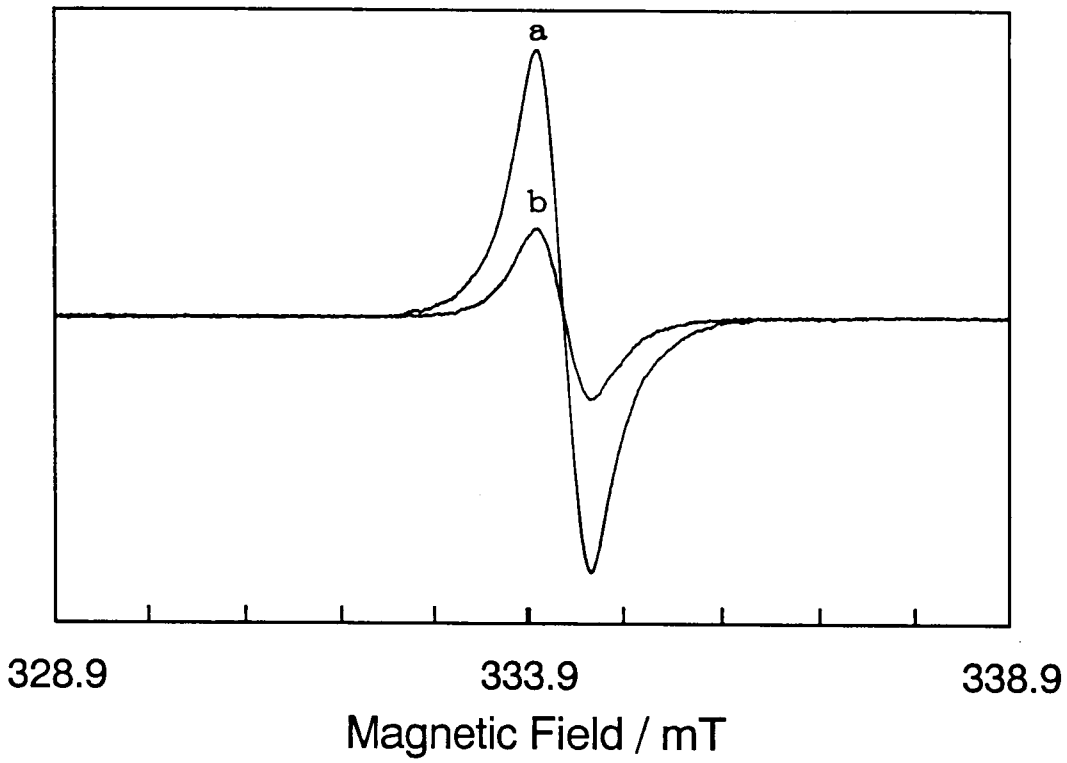

Figure 11. ESR spectra of poly(A/Cd/ZnTPP) in the presence of PMPS in aqueous solution: **a**, under irradiation of steady-state visible light; **b**, after standing in the dark for 45 min after irradiation was stopped: [ZnTPP](residue)=100 μM; [PMPS]=10 mM.

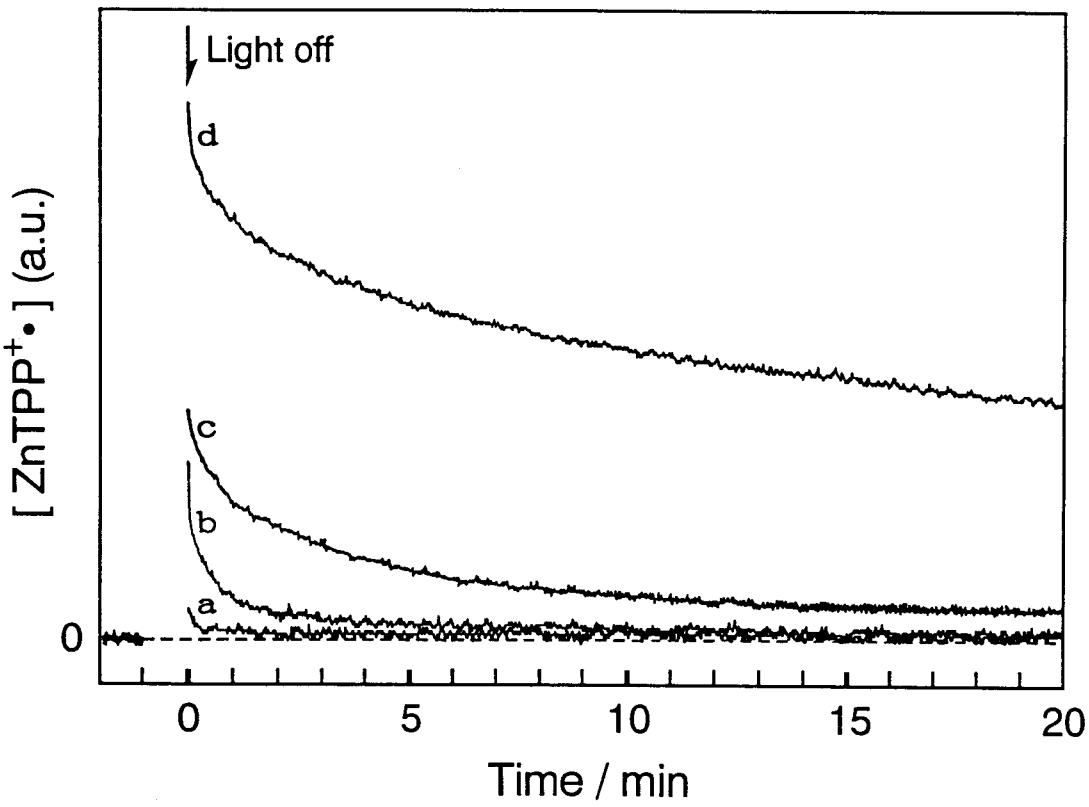

Figure 12. Decay profiles monitored at 333.9 mT for $ZnTPP^{+\bullet}$ moieties produced by irradiation of steady-state visible light for 1 min in the polymer-PMPS systems in aqueous solution: **a**, poly(A/ZnTPP); **b**, poly(A/La/ZnTPP); **c**, poly(A/Np/ZnTPP); **d**, poly(A/Cd/ZnTPP); [ZnTPP](residue)=100 μM; [PMPS]=10 mM.

Table II. Half-lives of the $ZnTPP^{+\cdot}$ moieties generated by photoinduced ET in the polymers in aqueous solution

sample code	time / s
poly(A/ZnTPP)	7
poly(A/La/ZnTPP)	15
poly(A/Np/ZnTPP)	120
poly(A/Cd/ZnTPP)	810
ZnTSPP [a]	6

[a] reference 10.

are summarized in Table III. Polyacrylamide was only obtained in the poly(A/Cd/ZnTPP)-PMPS system by irradiation. This result shows that the radical generated from PMPS in the poly(A/Cd/ZnTPP)-PMPS system initiated the radical polymerization of acrylamide. On the other hand, the radical generated from the reference copolymer-PMPS system could not initiate the radical polymerization. Although no ESR signal due to the carbon radical was detected, the radical in the poly(A/Cd/ZnTPP)-PMPS system may be long-lived to be able to attack acrylamide leading to the polymerization because the reaction of the radical with the $ZnTPP^{+\cdot}$ moiety (Scheme I) may be suppressed by the compartmentalization.

Table III Photoinduced Radical Polymerizations of Acrylamide (AA)

polymer code	[PMPS] / mM	irradiation	yield of polyAA (%)
poly(A/Cd/ZnTPP) [a]	6.7	yes [b]	13.4
poly(A/Cd/ZnTPP) [a]	0	yes [b]	0
poly(A/Cd/ZnTPP) [a]	6.7	no [c]	0
none	6.7	yes [b]	0
poly(A/ZnTPP) [a]	6.7	yes [b]	0

[a] Concentration of the ZnTPP residues was adjusted to 50 μM.

[b] Irradiation at 532 nm with 50 laser pulses.

[c] No irradiation.

6.4. Conclusions

The CT complexation with PMPS was completely suppressed by the compartmentalization of the ZnTPP moieties in the terpolymers.

The ET from S_1 of the ZnTPP moiety to PMPS for the reference copolymer occurred, but the compartmentalization completely suppressed it because of the steric protection by the

compartmentalizing hydrophobic groups.

The apparent rate constants of the ET from T_1 of the ZnTPP moiety to PMPS ($k_{q,T}$) for the terpolymer systems were two orders of magnitude smaller than that for the reference copolymer.

The accumulation of $ZnTPP^{+\cdot}$ as a result of the compartmentalization was observed by laser flash photolysis, absorption spectra, and ESR measurement. The naphthyl and cyclododecyl groups were effective to accumulate $ZnTPP^{+\cdot}$ which persisted over 20 min. The $ZnTPP^{+\cdot}$ moiety was eventually converted to the ZnTPP moiety.

Though no carbon radical generated from PMPS could be detected by ESR measurement, the carbon radical in the poly(A/Cd/ZnTPP)-PMPS system was long-lived enough to initiate the radical polymerization of acrylamide.

References

1) (a) Pappas, S. P.; Pappas, B. C.; Gatechair, L. R.; Schnabel, W. R. *J. Poly. Sci. Polym. Chem. Ed.* **1984**, *22*, 69. (b) Pappas, S. P.; Gatechair, L. R.; Jilek, J. H. *J. Poly. Sci. Polym. Chem. Ed.* **1984**, *22*, 77. (c) Crivello, H.; Lam, J. H. W. *Macromolecules* **1977**, *10*, 1307.

2) (a) DeVoe, R. J.; Sahyun, M. R. V.; Serpone, N.; Sharma, D. K. *Can. J. Chem.* **1987**, *65*, 2342. (b) DeVoe, R. J.; Sahyun, M. R. V.; Schmidt, E.; Serpone, N.; Sharma, D. K. *Can. J. Chem.* **1988**, *66*,

319.

3) Saeva, F. D.; Morgan, B. P. *J. Am. Chem. Soc.* **1984**, *106*, 4121.

4) Kalyanasundaram, K. *J. Chem. Soc., Faraday Trans. 2* **1983**, *79*, 1365.

5) Harriman, A. *J. Chem. Soc., Faraday Trans. 2* **1981**, *87*, 1281.

6) Fajer, J.; Borg, D. C.; Forman, A.; Dolphin, D.; Felton, R. H. *J. Am. Chem. Soc.* **1970**, *92*, 3451.

7) (a) Mosseri, S.; Mialocq, J. C.; Perly, B.; Hambright, P. *J. Phys. Chem.* **1991**, *95*, 2196. (b) Richoux, M.-C.; Neta, P.; Christensen, P. A.; Harriman, A. *J. Chem. Soc., Faraday Trans. 2* **1986**, *82*, 235. (c) Harriman, A.; Porter, G.; Walters, P. *J. Chem. Soc., Faraday Trans. 1* **1983**, *79*, 1335. (d) Dolphin, D.; Felton, R. H.; Borg, D. C.; Fajer, J. *J. Am. Chem. Soc.* **1970**, *92*, 743.

8) Wolberg, A.; Manassen, J. *J. Am. Chem. Soc.* **1970**, *92*, 2982.

9) Felton, R. H.; Dolphin, D.; Borg, D. C.; Fajer, J. *J. Am. Chem. Soc.* **1969**, *91*, 196.

10) Neta, P.; Harriman, A. *J. Chem. Soc., Faraday Trans. 2* **1985**, *81*, 123.

Chapter 7

Summary

We synthesized several new monomers containing metalloporphyrins as follows:

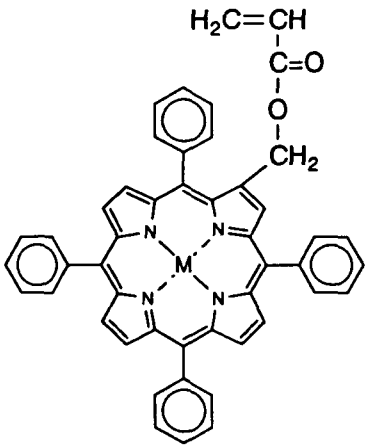

MAOMTPP
M=Cu(II)
VO(II)

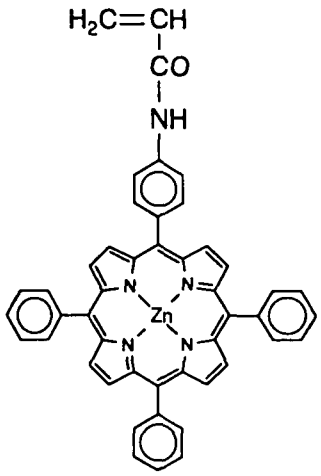

ZnAATPP

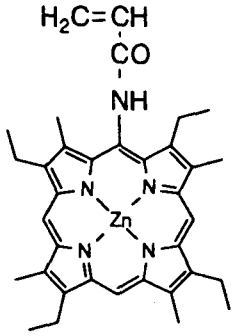

ZnAAEtio

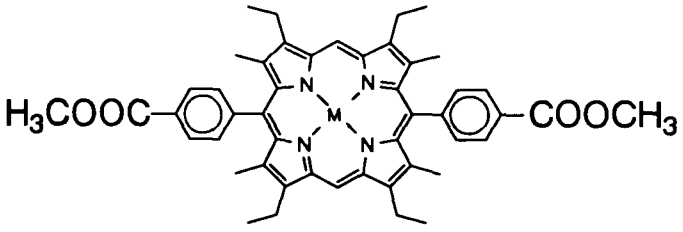

MCH$_3$OCODPE
M=Cu,VO, MnCl

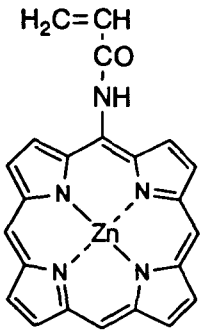

ZnAAPor

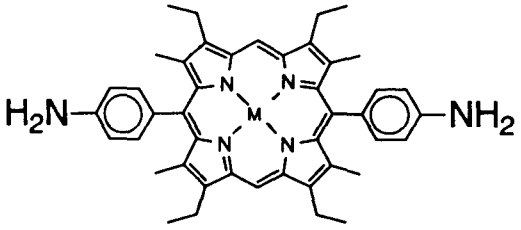

MNH$_2$DPE
M=Cu,VO, MnCl

Homopolymers of the acrylate monomers, CuAOMTPP and VOAOMTPP, with the weight average molecular weight of about 15000, were obtained by radical polymerizations. The order of the reactivities of the acrylamide monomers in radical polymerization increased in the order: ZnAAEtio < ZnAAPor < ZnAATPP. This order may be explained by the bulkiness of substitutes bound directly to the vinyl group. Polyamides obtained by condensation polymerization of DPE compounds were insoluble. These results are mentioned in Chapter 2.

In Chapter 3, a study on the magnetic behavior of the polymers containing paramagnetic metalloporphyrins is described. CuCuDPE, VOVODPE, MnMnDPE, CuMnDPE, and VOMnDPE, which were polyamides obtained by condensation polymerization, showed a weak antiferromagnetic interaction. PolyCuAOMTPP showed an antiferromagnetic interaction with a Weiss temperature of -38K, indicating that it has stronger magnetic interaction than polyAOTPPCu which was previously studied in our laboratory. The stronger magnetic interaction of polyCuAOMTPP is reasonably ascribed to the decrease in the distance between paramagnetic species due to the distance between the main chain of the polymer and the metalloporphyrin moiety. PolyVOAOMTPP was separated into a magnetoinactive part and a small magnetoactive part. In the ESR spectrum of the magnetoactive part, a broad signal, whose intensity was almost independent of the temperature, was observed along with signals due to paramagnetic polyVOAOMTPP. The magnetoinactive part showed a weak ferromagnetic interaction with a Weiss

temperature of +5K, indicating the formation of a magnetic domain where the arrangement of the magnetic sites was good enough to interact magnetically.

In Chapter 4, we studied photophysics of the ZnTPP chromophore compartmentalized in the hydrophobic aggregate of the amphiphilic polyelectrolytes in aqueous solution. Absorption maxima of the Soret band for the terpolymers in aqueous solution were longer than that for the reference copolymer because of differences in the environments around the ZnTPP moieties. We clarified that the compartmentalization was effective to lengthen the lifetimes of the triplet excited states of the ZnTPP moieties. Especially, the lifetimes for poly(A/Np/ZnTPP) and poly(A/Cd/ZnTPP) were almost equal to the value of ZnTPP itself in glassy solid at 77K. We are the first to observe phosphorescence and thermally activated delayed fluorescence of zinc porphyrins in fluid solution at room temperature, due to lengthened lifetimes of the triplet excited states by the compartmentalization.

In Chapters 5 and 6, we studied the photochemistry of the compartmentalized ZnTPP-MV^{2+} and ZnTPP-PMPS systems, respectively. The CT complexations were completely suppressed by the compartmentalization of the ZnTPP moieties in the terpolymers. The electron transfers of the compartmentalized systems were slower than those of reference systems. We could observe the accumulations of the $ZnTPP^{+\cdot}$ moieties as a result of the compartmentalization, i.e., the backward reactions were suppressed by the compartmentalization. We could detect the $ZnTPP^{+\cdot}$ moieties

which persisted for several milliseconds in the compartmentalized ZnTPP-MV^{2+} systems in spite of the reversible electron transfer systems. Moreover, when we used an irreversible acceptor PMPS, we could detect the $ZnTPP^{+\cdot}$ moieties persisted over 20 min. This result for the compartmentalized ZnTPP-PMPS systems was attributed to the suppressed the reaction between the $ZnTPP^{+\cdot}$ moiety and the radical generated from PMPS and that between the $ZnTPP^{+\cdot}$ moiety and other compounds. Though no carbon radical generated from PMPS could be detected by ESR measurement, the carbon radical in the poly(A/Cd/ZnTPP) system was long-lived enough to initiate the radical polymerization of acrylamide.

List of Publications

The content of this thesis have been published or will be published in the following papers:

1. New Polymers Containing Pendant Metalloporphyrins. Radical Polymerization of 2-[(Acryloyloxy)methyl]-5,10,15,20-tetraphenylporphinato metals.
   Aota, H.; Fujii, H.; Harada, A.; Kamachi, M.
   Chem. Lett. **1990**, 823.
2. Synthesis of Acrylamide Containing Zincporphine (ZnPor) and Its Polymerizability.
   Aota, H.; Harada, A.; Morishima, Y.; Kamachi, M.
   Chem. Lett. to be published.
3. Magnetic Behavior of Poly2-[(Acryloyloxy)methyl]-5,10,15,20-tetraphenylporphinato metals.
   Aota, H.; Fujii, H.; Harada, A.; Kamachi, M.; Mori, W.; Kishita, M.
   Chem. Lett. to be published.
4. Compartmentalization of Zinc(II) Tetraphenylporphyrin in a Hydrophobic Microdomain of an Amphiphilic Polyelectrolyte: A Physicochemical Model of Biological Metalloporphyrin Systems.
   Aota, H.; Morishima, Y.; Kamachi, M.
   Photochem. Photobiol. in press.
5. Photoinduced Electron Transfer to Methylviologene from Zinc(II) Tetraphenylporphyrin Compartmentalized in an Amphiphilic Polyelectrolyte.

Aota, H.; Morishima, Y.; Kamachi, M.

Photochem. Photobiol. to be published.

6. Photoinduced Electron Transfer to a Sulfonium Salt from Zinc(II) Tetraphenylporphyrin Compartmentalized in an Amphiphilic Polyelectrolyte.

Aota, H.; Morishima, Y.; Kamachi, M.

Photochem. Photobiol. to be published.

Other Related Papers:

1. Organic Ferromagnetism and Antiferromagnetism of 4-(Methacryloyloxy)-2,2,6,6-tetramethylpiperidin-1-oxyl and 4-(Acryloyloxy)-2,2,6,6-tetramethylpiperidin-1-oxyl.

Sugimoto, H.; Aota, H.; Harada, A.; Morishima, Y.; Kamachi, M.; Mori, W.; Kishita, M.; Ohomae, N.; Nakano, M.; Sorai, M.

Chem. Lett. **1991**, 2095.

2. Polymer Dependence of Boson Peak Frequency Studied by Hole Burning and Raman Spectroscopies.

Saikan, S.; Kishida, T. ;Kanematsu, Y.; Aota, H.; Harada, A.; Kamachi, M.

Chem. Phys. Lett. **1990**, *166*, 358.

3. Synthesis of Isophthalaldehyde Polymer and ESR Detection of High Spin States.

Nogami, T.; Kosaka, S.; Shirota, Y.; Aota, H.; Harada, A.; Kamachi, M.

Chem. Lett. **1989**, 1593.

4. Preparation and Properties of Magnetically-interacting Polymer with Copper(II) and Vanadyl (II) Porphyrins.
Kamachi, M.; Cheng, X. S.; Aota, H.; Mori, W.; Kishita, M.
Chem. Lett. **1987**, 2331.